SURFACTANT SELF-ASSEMBLY, KINETICS AND THERMODYNAMICS OF MICELLAR AND MICROEMULSION SYSTEMS

By

PAUL D. T. HUIBERS

A DISSERTATION PRESENTED TO THE GRADUATE SCHOOL
OF THE UNIVERSITY OF FLORIDA IN PARTIAL FULFILLMENT
OF THE REQUIREMENTS FOR THE DEGREE OF
DOCTOR OF PHILOSOPHY

UNIVERSITY OF FLORIDA

1996

Copyright 1996

by

Paul D. T. Huibers

I dedicate this dissertation to my parents, Elizabeth C. and Derk T.A. Huibers, for without their guidance and constant support I would not have given up my job, gone back to school, and embarked on a second career.

ACKNOWLEDGMENTS

Several organizations and people have helped me during my Ph.D. research. I would like to acknowledge the financial support of Kraft General Foods and ICI Americas Inc. for research funding, and ICI Surfactants and Rhone-Poulenc for surfactant donations. I have benefited from interactions with other departments, and would specifically like to thank Dr. Randolph Duran for use of his Langmuir trough equipment, and Dr. Wallace Brey for assistance in running NMR samples on surfactants. Many thanks go to Dr. Alan R. Katritzky and his QSPR group, especially Dr. Mati Karelson and Dr. Victor Lobanov, as our successful collaboration over the last year and a half has led to one of the three chapters in this thesis, and several papers. I would like to thank the graduate students who have graduated before me, and taught me a lot about interfacial phenomena: Dr. Seong-Geun Oh, Dr. Vinod Pillai, Dr. Promod Kumar, Dr. S. Hingorani, Dr. C.P. Singh, and Dr. Y.K. Rao. I would like to thank Merle Regino for her help and support through my Ph.D. program. Special thanks go to the late Dr. N.M. van Os for his help and to Dr. Christian Reichardt for his advice on solvatochromism and his invitation to me to speak at Phillips University in Marburg, Germany. Finally, I would like to acknowledge my advisor, Dr. Dinesh O. Shah, for his guidance and inspiration through these past four years. His advice has led me on many fruitful research paths, and his sponsorship has allowed me pursue interdisciplinary projects and to present my work at several national and international meetings.

TABLE OF CONTENTS

page

ACKNOWLEDGMENTS iv

LIST OF TABLES vii

LIST OF FIGURES ix

KEY TO SYMBOLS OR ABBREVIATIONS xiv

ABSTRACT xvi

CHAPTERS

1 INTRODUCTION 1

2 SURFACTANT QUANTITATIVE STRUCTURE-PROPERTY RELATIONSHIPS 4

Introduction 4
Nonionic Surfactant CMC 6
Anionic Surfactant CMC 11
Temperature Dependence of Anionic CMC 15
Nonionic Surfactant Cloud Point 23
Anionic Surfactant Krafft Point 28
Molecular Volume of Alkanes and Surfactant Hydrophobic Tails 34
Conclusions 47

3 MAXIMUM SOLUBILIZATION IN NONIONIC W/O MICROEMULSIONS 49

Introduction 49
Nonionic Surfactants 50
Microemulsions 54
Design of Water-in-Oil Microemulsions 62
Water/Hexadecane/Sorbitan Ester Microemulsions 69
Effect of Oil Phase on Water/Alkane/Sorbitan Ester Systems 84
Water/Cyclohexane/Nonylphenyl Ethoxylate Microemulsions 95
Other Solubilization Experiments 101
Conclusions 105

4 SURFACTANT MICELLAR LIFETIME 107

Introduction 108
Anionic Surfactants 109
Influence of Alcohol Cosurfactants on Micellar Lifetime 110
Influence of Glycerol on Micellar Lifetime 114
Influence of Counterion Size on Micellar Lifetime 122
Influence of Added Nonionic Surfactant on Micellar Lifetime 131
Influence of Added Electrolyte on Micellar Lifetime 136
Effect of Molecular Structure on Dynamic Surface Tension 142
Effect of Micellar Structure on ^{23}Na NMR Measurements 152
Cationic Surfactants 160
Micellar Lifetime 160
Effect of Micellar Lifetime on Processes 169
Nonionic Surfactants 175
Solvatochromism in Nonionic Surfactants 176
Determination of Aggregation Number by UV Rayleigh Scattering 179
Conclusions 191

SUMMARY AND CONCLUSIONS 194

APPENDIX. SURFACTANTS USED IN THIS RESEARCH 198

LIST OF REFERENCES 202

BIOGRAPHICAL SKETCH 212

LIST OF TABLES

Table		page
2-1.	CMC values (mM) for 16 structures, as a function of temperature, and Krafft points (^{o}C)	18
2-2.	Structure names for the 44 surfactants included in the Krafft point correlations	31
2-3.	Methods for estimating molecular volume	36
2-4.	Structure names for the 78 hydrocarbons and fluorocarbons used for the determination of molecular volume	40
3-1.	Approved daily intake values for some surfactants	52
3-2.	Specific roles of cosurfactant in microemulsion formulation	59
3-3.	The effect of oils on the PIT for volume ratio 1.0 water/oil emulsion containing 10% POE (9.6) nonylphenyl ether	61
3-4.	Expected structures for different R values	63
3-5.	Abe's microemulsion design rules	65
3-6.	Surfactant mixture studies	68
3-7.	Maximum solubilization for Spans and Tweens	81
3-8.	Maximum solubilization in different oils	88
3-9.	Mole fractions of Span and Tween 85 at the ratio of maximum solubilization in different alkane oil phases	93
3-10.	Maximum water solubilization for Igepal CO mixtures in hexadecane and cyclohexane	98
3-11.	Other successful maximum solubilization experiments	101

3-12. Unsuccessful maximum solubilization experiments 103

4-1. Solubility of n-aliphatic alcohols in water at 25°C 112

4-2. Rules for alcohol influence on micellar stability 114

4-3. Slow relaxation time estimates for 150 mM SDS + salt ($NaClO_4$) 125

4-4. Slow relaxation time (τ_2) and electrical conductivity for SDS micellar solutions with different concentrations of nonionic surfactants 132

4-5. Slow relaxation time (τ_2) and electrical conductivity for SDS micellar solutions with different concentrations of electrolytes 138

4-6. Surface tension values (dyne/cm) at 20°C 145

4-7. Surface tension and viscosity values (20°C, unless otherwise marked) 151

4-8. Absorbance peaks and solvatochromic shift of selected dyes in organic solvents 178

4-9. Absorbance peaks of Sudan Black B in selected micelles 179

4-10. Aggregation number of some typical nonionic surfactants as a function of temperature 183

A-1. HLB and structure of selected surfactants 198

LIST OF FIGURES

Figure page

2-1. Structures of the surfactants included in the nonionic CMC correlations 8

2-2. Scatter plot for calculated vs. experimental nonionic CMC for 77 surfactants, using three descriptors 10

2-3. Structures of the surfactants included in the anionic CMC correlations 13

2-4. Scatter plot for calculated vs. experimental anionic CMC for 119 surfactants, using three descriptors 14

2-5. Normalized CMC vs. temperature for a) sulfates and b) sulfonates 21

2-6. Structures of the surfactants included in the nonionic cloud point correlations 25

2-7. Scatter plot for calculated vs. experimental nonionic cloud point for 62 surfactants, using three descriptors 26

2-8. Topological descriptor values vs. carbon number for the different hydrophobic structures in the cloud point correlation 27

2-9. Structures of the surfactants included in the Krafft point correlations 30

2-10. Scatter plot for calculated vs. experimental Krafft point for 44 surfactants, using four descriptors 33

2-11. Scatter plot for the four descriptor regression of calculated to experimental molar volume of 78 diverse alkanes and alkenes 42

2-12. Scatter plot for the one descriptor ($^0\chi$) regression of calculated to experimental molar volume of 78 diverse alkanes and alkenes, showing structures with greatest steric influence on the molecular volume 44

3-1. W/O solubilization, binary mixtures of Spans with Tween 85 73

3-2. W/O solubilization, binary mixtures of Spans with Tween 80 74

3-3. W/O solubilization, binary mixtures of Spans with Tween 20 75

3-4. W/O solubilization, binary mixtures of Spans with Tween 21 76

3-5. W/O solubilization, binary mixtures of Spans with Tween 81 78

3-6. Solubilization assuming hydration, binary mixtures of Spans with Tween 85 79

3-7. W/O solubilization in ternary Span/Tween mixtures 83

3-8. W/O solubilization, weight % excursion for Tween 81 85

3-9. W/O solubilization, weight % excursion for Span 80/Tween 85 mixtures 86

3-10. W/S ratio vs. S/O ratio, for Span 80/Tween 85 N_{HLB}=10 mixture 87

3-11. W/O solubilization in C_{10}-C_{16} n-alkane/Tween 81 microemulsions 89

3-12. W/O solubilization in C_8-C_{16} n-alkane/Span 80/Tween 85 microemulsions 90

3-13. W/O solubilization in C_8-C_{16} n-Alkane/Span 20/Tween 85 microemulsions 91

3-14. W/O solubilization in C_8, C_{12}, C_{16} n-alkane/Span 20/Tween 85 microemulsions 92

3-15. Curvature model for the solubilization behavior of Span/Tween W/O microemulsions 94

3-16. W/O solubilization, binary mixtures with Igepal CO series surfactants in cyclohexane 97

3-17. Solubilization of electrolyte solutions in Igepal/cyclohexane W/O microemulsions 100

3-18. W/O solubilization in hexadecane/Span/ethoxylated Castor oil microemulsions 102

4-1. Effect of micellar lifetime (slow relaxation time) on technological processes 108

4-2. Variation of the slow relaxation time (τ_2) of 100 mM SDS as a function of alcohol concentration 111

4-3. Slow relaxation time for mixtures of SDS and higher alcohols. The concentration of the mixtures remains constant at 100 mM (SDS+alcohol)..... 113

4-4. Viscosity of glycerol/water mixtures..... 117

4-5. Conductivity of glycerol/water/SDS mixtures..... 118

4-6. Slow relaxation time of 100 mM SDS with different glycerol/water ratios..... 120

4-7. Slow relaxation time of SDS at a 1:1 glycerol/water ratio..... 121

4-8. Slow relaxation time (τ_2) vs. size of counterion, for 3 and 30 mM concentrations of tetraalkyl-ammonium chloride salts, where the alkyl group varies from methyl to pentyl..... 127

4-9. Slow relaxation time vs. concentration, for tetraethylammonium chloride in 150 mM SDS..... 129

4-10. Slow relaxation time vs. concentration, for tetraethylammonium chloride in 75 mM SDS..... 130

4-11. Slow relaxation time of mixed anionic and nonionic surfactants, for different mixtures of 100 mM combined SDS + Tween 80..... 134

4-12. Typical electrical conductivity vs. time traces for pressure-jump experiments. These examples show the decrease in signal as the proportion of nonionic surfactant increases..... 135

4-13. Slow relaxation time (τ_2) for mixed anionic and nonionic surfactants, for different mixtures of 0.5 wt% combined AOT + Arlacel 20..... 136

4-14. Slow relaxation time vs. additive concentration for 100 mM SDS with the additives glycerol, glycine and sodium octanoate..... 139

4-15. Slow relaxation time vs. concentration for mixed sodium octanoate/SDS micelles, compared with pure SDS micelles..... 140

4-16. Surface tension vs. concentration for sodium octanoate..... 141

4-17. Apparent dynamic surface tension of glycerol..... 149

4-18. Equilibrium surface tension of methanol/water mixtures..... 150

4-19. ^{23}Na chemical shift (δ) vs. SDS concentration for the entire range from 2 to 400 mM 156

4-20. Spin-lattice relaxation time (T_1) vs. SDS concentration for the entire range from 2 to 400 mM 157

4-21. ^{23}Na chemical shift (δ) vs. the inverse of the SDS concentration for the entire range from 2 to 400 mM 158

4-22. Spin-lattice relaxation time (T_1) vs. the inverse of the SDS concentration for the entire range from 2 to 400 mM, showing linear relationship of T_1 to 1/[SDS] over certain concentration ranges 159

4-23. Surface tension vs. concentration for CPC, establishing a CMC of 0.9 mM 163

4-24. Electrical conductivity vs. concentration for MTAB 164

4-25. Slow relaxation time (τ_2) vs. concentration for CPC 165

4-26. Slow relaxation time vs. concentration for MTAB 166

4-27. Slow relaxation time vs. concentration for CTAB 167

4-28. Slow relaxation time conductivity signal amplitude vs. concentration for CPC 168

4-29. Fabric wetting time vs. concentration for MTAB 171

4-30. Fabric wetting time vs. concentration for CTAB 172

4-31. Foam height vs. concentration for MTAB 173

4-32. Foamability vs. concentration for MTAB 174

4-33. Nonionic surfactant micellar kinetics via temperature-jump 177

4-34. Measuring light scattering with absorbance spectroscopy 184

4-35. Absorbance spectrum of Arlasolve 200 185

4-36. Log absorbance vs. log wavelength for Brij 78 186

4-37. Absorbance spectrum of SDS 187

4-38. Ultraviolet absorbance spectrum of water vs. temperature 188

4-39. Absorbance spectrum of Igepal CO-720 189

4-40. Absorbance spectrum of Brij 97 190

KEY TO SYMBOLS AND ABBREVIATIONS

Structure-Property Relationships

C#	carbon number, number of carbon atoms in a linear alkyl chain
CMC	critical micelle concentration
EO#	ethylene oxide number, number of ethylene oxide residues in poly(ethylene oxide)
F	F-statistic of regression
HGP	head group position in surfactant alkyl chain
KS3	Kier shape index of third order
MW	molecular weight
N	number of structures in regression
N_c	(see C#)
QSPR	quantitative structure-property relationships
r^2, R^2	square of correlation coefficient of regression
RNNO	relative number of oxygen and nitrogen atoms
s^2	square of standard error of regression
TDIP	total molecular dipole moment
t-KH0	Kier & Hall molecular connectivity index of 0th order for the hydrophobic domain
t-ASIC2	average structural information content of 2nd order for the hydrophobic domain

Microemulsions

HLB	hydrophile-lipophile balance (also N_{HLB})
O/W	oil-in-water (emulsions or microemulsions)
PIT	phase inversion temperature
POE	poly(ethylene oxide), or PEO
QELS	quasi-elastic light scattering
W/O	water-in-oil
w/v	weight to volume units, usually grams per ml of liquid

Micellar Lifetime

MBP	maximum bubble pressure (for measurement of dynamic surface tension)
TAA	tetraalkylammonium ions
η	viscosity, centipoise
τ_1	fast micellar relaxation time
τ_2	slow micellar relaxation time, micellar lifetime

Abstract of Dissertation Presented to the Graduate School
of the University of Florida in Partial Fulfillment of the
Requirements for the Degree of Doctor of Philosophy

SURFACTANT SELF-ASSEMBLY, KINETICS AND THERMODYNAMICS IN MICELLAR AND MICROEMULSION SYSTEMS

By

Paul D. T. Huibers

December, 1996

Chairman: Dr. Dinesh O. Shah
Major Department: Chemical Engineering

A greater knowledge of the physical properties of surfactants is important to future applications of new surfactants, as well as for improvements in product development with currently available surfactants. In this thesis, three areas are examined; (i) the development of unique new surfactant quantitative structure-property relationships (QSPR) using the latest advances in chemical topological indices and semi-empirical quantum-chemical calculations, (ii) synergism in mixtures of nonionic surfactants for the formation of optimum microemulsions, and (iii) additive effects on ionic surfactant micellar lifetime and the effect of micellar lifetime on processes of technological interest.

The ability to predict physical and chemical properties given only surfactant molecular structure has great potential in the screening of new surfactants for new applications. Molecules can even be considered that have not yet been synthesized. Modern

QSPR techniques have not previously been applied to surfactants. A wide variety of molecular descriptors have been screened against surfactant physical properties. Correlations are presented for critical micelle concentration, cloud point, Krafft point, and molecular volume as applied to surfactant tails.

Microemulsions have applications in such diverse areas as foods, pharmaceuticals, and nanoparticle synthesis, among others. It is desirable to be able to solubilize the maximum amount of the inner phase into the bulk liquid phase, using a minimum of surfactant. Synergism is possible by using surfactant mixtures, improving solubilization results over any single surfactant, in creating water-in-oil microemulsions. Rules for surfactant selection based on HLB, molecular ratio, and influence of oil phase are presented.

Micellar stability has been shown to influence many processes of technological importance, including foaming, fabric wetting, emulsification, etc. Any process where surface or interfacial tension is important, and new interface is being rapidly created, will be influenced by micellar stability. As no practical surfactant system uses pure surfactant, the influence of alcohols, glycerol, electrolytes and nonionic surfactants on sodium dodecylsulfate micellar lifetime is examined. Measurements of micellar lifetime were made for several cationic surfactants, as well as a comparison of lifetime to processes such as fabric wetting and foamability.

CHAPTER 1
INTRODUCTION

My years of research at the University of Florida have brought me down many interesting paths in the field of interfacial phenomena. In this thesis, I hope to pass on what unique observations I have made along the way. My contributions to this field of interfacial phenomena lie in three areas, with surfactant physical properties as the binding theme. These three areas are microemulsion formulation, ionic surfactant micellar lifetime, and surfactant structure-property relationships.

Thesis organization. This thesis contains three separate projects, as described in the abstract section, tied together by the common thread of the prediction of properties in surfactant systems.

Structure-property relationships. In the first section, surfactant structure-property relationships are investigated. The approach used has been successfully applied by chemists to physical properties of compounds (QSPR), and also by biologists and medicinal chemists to drug activity (QSAR). The validity and success of this method has led to the publication of at least two journals in this field, *JCICS* and *QSAR*. The group of Professor Katritzky in the Department of Chemistry have developed a powerful tool (CODESSA) to assist the scientist in finding such relationships. It is surprising to note that the QSPR approach has never been applied to surfactant chemistry. This thesis and associated publications [Huibers et al. 1996b; 1996c; 1996d] are the first attempts of applying QSPR to surfactants.

Microemulsions. In the second section, synergism in nonionic surfactant mixtures is studied, specifically applied to enhancing water solubilization in water-in-oil microemulsions. Much work has been done in this area by many researchers, examining microemulsions made from many different oils and surfactants, and in the introduction to this section the relevant work on nonionic microemulsions and attempts at design rules for microemulsions are extensively reviewed. For certain food and pharmaceutical applications, microemulsions without cosurfactants are desirable. There is hardly any literature on w/o microemulsions using only nonionic surfactants. In this thesis, the rules of w/o microemulsion formulation using mixtures of nonionic surfactants are clarified, and numerous examples of such microemulsions are presented.

Micellar stability. In the third section, micellar stability is investigated. Micellar stability has been shown to influence numerous technological processes involving surfactant solutions. Also, the effects of additives to the surfactant solution on the micellar stability have been studied. This thesis extends the knowledge of the effects of additives on the model anionic surfactant system, SDS. The micellar stability of cationic surfactants at high concentrations is studied for the first time, along with the effect of cationic micellar stability on some technological processes. There is no established technique for the measurement of nonionic micellar lifetime. The potential of two possible detection techniques are investigated; 1) spectral absorbance shift in solvatochromic dyes, and 2) UV Rayleigh scattering in the 200-220 nm region. Both of these techniques may be used as detection

methods for a temperature-jump perturbation. The magnitude of potential changes by these two methods as a function of temperature is presented.

CHAPTER 2
SURFACTANT QUANTITATIVE STRUCTURE-PROPERTY RELATIONSHIPS

Introduction

In principle, the structural formula of a surfactant should encode all of the information that will determine its physical properties. In practice, though, our knowledge of chemistry and intermolecular forces is incomplete and does not allow us to calculate all properties from first principles. The use of quantitative structure-property relationships (QSPR) lies between the two extremes in determining surfactant physical properties.

On the one hand, given accurate thermodynamic models, along with accurate calculations of molecular orbitals, molecular conformations, and the interactions among molecules, all physical properties should be precisely determinable. On the other hand, given no such knowledge, physical properties can be measured experimentally. With our QSPR approach we attempt to stake out a middle ground, combining databases of physical properties with quantum chemical and topological calculations based on the molecular structure, in order to find relationships that can be used to make property predictions for structures without such property measurements. This can be summed up by the following quote:

> One need not attempt to derive chemical properties from physical structures by first principles; one need only choose a mathematical way of assigning numbers to molecules and then correlate those numbers with the vast base of known chemical properties. D.H. Rouvray, *Scientific American*, 1986.

Correlating chemical properties to parameters calculated from molecular structure has been around for decades. An early topological index that correlated alkane structure to boiling point was developed by Weiner [1947], although real progress in this area was limited by the ability to compute the indices. The modern era of such research began in 1975 with the development of a variety of topological indices of molecular structure by Randic [1975], Kier and Hall [1976] and others. Since that time, these indices have been applied to the prediction of a wide variety of physical properties [Kier and Hall, 1986; Rouvray, 1986]. More recently, partial charge [Stanton and Jurs, 1990] and quantum-chemical molecular descriptors [Katritzky et al., 1995; Lobanov, 1996] have been added to the inventory of successful molecular descriptors in QSPR studies.

Correlations of surfactant properties to aspects of molecular structure has been in a much more primitive state than that seen in general physical chemistry, and mostly limited to correlations of the carbon number of surfactants to properties, within a limited subclass of compounds. I have taken the QSPR tools developed by others and successfully applied them to predicting a number of properties, creating predictive formulas with a much more general applicability. In the following sections I will cover more details of the prediction of nonionic surfactant critical micelle concentration (CMC) [Huibers et al., 1996b], anionic CMC [Huibers et al., 1996c], nonionic cloud point [Huibers et al., 1996d], anionic Krafft point, and the molecular volume of a variety of hydro- and fluorocarbon surfactant tails.

Previous work. Only recently has there been QSPR-like work related to surfactants, besides simple relationships between properties such as the CMC and chain length for

surfactants with linear alkyl tails, as reviewed by Rosen [1989] and covered by Huibers et al. [1996b, 1996c, 1996d]. Two such QSPR works are known. Lindgren [1995], Lindgren and Sjöström [1994], and Lindgren at al. [1995] performed a multivariate QSPR study correlating nonionic surfactant properties to empirically derived parameters. The surfactants considered were commercial nonionics of the linear alkyl and alkylphenyl ethoxylate classes. Properties correlated were toxicity, detergency and CMC. Parameters used were constitutional descriptors based on the carbon number, HLB, and cloud point. [Richter et al., 1996] correlated three detergency parameters to nonlinear functions of the Kier and Hall molecular connectivity indices calculated for the surfactant head and tail.

Nonionic Surfactant CMC

Introduction. Until the 1980s, the only structure-property relationship in the surfactant literature was the Klevens' rule, after Klevens [1953] noted the relationship between the logarithm of the CMC and the carbon number of series of related surfactants. Some examples are given in Rosen [1989] for several different classes of surfactants, at different temperatures (see also Huibers et al. [1996b]), for example the following equation for C_nE_6 at 25°C.

$$\log_{10}\text{CMC} = 1.8 - 0.49\ C\# \qquad [1]$$

Becher [1984] first introduced a relationship similar to the Klevens rule, with a term for the number of ethylene oxide residues (*EO#*) in addition to the number of carbon atoms

(*C#*). Ravey et al. [1988] achieved even better results by including a nonlinear term, the product between *EO#* and *C#*, arriving at the following equation for alkyl ethoxylates:

$$\log_{10}\text{CMC} = 1.77 - 0.52\ C\# + 0.032\ EO\# + 0.002\ C\#EO\# \qquad [2]$$

From the theoretical direction (as opposed to these strictly empirical relationships), both Puvvada and Blankschtein [1990] and Nagarajan and Ruckenstein [1991] proposed thermodynamic models that could predict surfactant physical properties such as the CMC. These models are somewhat limited by the lack of understanding of head group interactions, and thermodynamics of tail interactions (limiting the models to linear alkyl tails only), resulting in predictions of limited accuracy, for a limited set of surfactants.

The QSPR approach takes the middle road between these two extremes, developing empirical rules similar to the Klevens rule, but with much more complicated descriptors than the simple carbon number (*C#*), and also applying several descriptors in one multiple linear regression. The empirical rules developed here are valid for a broader range of structures than either the Klevens relationships or the thermodynamic models are capable of handling. The full details of this effort are described in Huibers et al. [1996b]. The best three descriptor relationship developed for 77 diverse nonionic surfactants (Figure 2-1) at 25°C is

$$\log_{10}\text{CMC} = -1.80 - 0.567\ t\text{-}KH0 + 1.054\ t\text{-}ASIC2 + 7.51\ RNNO \qquad [3]$$
$$R^2 = 0.983,\ F = 1433,\ s^2 = 0.0313,\ N = 77$$

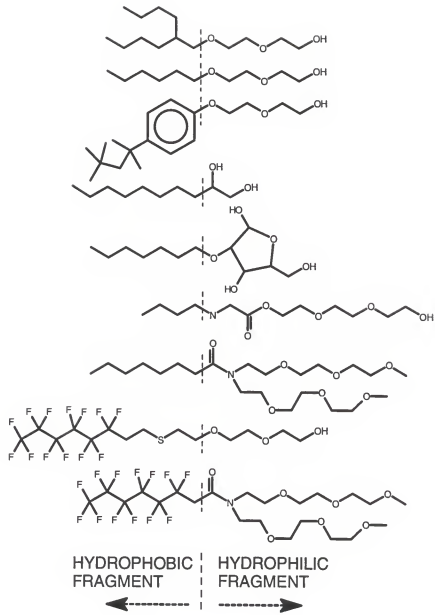

Figure 2-1. Structures of the surfactants included in the nonionic CMC correlations.

This formula uses two topological descriptors calculated from the hydrophobic tail, the Kier and Hall index of zero order (*t-KH0*) and the average structural information content index of second order (*t-ASIC2*), which together capture the influence of structural variation of the tail on CMC. The final descriptor, the relative number of nitrogen and oxygen atoms in the molecule (*RNNO*), captures the influence of the hydrophilic head group. The scatter plot of this correlation can be seen in Figure 2-2. The selection of these three descriptors over the hundreds of others available (with literally millions of combinations) was achieved by a heuristic search algorithm coded into the CODESSA program [Katritzky et al., 1994], which was also used for the generation of descriptors and the calculation of statistical parameters for the resulting regressions.

The two major accomplishments of this research effort were the first application of the QSPR techniques developed in other fields of chemistry to surfactant chemistry, and the successful application of descriptors calculated from molecular fragments to a QSPR problem. Surfactant physical properties were an excellent choice for the use of fragment descriptors, because what makes surfactants unique is the existence of two distinct domains, one hydrophobic and one hydrophilic, within the same molecule. Also, the changes that occur in the description of a physical property, such as CMC, effect the two fragments differently. The CMC is a perfect example, as when surfactant molecules form micelles, the hydrophobic domain undergoes a major environmental change, from aqueous to micellar interior (hydrophobic), while the hydrophilic fragment stays in the aqueous environment.

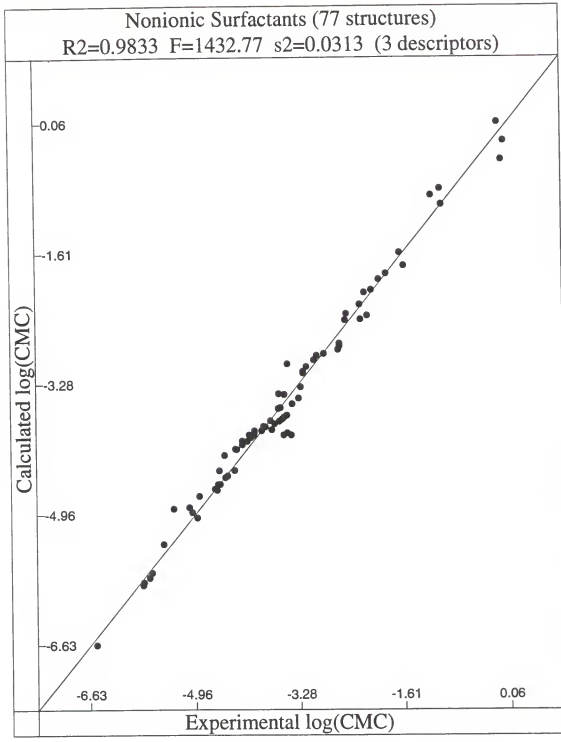

Figure 2-2. Scatter plot for calculated vs. experimental nonionic CMC for 77 surfactants, using three descriptors.

Thus, it was no surprise that the descriptors calculated from the two fragments performed better than those calculated in the traditional method from the whole molecule.

The success of this initial study of QSPR techniques applied to surfactants [Huibers et al. 1996b] led us to try CMC prediction for additional surfactant classes, as well as prediction of different surfactant properties. There is value in this analysis besides the regressions themselves. Ideally the choice of descriptors by CODESSA will give insight into what aspect of the molecule is influencing the property of interest, increasing the knowledge of surfactant structure effects on properties.

Anionic Surfactant CMC

The success with the nonionic surfactant CMC prediction led us immediately to try the other most important class of surfactants, the anionics. The details of the anionic CMC predictions can be found in Huibers et al. [1996c]. Together, the nonionics and anionics make up over 90% of the production (and use) of surfactants. A search of the literature resulted in 119 anionic surfactants with CMC values at or near 40°C. Although many CMC values are available at both 25 and 40°C, the higher temperature was used here because the solubility (Krafft point) is often limited for surfactants with larger hydrophobic domains at the lower temperature, and thus CMC is not reached before the surfactant precipitates out of the solution. As the head group for most of the anionics was either a sulfate or sulfonate group (many with additional oxygen or nitrogen atoms in the head group), the majority of the variation seen in the data set was in the hydrophobic domain. Again, we were able to

come up with good three descriptor relationships. The first relationship is for the overall data set of 119 structures (Figure 2-3),

$$\log_{10}\text{CMC} = (1.89\pm0.11) - (0.314\pm0.010)\textit{t-sum-KH0} - (0.034\pm0.003)\textit{TDIP} - (1.45\pm0.18)\textit{h-sum-RNC} \quad [4]$$
$$R^2 = 0.940,\ F = 597,\ s^2 = 0.0472,\ N = 119$$

and the second is for a subset of 68 where the head groups were only sulfates and sulfonates.

$$\log_{10}\text{CMC} = (2.42\pm0.07) - (0.537\pm0.009)\ \textit{KH1} - (0.019\pm0.002)\ \textit{KS3} + (0.096\pm0.005)\ \textit{HGP} \quad [5]$$
$$R^2 = 0.988,\ F = 1691,\ s^2 = 0.0068,\ N = 68$$

This second relationship (Eq. 5) had a much higher correlation coefficient and smaller standard error in the predicted CMC value compared to the literature value. Both of these relationships have just two descriptors calculated from the hydrophobic tail, and one for the hydrophilic head group. In Eq. 4 the head group contribution is represented by the dipole moment of the molecule (this accounts for the position of the charged head group relative to the center of mass of the molecule) and in Eq. 5 the contribution is captured in the head group position, which is the number of the carbon where the head group is attached. The scatter plot for Eq. 4 can be seen in Figure 2-4.

The occurrence of the Kier and Hall molecular connectivity indices (of order 0 and 1) in the regressions for both the nonionic and anionic surfactants is important. In all three regressions, this is the dominant descriptor. It has been noted [Kier and Hall, 1976] that this descriptor correlates highly to both molecular volume and molecular surface area. This is a

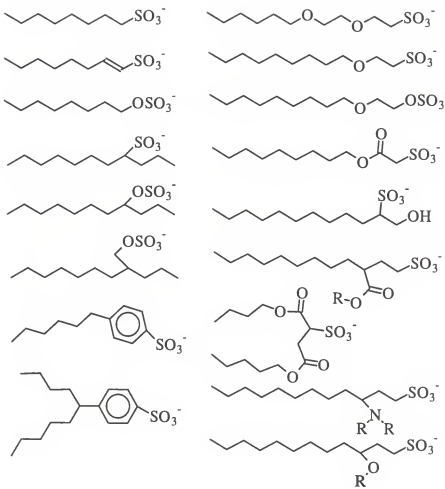

Figure 2-3. Structures of the surfactants included in the anionic CMC correlations.

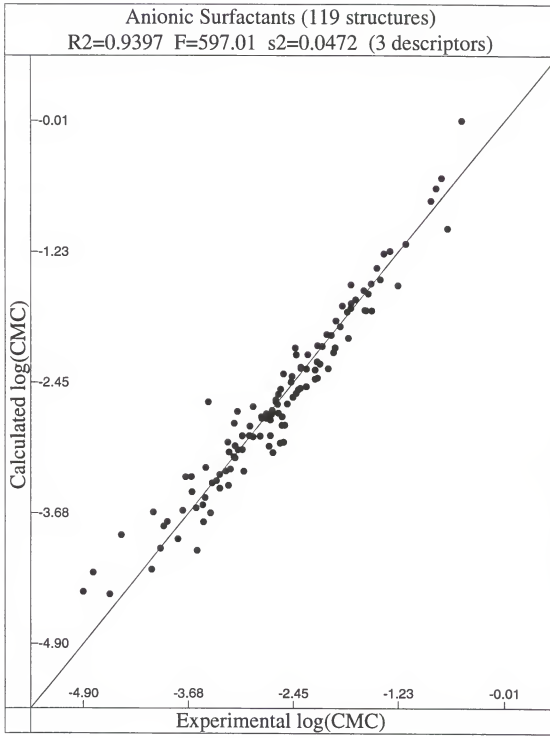

Figure 2-4. Scatter plot for calculated vs. experimental anionic CMC for 119 surfactants, using three descriptors.

satisfying result, as the qualitative picture for the solubilization of a hydrophobic entity such as the surfactant tail is that the water must form a cage around the solute. This cage results in water forming strained or broken hydrogen bonds, which are energetically unfavorable. These water molecules at the interface are also more restricted in their motion and orientational freedom, thus suffering a entropically unfavorable situation also. Both of these unfavorable situations would scale with the surface area of the interaction. Thus for hydrophobic solutes it is expected that the solubility or CMC (basically the solubility of the tail) would scale with the surface area of the hydrophobic domain. The two K&H indices correlate with surface area ($R^2 \approx 0.97$) and thus corroborate this qualitative picture of micellization.

Temperature Dependence of Anionic CMC

In order to allow the inclusion of more anionic surfactants in the QSPR study described in the previous section and in Huibers et al. [1996c], it was important to try to develop some scaling laws for CMC as a function of temperature. This would also be useful in applying the QSPR modeling results to other temperatures. There is various experimental evidence for a parabolic relationship between the critical micelle concentration (CMC) and temperature for anionic surfactants. The temperature dependence is the result of entropic and enthalpic contributions from both the surfactant and the surrounding water. There is a minimum in CMC around 25°C, although the minimum temperature appears to be dependent on the size of the surfactant molecule. A general model is proposed for the

temperature dependence of anionic surfactant CMC in the 10 to 70°C range, taking into account the size of the hydrophobic domain.

While not as temperature dependent as the nonionic surfactants, the CMC of anionic surfactants clearly has a temperature dependence. This dependence has been described as a complex competition between enthalpic and entropic effects, both of the surfactant molecules and the water surrounding them. Several thermodynamic models exist, though none are at the level where accurate temperature dependence can be predicted. Thus, it would be of value to define an empirical model for the temperature dependence of anionic surfactant CMC. This model should have certain features, such as a parabolic dependence of the CMC with temperature, and a shift in the minimum CMC with surfactant structure. It should also be simple to calculate and should be valid for a wide range of structural variation among the anionic surfactants.

Measurements of CMC for a large number of anionic surfactants have been performed by many research groups over the last several decades. The majority of these measurements were made at either 25 or 40°C. It would be valuable to have general scaling laws to make CMC estimates at other temperatures. A general model can be used to estimate CMC in the range of 10-70°C, given a single CMC value in that range. Care must be taken at the lower end of this range with respect to the Krafft point of the surfactant of interest. Below the Krafft point, the CMC may not be reached, as the surfactant will precipitate out of solution before sufficient concentration is achieved for micelles to be

formed. For a means of predicting Krafft point from molecular structure, some models have been developed by Gu and Sjöblom [1991; 1992].

A parabolic model in the form of Eq. 6 has been proposed by van Os et al. [1987; 1988] for the sodium p-(x-decyl)benzenesulfonates and p-(3-alkyl)benzenesulfonates.

$$\log CMC = a + bT + cT^2 \qquad [6]$$

This functional form is an excellent fit to the data, but the three coefficients must be calculated for each surfactant structure.

Data and Methodology

Sources of CMC data. The CMC values for the various anionic surfactants were taken from the compilation by van Os et al. [1993] and Mukerjee and Mysels [1971]. A total of 103 CMC measurements for 16 different structures are summarized in Table 2-1, along with the Krafft points and estimated carbon number. All alkylbenzenesulfonate structures are substituted at the para position of the ring.

In order to develop the most accurate data set, CMC values were only used from researchers who conducted measurements at several temperatures. It is difficult to compare measurements at different temperatures from different researchers, as the systematic error in CMC between labs is often greater than the expected change due to temperature. CMC data with at least four temperature values have been measured by Klevens [1948] (C_{10}) for the linear alkyl sodium sulfonates, Rouviere et al. [1983] (C_7, C_8) and van Os et al. [1988] (3-C_9, 3-C_{12}) [1987] (5-C_{10}) for the alkyl sodium benzenesulfonates, and Moroi et al. [1975] (C_8, C_{10}, C_{12}, C_{14}) and Rassing et al. [1973] (C_8) for the linear alkyl sodium sulfates.

Table 2-1. CMC values (mM) for 16 structures, as a function of temperature, and Krafft points (°C).

T(°C)	C7 BSO3	C8 BSO3	3C9 BSO3	2C10 BSO3	3C10 BSO3	5C10 BSO3	3C12 BSO3	6C12 BSO3
10								
15			10.43			8.31	1.99	2.10
20			10.40	4.35	6.03	8.14	2.16	2.29
25	22.8	11.4	10.27	4.63	6.02	8.01	2.22	2.38
30	24.0	12.0	10.41	4.86	6.04	8.13	2.35	2.50
35	25.0							
40	26.2	12.7	10.80	4.98	6.31	8.98	2.48	2.60
45	27.4							
50		13.5	11.64	5.50	6.78	9.06	2.69	
55								
60		14.7	12.84	6.07	7.39	10.34	3.04	
65								
70		15.8	14.13	6.92	8.35	11.39	3.30	
KP	9	18.5	<0	22	4	<0	14	

T(C)	C8 SO3	C10 SO3	C8 SO4	C10 SO4	C12 SO4	C14 SO4	2C14 SO4	4C14 SO4
10			141.6	35.0	8.66			
15			136.8	33.9	8.43			
20			133.3	33.3	8.25			
25	155	41	130.2	33.0	8.16	2.05	3.27	5.12
30			131.8	32.9	8.24	2.08		
35		42	133.7	33.3	8.38	2.14		
40	162		135.9	33.7	8.56	2.22		
45		45	138.6	34.5	8.85	2.31		
50	177		142.1	35.5	9.18	2.43		
55		49	146.6	36.9	9.61	2.59		
60							4.04	5.85
65		55						
70								
KP		22	<0	<0	8	21	11	

Note: Abbreviations for the structures are BSO3 (benzenesulfonate), SO4 (sulfate), Cn (linear alkyl fragment of n carbons) and mCn (branched alkyl fragment, n carbons, substitution at m carbon).

One of the available data sets was omitted (Kovtunenko) which showed contrary temperature dependence to measurements of other researchers and three CMC values (3-C_{12-15}, 3-C_{20}, 2-C_{10-20}) at low temperatures [van Os et al., 1988] were omitted that deviated strongly from the empirical relationships, and were determined statistically (*t* test) to be anomalous and omitted from the coefficient calculations.

Statistical analysis. The determination of the optimum descriptor coefficients and the calculation of statistical parameters for the multiple regression were done using the CODESSA program [Katritzky et al., 1994]. This program has been designed for discovering general quantitative structure-property relationships (QSPR) and allows quick comparison of several different proposed models.

Results and Discussion

The functional form of the proposed model (Eq. 7) takes the form of a partition function, with a multiplicative factor (G) on the order of one calculated used to scale a known CMC value to another temperature. The right hand side of Eq. 8 is the logarithm (base 10) of the factor G. The difference of the logarithms is equivalent to the ratio of the CMC values.

$$CMC_T = CMC_{25}\, G(Nc,T) \qquad [7]$$

$$\log CMC_T - \log CMC_{25} = a_0 + a_1T + a_2T^2 + a_3N_cT + a_4N_cT^2 \qquad [8]$$

or

$$\log [CMC_T/CMC_{25}] = a_0 + (a1 + a_3N_c)T + (a_2 + a_4N_c)T^2$$

Temperature values (T) have units of Kelvin, CMC has units of 10^{-3} moles/liter (mM), and N_c is the alkane carbon number of the surfactant. Estimation of N_c for other than linear alkyl sodium sulf(on)ates will be discussed later.

The best fit and statistical parameters of the coefficients can be seen in the equations below. Models with and without alkyl chain length dependence are presented.

$$\log G(N_c,T) = 6.549 - 4.401\times10^{-2}\,T + 7.400\times10^{-5}\,T^2$$
$$r = 0.959,\ F = 420,\ s^2 = 0.0002,\ N = 76$$
Model One. No molecular size dependence.

$$\log G(N_c,T) = 5.382 - 3.305\times10^{-2}\,T + 5.042\times10^{-5}\,T^2 - 2.923\times10^{-4}\,N_cT + 9.762\times10^{-7}\,N_cT^2$$
$$r = 0.982,\ F = 470,\ s^2 = 0.0001,\ N = 76$$
Model Two. Molecular size dependence.

In these equations, r is the correlation coefficient, F is the F-statistic representing the quality of the model in fitting nonrandom changes in the data, s is the standard error, and N is the number of data points used in the calculation.

The quality of the fit of the model equations can be seen graphically in Figure 2-5. The calculated results clearly show both trends apparent in the data: the change in the parabolic fit, and a shift in the temperature of the minimum CMC value, with a change in the size of the hydrophobic domain of the surfactant. The model is a good fit for a wide variety of anionic surfactant structures, including linear, branched, and aromatic sulfates and sulfonates.

Estimation of carbon number. The carbon number (N_c) is originally defined as the number of carbons in the linear alkyl portion of a surfactant. It has been demonstrated that the logarithm of CMC is proportional to N_c. For the linear alkyl sulfates and sulfonates, the

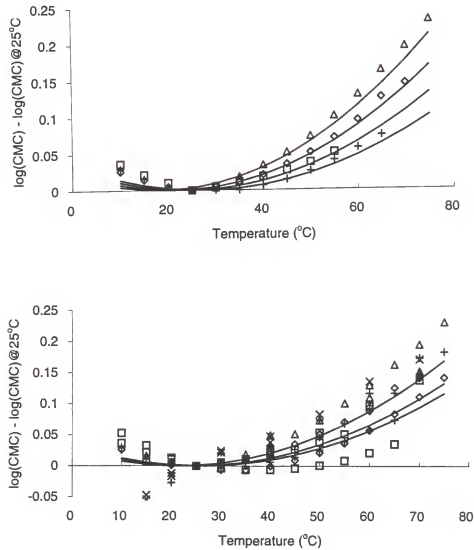

Figure 2-5. Normalized CMC vs. temperature for: a) sulfates and b) sulfonates.

following equation [Rosen, 1976] describes this relationship between CMC and N_c at 25°C. Coefficient values for Eq. 9 at temperatures are tabulated by Rosen [1989].

$$\log CMC_{25} = 1.51 - 0.30\,N_c \qquad [9]$$

A problem arises when the hydrophobic structure is more complex than a linear carbon chain. For branched and aromatic structures, an 'effective' carbon number can be defined, which when used in Eq. 8 predicts the CMC correctly. It is well established that branching and aromatic ring structures have lower effective carbon numbers than the actual number of carbon atoms present in the molecule.

Two methods are proposed for the estimation of carbon number for use in Eq. 8. The first is simply using a known CMC value of the surfactant and Eq. 10 to estimate N_c. Equation 10 is simply Eq. 9 solved for N_c.

$$N_c = 5.03 - 3.33 \log CMC_{25} \qquad [10]$$

A second approach uses a topological index, the ${}^0\chi^v$ developed by Kier and Hall [1976]. This approach assigns a contribution to each carbon atom based on its valence and number of attached hydrogens and sums the contributions of all carbon atoms in the hydrophobic domain of the surfactant.

$${}^0\chi^v = \Sigma\,(\delta^v_i)^{-1/2} \text{ where } \delta^v_i = (Z^v_i - H_i)/(Z_i - Z^v_i - 1) \qquad [11]$$

Z_i is the total number of electrons in the *i*th atom, Z^v_i is the number of valence electrons, and H_i is the number of hydrogens directly attached to the *i*th atom. For hydrocarbon chains, valence delta values are ($(\delta^v_i)^{-1/2}$) 1.0 for CH_3, 0.707 for CH_2, 0.577 for CH, 0.500 for C, and 3.308 for a phenyl group with two substitutions. For fluorocarbons, values are 1.634 for

a CF_3 group and 1.256 for a CF_2 group. Given the calculated value of ${}^0\chi^v$ for the hydrophobic domain, the carbon number can be estimated by the following equation.

$$N_c = 1.414\ {}^0\chi^v - 0.414 \qquad [12]$$

The applicability of the molecular connectivity index for predicting the effect of the hydrophobic domain on CMC has been established by Huibers et al. [1996b]. The value of this approach is that it is independent of temperature and does not require a CMC value for determination, as it is calculated exclusively from molecular structure.

Conclusion. An empirical model has been developed for the temperature dependence of CMC for anionic surfactants. A high correlation was found for this model ($r = 0.982$) given a set of 103 CMC values for 16 surfactants, representing linear, branched, and aromatic sodium sulfates and sulfonates, at temperatures in the range of 10 to 70°C.

Nonionic Surfactant Cloud Point

With the success of applying the QSPR methodology to the prediction of CMC, we attempted another surfactant physical property. For the nonionic surfactants, a phase transition is sometimes observed upon heating of the surfactant solution. A transition occurs from a single phase micellar solution to surfactant rich and surfactant poor phases. This has been attributed to the weakening of the hydrogen bonds necessary for solubilizing the hydrophilic domain of the molecule. Again, details of this effort are described by Huibers et al. [1996d], and a brief summary follows.

Similar to the Klevens rule for CMC prediction, the relationships among the cloud point, the carbon number, and the ethylene oxide number have long been known. For the

data considered here, we recalculate the equation, including error terms and other statistical parameters, for 46 linear alkyl ethoxylates:

$$CP = (87.1\pm3.3)\ \log EO\# - (5.78\pm0.38)\ C\# - (40.7\pm5.2)$$
$$R^2=0.943,\ F=355,\ s^2=40.4,\ N=46 \qquad [13]$$

Given the success of the topological descriptors in accounting for the variation of the hydrophobic domains for the prediction of CMC, we believed that the same method would be successful for the prediction of cloud point for a wide variety of hydrophobic structural features. For 62 structures (Figure 2-6), the best relationship for cloud point (^oC) was as follows:

$$CP = (-264.\pm17.) + (86.1\pm3.0)\ \log EO\#$$
$$+ (8.02\pm0.78)\ {}^3\kappa - (1284\pm86)\ {}^0ABIC - (14.26\pm0.73)\ {}^1SIC$$
$$R^2=0.937,\ F=211,\ s^2=42.3,\ N=62 \qquad [14]$$

This regression was found to fit a range of linear alkyl, branched alkyl, cyclic alkyl, and alkylphenyl ethoxylates with a standard error of 6.5 ^oC. The scatter plot for this correlation can be found in Figure 2-7. Three descriptors account for the hydrophobic structure variation. In Figure 2-8, we show graphically the specific values of the descriptors for the different hydrophobic fragments, showing how they account for different structural features with different weightings. The hydrophilic variation is accounted for by the logarithm of the ethylene oxide number, which is the descriptor used in the Klevens-like relationships. Although different hydrophilic descriptors were tried, none were noticeably superior to this descriptor.

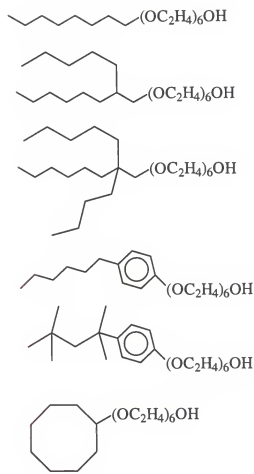

Figure 2-6. Structures of the surfactants included in the nonionic cloud point correlations.

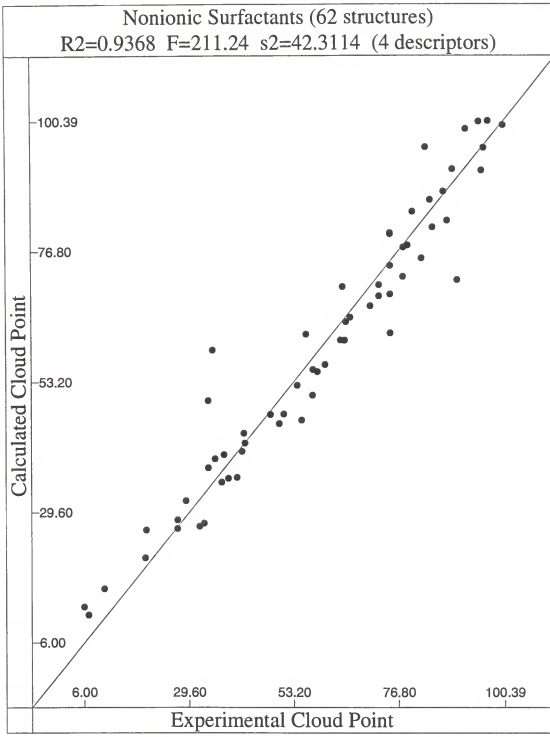

Figure 2-7. Scatter plot for calculated vs. experimental nonionic cloud point for 62 surfactants, using three descriptors.

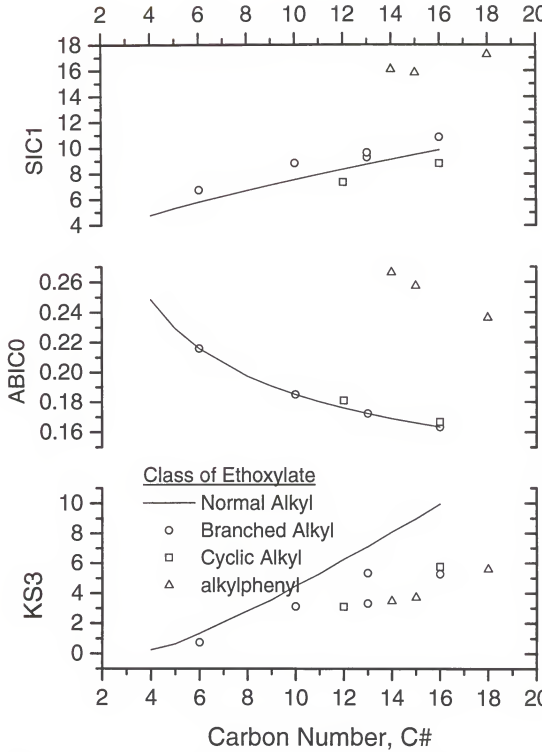

Figure 2-8. Topological descriptor values vs. carbon number for the different hydrophobic structures in the cloud point correlation.

Anionic Surfactant Krafft Point

The Krafft point is an important physical property of ionic surfactants, establishing the minimum temperature at which a surfactant can be used. The solubility of ionic surfactants in water is influenced by temperature, and the Krafft point is the temperature at which a hydrated surfactant crystalline solid melts and forms micelles in solution [Krafft and Wiglow, 1895]. Below this temperature, there are surfactant monomers in solution, in equilibrium with the solid, but the concentration is below CMC so the solubility is limited. If a micellar solution is cooled below the Krafft point, it will precipitate out of solution and the detergency of the solution will be lost.

Several aspects of the influence of molecular structure on Krafft point are known. Gu and Sjöblom [1991, 1992] established that for a wide variety of anionic surfactants, the Krafft point increases on average 5.5°C for each methylene (-CH_2-) group in the hydrophobic tail. Also, for the one case available, there is an average decrease of 9°C per ethylene oxide residue (-CH_2CH_2O-) in the hydrophilic head group. Finally, no systematic formula could be developed for the influence of the head group, and so they developed a table of constant terms for the contributions from different head groups. As can be seen in these constants and also noted by others [Matsuki et al., 1996], the counterion plays a significant role and can change the Krafft point by over 10°C. It is interesting to note that as it has also been established that there is a linear relationship between the logarithm of CMC and the carbon number, it follows that there is a linear relationship between the Krafft point and log(CMC) for a given homologous series of surfactants.

Results. In order to study the influence of the molecular structure on Krafft point, it is desirable to develop the largest possible set of surfactants with reliable Krafft point measurements. Due to the limited amount of Krafft point data in the literature, this effort focused on anionic surfactants that were sodium salts. Sodium is the most prevalent counterion, and if structure-property relationships can be generally developed for this subset, it provides a good base to expand the study to examine specific counterion effects. Besides the anionic surfactants, there are extremely few published Krafft point values for cationic or zwitterionic materials.

Included in this investigation are 44 linear alkyl sulfates and sulfonates, branched alkylbenzene sulfonates, perfluorinated alkyl sulfonates and acids, and sulfates and sulfonates with an ether or ester linkage to the hydrophobic tail (Figure 2-9). Sources for the Krafft point data include the texts of Rosen [1989], van Os et al. [1993], and additional data from Püschel and Todorov [1968], etc. and listed in Table 2-3. For each structure, descriptors were calculated for the entire molecule, as well as for the hydrophobic and hydrophilic fragments, as described in previous sections. In the regressions that were chosen as statistically the best, certain hydrophobic fragment descriptors appeared often, but no hydrophilic fragment descriptors were chosen for the final regressions. The influence of the head group was handled by whole molecule descriptors.

For the 44 surfactants in Table 2-2, a regression with a standard error of 5.3°C has been developed, using four descriptors,

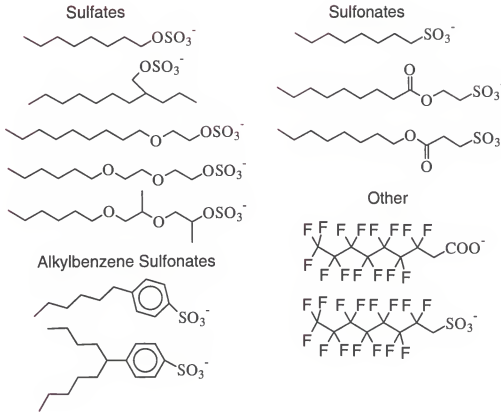

Figure 2-9. Structures of the surfactants included in the Krafft point correlations.

Table 2-2. Structure names for the 44 surfactants included in the Krafft point correlations.

Name	KP (°C)
C10SO4	8
C11SO4	7
C12SO4	16
C13SO4	20.8
C14SO4	30
C15SO4	31.5
C16SO4	45
C18SO4	56
C10SO3	22.5
C12SO3	38
C14SO3	48
C16SO3	57
C17SO3	62
C18SO3	70
C07BSO3	9
C08BSO3	18.5
2C10BSO3	22
2C12BSO3	31.5
2C14BSO3	46
2C16BSO3	54.2
2C18BSO3	60.8
3C10BSO3	4
3C12BSO3	14
2C13CSO4	11
2C15CSO4	25
2C17CSO4	30
C16E1SO4	36
C16E2SO4	24
C16E3SO4	19
C18E3SO4	32
C18E4SO4	18
C08AESO3	0
C10AESO3	8.1
C12AESO3	24.2
C14AESO3	36.2
C08PSO3	0
C10PSO3	12.5
C12PSO3	26.5
C14PSO3	39
C16P2SO4	19
C18P2SO4	31
CF7SO3	56.5
CF8SO3	75
CF7COO	8

Note: nCm is n-substituted Cm, B is phenyl [-C_6H_4-], E# is ethoxylate [-$(OC_2H_4)_{\#}$-], A is [-C(O)-], P is [-$OC(O)C_2H_4$-], P2 is [-$(OCH_2CH(CH_3))_2$-]. All carbons are hydrogenated except fluorinated cases (CF).

$$KP = (231\pm15) + (3.02\pm0.23)f\text{-}KS1 - (41.7\pm3.2)f\text{-}AIC2 + (20.6\pm2.2)NDB - (231\pm15)AVO \quad [15]$$

$$R^2=0.932,\ F=134,\ s^2=28.1,\ N=44$$

where *f-KS1* is the Kier shape index of first order, *f-AIC2* is the average information content of second order, *NDB* is the number of double bonds, and *AVO* is the average valence of an oxygen atom. The scatter plot of this correlation can be seen in Figure 2-10.

In an attempt to find better correlations for more limited sets of structures, the structures with linking ether and ester bonds between the head group and tail were eliminated, resulting in 28 linear branched, aromatic and perfluorinated sulfates and sulfonates. Using three descriptors (because of the limited number of structures), a regression of similar quality was achieved, with $R^2=0.947$, $F=143$, $s^2=26.1$, $N=28$, which was not a useful improvement on the regression of the 44 structures. As it is well established that the linear alkyl compounds have a strong linear relationship with chain length, a regression was developed for just the 16 linear alkyl and perfluorinated sulfates and sulfonates, resulting in the following:

$$KP = -(56.6\pm3.5) + (6.39\pm0.44)f\text{-}R2 + (1.09\pm0.57)f\text{-}KH2 \quad [16]$$

$$R^2=0.986,\ F=466,\ s^2=7.46,\ N=16$$

where *f-R2* is the Randic index of second order for the hydrophobic fragment, and *f-KH2* is the Kier and Hall molecular connectivity index of second order for the hydrophobic fragment. This error of 2.7°C is probably the best accuracy achievable, given the experimental error of the measurements, and the difference between researchers.

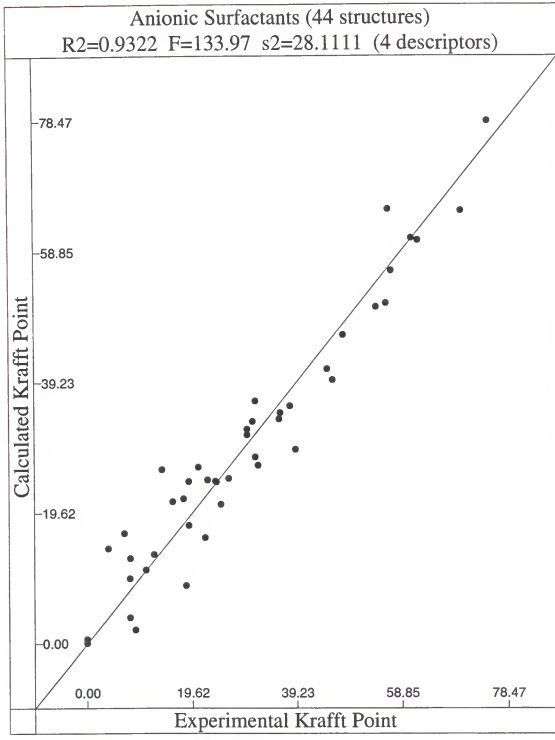

Figure 2-10. Scatter plot for calculated vs. experimental Krafft point for 44 surfactants, using four descriptors.

Conclusions. Kier and Hall [1976] noted the difficulty of achieving good correlations with melting point data, as compared to boiling point data, as the melting point transition involves ordering and more complex intermolecular interactions that must be accounted for, when compared to the boiling point transition. As the Krafft point is basically a melting phenomenon of hydrated surfactant crystals, it was expected that the correlations would not be as good as the CMC correlations. The results achieved, though, were of similar quality to the CMC correlations, although the data set was somewhat limited. From this work it appears that Krafft point can be estimated to within several degrees for sodium salts of anionic surfactants, given only the molecular structure. As the influence of the counterion is known to be significant, a systematic study of the counterion effect would make this a more complete predictive tool.

Molecular Volume of Alkanes and Surfactant Hydrophobic Tails

From the CMC investigations [Huibers et al., 1996b; 1996c], and from examining other works on aqueous solubility [Yalkowsky and Banerjee, 1992], it became clear that the knowledge of molecular volume and surface area of hydrophobic domains plays an important role in correlations of several molecular properties. For a hydrophobic molecule or hydrophobic domain of a surfactant, solubilization in water involves the formation of a 'cage' of hydrogen bonded water around the molecule with which water cannot form any specific interactions. Without these favorable specific interactions, such as polar-polar or hydrogen bonding interactions, the unfavorable interactions should be

proportional to the surface area of contact. The molecular volume often appears to correlate well because it correlates highly to the molecular surface area.

Previous volume prediction methods. For theoretical studies of surfactant self assembly, a means of calculating the geometric aspects of the surfactant molecules is necessary. Geometrical parameters such as the head group surface area, tail length and tail volume have been applied to models that describe the optimal aggregation state, such as the Israelachvili and coworkers [1976, 1992] packing parameter. Tanford [1972] provided the following equation for his model of the optimum aggregation number of micelles to have a spherical shape, given the tail length and volume,

$$v = 27.4 + 26.9\, N_c \qquad [17]$$

where v is the tail volume in $Å^3$ and N_c is the number carbons in the linear alkane tail. This equation has been referred to in many studies since, and most micellar models only consider surfactants with linear alkyl chains for the hydrophobic domain. In order to allow future models to be more general, volume calculation techniques need to be improved to allow for calculations on branched, aromatic, and fluorinated alkyl tails.

The most direct and simple means of estimating volume from group contribution methods, where each molecular subgroup is assigned an additive contribution. Tanford's [1972] method is just that, with 26.9 $Å^3$ assigned to the CH_2 group and 54.3 $Å^3$ assigned to CH_3. van Krevelen [1990] collected and compared many previous efforts at group contribution methods for predicting molar properties.

While the group contribution methods provide a good estimate, it cannot be exact as molecular volume is not strictly an additive property, but rather a constitutive property, which is defined as having a dependence on the arrangement of constituent atoms. To address this molecular connectivity dependence, several different approaches have been used, as summarized in Table 2-3.

Table 2-3. Methods for estimating molecular volume.

- group contribution
- sum of overlapping van der Waals spheres
- group contribution corrected for number of gauche conformations
- topological indices (molecular connectivity indices)

The method of overlapping van der Waals spheres is a means of calculating volume given only the van der Waals radii of the constituent atoms and the bond lengths. The molecular is simply the sum of the atomic volumes, minus the overlap in the spheres, as the bond lengths are always less than the sum of radii between two atoms. To be more accurate, precise methods have been developed assuming that no more than three spheres overlap at any one point in space.

One problem with the overlapping spheres method is that it does not accurately account for the void space between atoms, unreachable by solvent or neighboring molecules, that realistically makes up part of the molecular volume. Edward et al. [1978] developed a method for calculating the partial molal volumes of alkanes, accounting for these dead spaces by determining the number of gauche arrangements in the alkane. His

formula for the partial molal volumes for linear and branched alkanes in carbon tetrachloride was

$$V^o = 26.85\ CH_3 + 17.36\ CH_2 + 10.35\ CH + 3.40\ C + 11.61 - 2.5\ Z_g \quad [18]$$

where V^o is the partial molal volume in mL/mol, and Z_g is the Pitzer steric partition function. It is interesting to note that many of these group contribution methods have a constant term, in this case 11.61 mL/mol, which is called the covolume, initially recognized by Traube [1899]. There has been much debate as to the meaning of this covolume, and it poses a compromise to the group contribution methods, as it depends on no group, and cannot be eliminated without making the regressions for molecular volume worse.

Application of topological indices. The method we consider here for calculation of molecular volume is that of Kier and Hall [1976], using their topological indices, the molecular connectivity indices, for predictions. This method also has the desirable property of accounting for the arrangement of the constituent atoms. As a data driven approach, where relationships between the topological indices and property values are developed, it allows direct prediction of molecular volume in the liquid phase.

In the initial text of Kier and Hall [1976] relationships related to the molecular volume were investigated, including liquid density and molar refraction. The molecular volume (V^o) can be derived from the molecular weight (M) and the liquid density (ρ) by $V^o = M/\rho$. The best relationship for 82 linear and branched alkanes was

$$\rho = 0.7348 - 0.2929\ (^1\chi)^{-1} + 0.0030\ ^3\chi_P \quad [19]$$
$$R^2=0.979,\ s=0.0046,\ N=82$$

The authors developed a second relationship, using only the density numbers where they were assured of values with five or six significant figure accuracy, and arrived at a five descriptor model with $R^2 = 0.994$, s = 0.0024, N = 46. Density relationships were also developed for 40 alcohols, 13 ethers, and 20 aliphatic acids. Molar refraction (R_m) relationships were developed for 70 alkylbenzenes, where R_m is defined as

$$R_m = V_o(n^2-1)/(n^2+2) \qquad [20]$$

where n is the index of refraction. Again, an excellent formula could be found with just two descriptors:

$$R_m = 6.265 - 7.548\ {}^1\chi^v + 2.501\ {}^2\chi \qquad [21]$$
$$R^2=0.997,\ s=0.270,\ N=70$$

In their later text [Kier and Hall, 1986] they analyze the partial molal volume data from Edward et al. [1978], whose gauche arrangement correction methods were described in a previous section, to arrive at the following formula:

$$V_o = 39.79 + 24.87\ {}^1\chi + 11.86\ {}^2\chi + 2.844\ {}^4\chi_{pc} \qquad [22]$$
$$R^2=0.999,\ s=1.17,\ F=86615,\ N=37$$

The standard error of 1.17 is less than 1% of the molar volume, which ranges from 116 to 566 mL/mol for the data set. This method provides good estimates for alkanes with the exact same number and type of groups present, such as the dimethylpentanes and dimethylheptanes. In these classes there is a range of molar volumes, depending on the location of attachment of the two methyl groups, and different volumes for each unique structure are predicted, unlike the group contribution methods, which would predict the same volume for these different isomers.

Results. For modeling the molecular volume of surfactant tails, it is necessary to include more structural variation than just the linear and branched alkanes. We add alkenes, alkylbenzenes, fluorobenzenes, and perfluorinated alkanes to the set of structures considered, for a total of 78 structures (Table 2-4). The CODESSA program [Katritzky et al., 1994] is used to obtain

$$V_o = (25.2\pm0.7) + (5.05\pm0.05)N_H + (0.0931\pm0.0008)\ G \quad [23]$$
$$- (136\pm8)\ RNB - (6.0\pm0.5)\ {}^3\chi$$
$$R^2=0.999,\ s=1.32,\ F=21124,\ N=78$$

where N_H is the number of hydrogen atoms, G is the gravitation index (all bonds), RNB is the relative number of benzene rings, and ${}^3\chi$ is the Kier and Hall molecular connectivity index of third order. Here we come up with an excellent correlation (Figure 2-11), with a very small standard error, for a much more diverse data set than for the alkanes previously studied. We can do this by considering many more types of molecular descriptors than just the topological descriptors. Although the geometric, electrostatic, and quantum-chemical descriptors available in the CODESSA program did not show up in the best correlations, some simple constitutional descriptors (N_H and RNB) allowed for the development of an excellent regression equation. If just topological descriptors were employed, the best four descriptor correlation using Kier and Hall molecular connectivity indices along with Kier shape indices had statistical parameters of R^2=0.991, s=4.29, F=1992, N=78.

It is interesting to note that the best individual descriptor is the Kier and Hall molecular connectivity index of zero order, resulting in a good correlation of R^2=0.97, in

Table 2-4. Structure names for the 78 hydrocarbons and fluorocarbons used for the determination of molecular volume.

M.V. (cm^3/mol)	M.W. (g/mol)	Density (g/cm^3)	Structure Name
116.4	72.15	0.6197	2-methylbutane
115.2	72.15	0.6262	n-pentane
130.7	86.18	0.6594	n-hexane
146.6	100.21	0.6838	n-heptane
162.6	114.23	0.7025	n-octane
178.7	128.26	0.7176	n-nonane
194.9	142.29	0.7300	n-decane
227.5	170.34	0.7487	n-dodecane
114.6	104.14	0.9090	styrene
89.1	78.12	0.8765	benzene
106.3	92.13	0.8669	toluene
139.1	120.20	0.8642	1,3,5-trimethylbenzene
149.0	134.21	0.9010	1,2,3,4-tetramethylbenzene
94.0	96.11	1.0225	fluorobenzene
97.6	114.09	1.1688	1,4-difluorobenzene
115.0	186.06	1.6184	hexafluorobenzene
143.5	100.21	0.6982	3-ethylpentane
144.2	100.21	0.6951	2,3-dimethylpentane
144.5	100.21	0.6933	3,3-dimethylpentane
145.9	100.21	0.6868	3-methylhexane
147.7	100.21	0.67869	2-methylhexane
148.7	100.21	0.6739	2,2-dimethylpentane
149.0	100.21	0.6727	2,4-dimethylpentane
157.0	114.23	0.7274	3-ethyl-3-methylpentane
157.3	114.23	0.7262	2,3,3-trimethylpentane
158.8	114.23	0.7193	3-ethyl-2-methylpentane
158.8	114.23	0.71923	3,4-dimethylhexane
158.9	114.23	0.7191	2,3,4-trimethylpentane
159.5	114.23	0.7161	2,2,3-trimethylpentane
160.4	114.23	0.71214	2,3-dimethylhexane
160.9	114.23	0.71	3,3-dimethylhexane
161.8	114.23	0.70583	3-methylheptane
162.1	114.23	0.70463	4-methylheptane
163.1	114.23	0.70036	2,4-dimethylhexane
163.7	114.23	0.6979	2-methylheptane
164.3	114.23	0.69528	2,2-dimethylhexane
164.7	114.23	0.69354	2,5-dimethylhexane
165.1	114.23	0.6918	2,2,4-trimethylpentane

Table 2-4 (continued).

M.V. (cm^3/mol)	M.W. (g/mol)	Density (g/cm^3)	Structure Name
175.6	128.25	0.7304	3,3-dimethylheptane
176.4	128.25	0.727	2,3-dimethylheptane
178.2	128.25	0.7198	2,5-dimethylheptane
178.5	128.25	0.7185	2,2,4,4-tetramethylpentane
179.2	128.25	0.7158	2,4-dimethylheptane
178.2	128.26	0.7199	4-methyloctane
180.5	128.26	0.7107	2-methyloctane
188.4	140.27	0.7445	cis-5-decene
189.3	140.27	0.7408	1-decene
189.5	140.27	0.7401	trans-5-decene
192.9	142.28	0.7377	2,3-dimethyloctane
193.5	142.28	0.7354	3-methylnonane
194.2	142.28	0.7326	5-methylnonane
194.3	142.28	0.7323	4-methylnonane
194.6	142.28	0.7313	2,6-dimethyloctane
195.4	142.28	0.7281	2-methylnonane
196.5	142.28	0.7240	2,7-dimethyloctane
210.6	156.31	0.7422	3-methyldecane
212.1	156.31	0.7368	2-methyldecane
222.0	168.33	0.7584	1-dodecene
243.7	184.37	0.7564	tridecane
260.1	198.40	0.7628	tetradecane
276.4	212.42	0.7685	pentadecane
292.8	226.45	0.7733	hexadecane
327.6	254.51	0.7768	octadecane
224.3	388.7	1.7333	perfluoroheptane
132.5	118.18	0.8920	allylbenzene
139.4	120.20	0.8620	propylbenzene
154.9	134.22	0.8665	tertbutylbenzene
155.7	134.22	0.8621	secbutylbenzene
156.1	134.22	0.8601	butylbenzene
157.3	134.22	0.8532	isobutylbenzene
170.2	148.25	0.8710	1-butyl-2-methylbenzene
172.1	148.25	0.8612	1-tertbutyl-4-methylbenzene
172.6	148.25	0.8590	1-butyl-3-methylbenzene
172.7	148.25	0.8586	1-butyl-4-methylbenzene
172.7	148.25	0.8585	pentylbenzene
205.8	176.30	0.8567	heptylbenzene
238.1	204.35	0.8584	nonylbenzene
288.2	246.43	0.8551	dodecylbenzene

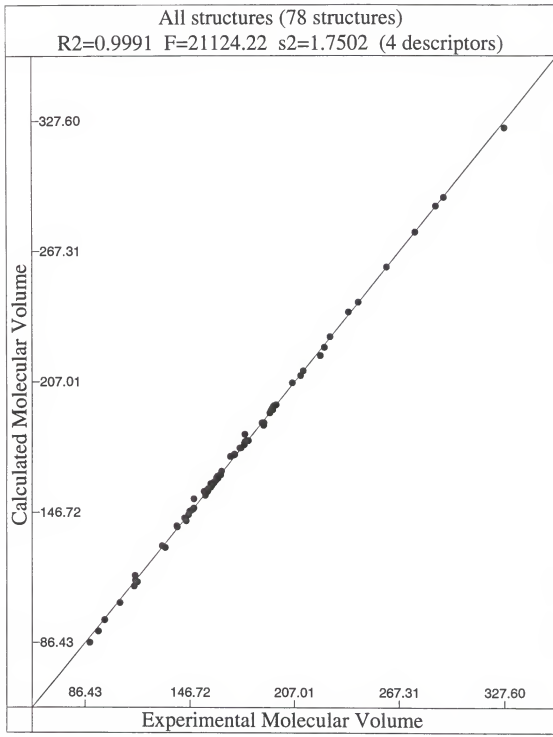

Figure 2-11. Scatter plot for the four descriptor regression of calculated to experimental molar volume of 78 diverse alkanes and alkenes.

accordance with the comments of Kier and Hall [1976] that the zero and first order indices correlate most highly with molecular volume and surface area (Figure 2-12).

$$V_o = (4.7\pm3.4) + (23.81\pm0.47)\ {}^0\chi \qquad [24]$$
$$R^2=0.971,\ s=7.48,\ F=2572,\ N=78$$

This result is quite reasonable when it is considered that ${}^0\chi$ is calculated from individual contributions of each atom, where the contributions are weighted by the number of valence electrons [Huibers et al., 1996c]. Thus, a methyl group (CH_3) will have a larger group contribution than a methylene (CH_2), which will have a larger contribution than a methine (CH), etc. Also, as ${}^0\chi$ is calculated from the (hydrogen free) carbon backbone, the fluorinated groups have much larger contributions then hydrogenated groups (a CF_2 group is 1.7 times the contribution of a CH_2 group), as fluorines are counted where hydrogens are not in the index contributions [Huibers et al., 1996c]. Also, the error on the constant term is large with respect to the coefficient, indicating that ${}^0\chi$ is practically directly proportional to the molecular volume. By examining the residual volume plot (calculated minus experimental volume) for this descriptor, the structures which have volumes most influenced by steric factors are highlighted.

The ${}^0\chi$ correlation can be greatly improved by the addition of the Kier shape index of third order (${}^3\kappa$), which results in the best two descriptor correlation using topological descriptors:

$$V_o = (16.8\pm2.0) + (20.06\pm0.36)\ {}^0\chi + (2.63\pm0.19)\ {}^3\kappa \qquad [25]$$
$$R^2=0.992,\ s=3.92,\ F=4788,\ N=78$$

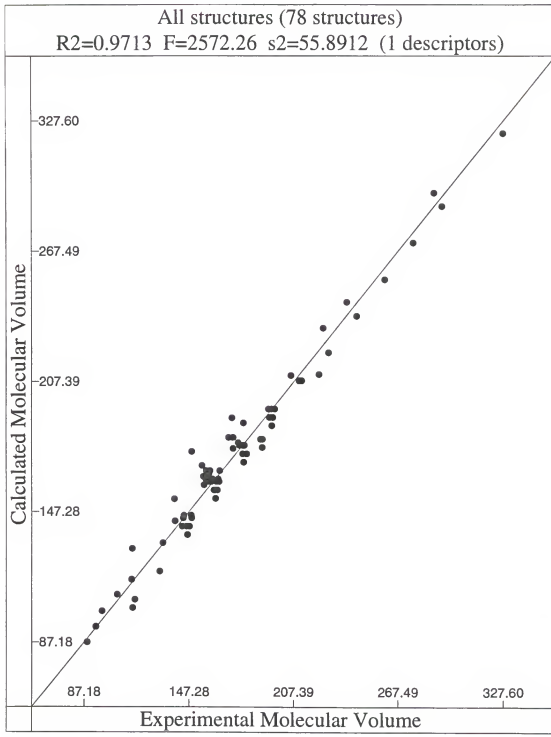

Figure 2-12. Scatter plot for the one descriptor ($^0\chi$) regression of calculated to experimental molar volume of 78 diverse alkanes and alkenes, showing structures with greatest steric influence on the molecular volume.

The Kier shape index [Kier, 1990] was developed specifically to handle aspects of the molecular shape, allowing a number to be calculated to quantify the extended vs. bulky nature of the molecule. As can be seen in its ability to improve the $^0\chi$ correlation, it serves this role well in improving the $^0\chi$ (essentially a group contribution method) correlation to handle steric influences.

Surfactant tail volume. Ideally, volume data would be available for a wide variety of fragments, and thus correlations could be developed directly for the fragment volume. Unfortunately, no such comprehensive measurements are known to the author. The best compromise is to use the means developed for predicting alkane volumes to predicting the volumes of the hydrophobic surfactant tails.

In order to calculate the molecular volume of surfactant hydrocarbon (and fluorocarbon) tails, the same four descriptor relationship developed for the liquid alkanes can be used. The major issue with the direct application of the formula is the handling of the constant term. As with the group contribution techniques, with their covolume term, this term is apparently a property of the whole molecule, and cannot be partitioned among the substituent atomic groups in the molecule. When considering the hydrophobic domain of the surfactant molecule, we are dealing with a fragment of the molecule rather than the whole. How, then, should this constant term be divided? It makes no sense to include the entire term, since if a molecule was split in half and the formula applied to each half, the resulting volume would potentially be more than the entire molecule. Also at issue is that some of the descriptors are based on normalizing by whole molecule parameters, such as

the gravitation index (G), or include contributions from neighboring groups, and thus would be a problem for the calculation of contributions from atoms near the division between fragments, such as the higher order molecular connectivity indices (ex. $^{3}\chi$). Another possible estimate would be to weight the constant term by the size, mass, or some other term, so that if, for example, 75% of the mass of the molecule was in the hydrophobic domain, then 75% of the constant term should be applied to the volume estimate. The major problem with any weighting method is that it contracts the basic nature of the covolume term, as by definition it is a whole molecule property, and not an additive property of the components of the molecule.

The best estimate offered here would be to use half of the constant term. Recognizing that the sum of the volume estimates of two halves of any of the molecules used here, using one half of the constant term for each, will almost certainly not result in the same volume as that calculated for the whole, as the descriptors used are not strictly additive. Assuming that the magnitude of the error is small, this leads to the best available estimate for the volume of surfactant hydrophobic tails. A compromise may be to use correlations that have poorer statistical results than the best correlation above, but use descriptors that are more additive in nature, assuring that the constant term for the fragments is more related to the covolume. Another possible way to address this in the future would be to examine data from molar volumes of alcohols, where the volume of the hydroxyl group could be accounted for by group contribution estimates, allowing the

hydrophobic fragment molecular volume to be studied. Possible sources of data are in Kier and Hall [1976, 1986] and more recently data from Sakurai et al. [1994].

Conclusion. An excellent correlation has been developed for estimating the molecular volume, allowing the prediction of volume to a standard error of 1.32 mL/mol, for a set of 78 molecules of diverse structures, including linear and branched alkanes, alkenes, alkylbenzenes, fluorobenzenes, and perfluorinated alkanes. The possibilities of applying this formula to the prediction of the molecular volume of surfactant hydrophobic tails is discussed, with the major issue being the handling of the constant (covolume) term in the fragment.

Conclusions

As the examples in the previous six sections demonstrate, the QSPR approach can be successfully applied to surfactant property prediction. Very good correlations can be found for nonionic and anionic CMC, cloud point and Krafft point, as well as related properties such as molecular volume and alkane solubility. The separate consideration of the surfactant head (hydrophilic) and tail (hydrophobic) domains by calculating descriptors specifically for just these molecular fragments is one key to getting the best correlations. The dominant descriptors tend to be topological, although one should not discount the potential of the other constitutional, geometrical, electrostatic, and quantum-chemical descriptors.

This QSPR approach has been successfully applied to a wide variety of chemical properties such as boiling point, GC retention time, refractive index, and partition

coefficient; and a diverse set of activities, such as corrosion, anesthetic effect, pollutant spreading, and carcinogenicity. The subset of topological descriptors have been applied for over twenty years in different areas, so it was just a matter of time before someone applied them to surfactant chemistry. This can be summed up by a quote from a decade ago:

> That the topological method is applicable to all these fields is now well established; the only question is how long it will be before the method is exploited to its full potential. D.H. Rouvray, *Scientific American*, 1986.

The major conclusions that can be drawn from this research are as follows:

1. Surfactant properties can be predicted to good accuracy with the quantitative structure-property relationships (QSPR) approach.
2. Good correlations have been found for nonionic and anionic surfactant CMC, nonionic cloud point and anionic Krafft point, and molecular volume of hydrocarbons and fluorocarbons.
3. Better correlations are found if descriptors are considered that have been calculated for the head group and tail fragments of the molecule, rather than for the whole molecule.
4. Topological descriptors are the most useful class in predicting surfactant properties.
5. General QSPR's allow the estimation of molecular properties for compounds that have not yet been synthesized, as they can be calculated solely from the molecular structure. This also opens up the possibility for molecular design to achieve certain values of properties.

CHAPTER 3
MAXIMUM SOLUBILIZATION IN NONIONIC W/O MICROEMULSIONS

Introduction

A microemulsion can be defined as a thermodynamically stable, transparent dispersion of two immiscible liquids, stabilized by an interfacial film of surfactants. Microemulsions have many applications in such diverse areas as pharmaceutical preparations, cosmetics, enhanced oil recovery, etc. An important aspect of microemulsion design is the ability to solubilize the maximum amount of one liquid (dispersed phase) into another (continuous phase). This can also be considered as the ability to solubilize a fixed amount of the dispersed phase with a minimum amount of surfactant.

There have been extensive studies done on microemulsions in the last few decades. Many works focus on microemulsions made using ionic surfactants, and most involve one surfactant. As it has been demonstrated that single surfactants will not necessarily produce the best microemulsions, many studies involving addition of a cosurfactant have also been done. This cosurfactant is usually a short chain alcohol, ranging from two carbons (ethanol) to four carbon atoms (butanol), though alcohols up to decanol have been studied by some investigators. Also, the effect of salt in the water phase has also been of great interest, so many studies exist on the effect of pH or electrolyte concentration on microemulsion properties.

The use of mixtures of nonionic surfactants is essential because the benefit of a cosurfactant such as a short chain alcohol is not available. These alcohols are not considered edible and may be irritating to the skin. Since it is known that a single surfactant alone is generally not optimum, mixtures are used to get an improvement in microemulsion properties similar to those obtained by the addition of a cosurfactant.

This chapter of the dissertation will demonstrate the value of mixtures of surfactants in the formulation of microemulsion systems that solubilize large amounts of water in oil. This research will be performed using nonionic surfactants and W/O microemulsions. In order to be more generally useful, we try to develop general rules for the formation of highly solubilizing microemulsions, that will hopefully be more widely applicable than just to the systems studied here. Current design of microemulsion systems involves trial and error methods to arrive at an optimum formulation. The intention of this research is to improve the understanding of the synergism between surfactants in a microemulsion environment, so that highly solubilizing microemulsion systems can be formulated in a more rational, scientific fashion.

Nonionic Surfactants

Nonionic surfactants are studied in the present work because of their unique nature: compared to ionic surfactants they are much less harmful to humans and thus can be considered for food, pharmaceutical, and cosmetic applications. Nonionics are compatible with all other types of surfactants, and are resistant to polyvalent cations (hard water) and high ionic strength solutions.

A good surfactant should have a low solubility in both the bulk and dispersed phases. Nonionic surfactants generally have lower solubility and CMC than ionics. This can be seen by the critical micellization concentration (CMC), which is 8 mM for the anionic surfactant sodium dodecylsulfate, and only 0.06 mM for the nonionic $C_{12}E_4$ (lauryl tetraethoxylate). These values demonstrate the low solubility of the nonionic surfactant monomer in water.

The molecular structures of nonionic surfactants are usually one of the following: polyoxyethylenated alkylphenols (mostly p-octyl-, p-nonyl-, p-dodecyl-, dinonylphenols), polyoxyethylenated straight chain alcohols, polyoxyethylenated polyoxypropylene glycols, polyoxyethylenated mercaptans, long chain carboxylic acid esters (glyceryl and polyglyceryl esters of natural fatty acids, propylene glycol, sorbitol, and polyoxyethylenated sorbitol esters, polyoxyethylene glycol esters) and alkanolamines (diethanolamine-, isopropanolamine-fatty acid condensates). The edible surfactants are mainly the esters based on glycerol, sorbitol, and propylene glycol [Rosen, 1989].

Surfactants used in foods are usually called emulsifiers [El-Nokaly et al., 1991]. Many of these have been assigned an Acceptable Daily Intake (ADI) value by the FDA. Many food surfactants are fatty acid esters. Raw materials in the synthesis of these surfactants are usually naturally occurring fats and oils. Most are nonionic, the exceptions being succinic, citric, and diacetyl tartaric acid esters. Lecithin is the only approved surfactant containing a positive charge. The following table summarizes some ADI values for emulsifiers.

Table 3-1. Approved daily intake values for some surfactants.

Surfactant Type	ADI Values (mg/kg body weight/day)
mono- and diglycerides	not limited
lecithin	not limited
Monoglycerides:	
lactic acid esters	not limited
acetic acid esters	not limited
citric acid esters	not limited
diacetyl tartaric acid esters	not limited
succinic acid esters	3 wt% in shortening
Fatty Acids:	
POE esters	25
POP esters	25
sorbitan esters	25
sucrose esters	10
POE sorbitan esters	25

For cosmetic applications, the preferred nonionic surfactants include polymeric ethers, alkoxylated amines, and ethoxylated sorbitan esters. Specific examples include blends of glyceryl stearate and POE (100) stearate, isostearic acid, cetearyl alcohol, choleth-24, ceteath-24, and stearyl triethanolamine [Zecchino et al., 1991].

Rosen [1992] suggests that commercially available surfactants should be studied, because questions of toxicity, biodegradability, and general environmental impact must now be addressed whenever FDA approval is sought for a new compound, a costly and time consuming procedure. So, in the search for improved surfactant performance and properties, a less costly approach is to investigate combinations of existing acceptable surfactants that show synergy, rather than designing new chemical structures.

HLB: Definition and application. HLB, the hydrophilic-lipophilic balance, has proven to be a useful tool for the design of emulsions. The HLB number is a parameter that

has been assigned to each surfactant molecule, and has a range of 0 to 20 for nonionic surfactants [Griffin, 1949; 1954]. A higher number represents a more hydrophilic molecule. This system was designed to score nonionic surfactants, but has been applied to ionic surfactants also. It has been suggested that the HLB number of nonionic surfactants should be a function of temperature, as nonionic surfactants become increasingly hydrophobic with increasing temperature [Shinoda and Friberg, 1986, p. 56].

The HLB temperature, or PIT (phase inversion temperature) is an important parameter for microemulsions containing nonionic surfactants. As temperature is increased through this value, the microemulsion will go through a change from O/W to W/O. There is some correlation between HLB number and PIT, and empirical estimates of the former can be made from the former [Shinoda and Friberg, p. 63]. Shinoda found nonlinear, but monotonic relationship between PIT and HLB for emulsions, using heptane as the oil phase, and various surfactants; POE nonylphenyl ethers, dodecylphenyl ethers, Tweens, and some binary mixtures of the three classes [Shinoda and Friberg, p. 113].

HLB number is used in the design of emulsions by applying the concept of required HLB (RHLB). There are two RHLB values assigned to each oil, one where W/O emulsions should be formed and one for O/W emulsions. These numbers are approximate, to within ±1 HLB number. It is possible to make a mixture of surfactants, one surfactant with HLB below the RHLB and one surfactant with HLB above, so that a mixture of the surfactants can be found that will have the RHLB value. The HLB of a surfactant mixture is simply the weighted average of the HLB of the two individual components:

$$HLB_{MIX} = W_A HLB_A + W_B HLB_B$$

Ideally, the RHLB should be independent of the surfactants selected. RHLB is expected to be in the range 3-6 for W/O emulsions and 8-18 for O/W emulsions [ICI, 1984].

HLB number can be estimated in several different ways [Shinoda and Friberg, 1986, p. 66]. One method for polyhydric alcohols with polyoxyethylene is to multiply the ratio of the weight of the hydrophilic part of the molecule with the total weight of the molecule, as in [Griffin, 1949]

$$HLB = 20\ (MW_{EO}) / MW_{TOT}$$

Another method for polyhydric alcohol fatty acid esters determines the HLB number as a function of saponification number of the ester and acid number of the acid [Shinoda and Friberg, 1986, p. 69]. A third method assigns a number to each functional group in a molecule, which are combined to compute the HLB number [Shinoda and Friberg, p. 84].

Shinoda et al. [1984] attempt to clarify confusion about HLB number and HLB. The HLB number of a surfactant is a parameter defined by Griffin [1949], and is fixed. HLB, on the other hand, is the hydrophile-lipophile balance of a surfactant, and will change in response to such environmental variables as surfactant composition, type of oil, temperature, valence of counterions, salt concentration, etc. The point is made that solubilization should be studied as a function of the HLB.

Microemulsions

The solubilization of one phase into another in a microemulsion system is affected by a balance of attractive and repulsive forces. As microemulsions are thermodynamically stable, the droplets will not coalesce and precipitate over time. The nature and environment of emulsion and microemulsion droplets must be considered to be completely different.

Emulsion droplets are much larger, generally greater than a micron, while microemulsion droplets are in the 10-100 nanometer range. It is clear from this size difference that the curvature at the interface is much more significant for microemulsion droplets. Droplets of both types are affected by thermal motion of the solution and will collide with each other. The interface of emulsion droplets can be considered as a monolayer of surfactant. Colliding emulsion droplets will either repel each other or coalesce. This coalescence is a monotonic process, it will continue to occur over time, resulting in an increase in the average droplet size over time. Microemulsion droplets, on the other hand, behave quite differently. One may consider the interface to be less perfect, with the dispersed phase coming in contact with the continuous phase. Collisions between droplets occur, and while most will repel, some will coalesce and then spontaneously break apart again. This results in a mixing of the contents of the microemulsion droplets. There must be a balance of forces present to drive the coalesced microemulsion droplets into splitting again. Over time, the average droplet size of a microemulsion will remain constant.

A microemulsion can be characterized by the amount of the dispersed phase solubilized in the continuous phase, at a given temperature. This can be done by titration with the dispersed phase while stirring, until a final clear to cloudy transition is observed. A solubilization parameter can be defined as the ratio of the volume of dispersed phase to the volume of the continuous phase present in the microemulsion. Another characterization technique [Abe et al., 1986] is by production of a middle phase (Winsor III) microemulsion, where the microemulsion is in equilibrium with an excess oil phase and an excess water

phase. The middle phase contains an equal amount of water and oil, and the solubilization parameter can be defined as the volume ratio of oil (or water) to surfactant.

Maximum solubilization has been reported for many different systems. As an example, Bansal et al. [1979] reports a water/oil ratio of 0.48 in a W/O microemulsion system consisting of sodium stearate, hexadecane, water, and one of three cosurfactants, either n-pentanol, n-hexanol, or n-heptanol. The initial system was composed of 1 g sodium stearate, 4 ml alcohol, and 10 ml hexadecane. A linear relationship is shown between maximum solubilization of water and the surfactant/oil ratio. Reported w/o ratios of 0.16 and 1.12 for 5% and 20% w/v sodium stearate/hexadecane, respectively, were reported.

The theoretical maximum ratio of dispersed phase to total volume is 0.74. This is the volume fraction assuming equal sized spheres packed in the face centered cubic (FCC) or hexagonal close packing (HCP) configurations. The solubilization parameter presented here is the ratio of volume of dispersed phase to volume of continuous phase, so the theoretical maximum of this parameter is 2.85. Several factors work to reduce this value. First, the thickness of the interface is not zero, but rather finite, and gains more relative importance as the radius of the particles diminishes. For an interface 1% of the radius, the theoretical maximum parameters fall to 0.72 and 2.76, and for an interface 10% of the radius these parameters fall to 0.56 and 2.14. One cannot also assume a monodisperse size distribution of particles. Second, a distribution in the particle size will also result in lower maximum parameters, as the ideal packing structure will be disrupted.

Nature of microemulsion droplet. What does a microemulsion droplet look like, and what is its dynamic behavior? Perhaps it is helpful to think of a microemulsion droplet as

an intermediate between a micelle and an emulsion droplet. Some researchers even consider a W/O microemulsion droplet to be a hydrated reverse micelle. One can consider an emulsion droplet to be a rather static structure, a large droplet of water suspended in a continuous phase of oil, with the oil/water interface stabilized by a monolayer of surfactant. On the other hand, a micelle is a very dynamic structure. It is a bit deceiving to see drawings of micelles in journals, because this representation is by necessity static, and micelles are actually dynamically changing and loosely bound aggregates. There is an equilibrium and a constant exchange between surfactant monomers and surfactant in the micellar aggregation. Micelles may have lifetimes as short as milliseconds, while emulsion droplets have long lifetimes, without the disintegration we see in micelles, but potentially with the occurrence of some coalescence over time. Given these two extremes of micelles and emulsion droplets, what will be our model for microemulsion droplets? It is known that the contents of mixed microemulsions do mix, this allows reactions to occur using microemulsion droplets as tiny microreactors [Kumar et al., 1993]. Because the water droplet is so small, we know through NMR studies that there exist two significant states of water, the "free" water in the interior of the droplet, and the water at the interface, associated with the surfactant molecules. Since we know that some fraction of microemulsion droplet collisions result in coalescence, yet the mean droplet size in the microemulsion remains constant over time, there must be a driving force to break up these aggregates again. Positive interfacial tension is the driving force for decreasing interfacial area of a given droplet, so there must be some "negative" interfacial tension present to force an increase in interfacial area and the resulting breakup of microemulsion droplets that are too large. At the optimum droplet size,

the forces are balanced and the interfacial tension must approach zero. We can envision a microemulsion as a dynamic entity, a tiny droplet surrounded by a monolayer or aggregate of surfactant, sometimes combining with its neighbors, and subsequently breaking apart, sometimes exposing the water phase to the oil phase.

Microemulsions using nonionic surfactants. For oil-in-water (O/W) microemulsions made with ionic surfactants, the primary force preventing coalescence is electrostatic charge repulsion. These microemulsions display the greatest ability to solubilize one phase within another. For W/O microemulsions, and microemulsions made with nonionic surfactants, there is only steric hindrance preventing coalescence of the droplets. This is a weaker force than electrostatic repulsion, so these microemulsions display less solubilization ability. Steric hindrance is affected only by the part of the surfactant molecule exposed to the continuous phase, for example, the hydrophobic region in a W/O microemulsion. Repulsion is enhanced by the length of this region, as well as disorder introduced by such features as double bonds, which introduce bends and interfere with orderly packing of the surfactant molecules at the interface.

Importance of cosurfactant free microemulsions. Microemulsions have traditionally been formed using a single surfactant and a cosurfactant, usually a small molecule. Typical cosurfactants are short chain alcohols, ethanol to butanol, glycols such as propylene glycol, or medium chain alcohols, amines, or acids.

The suitability of cosurfactant depends on the application. For cosmetics [Zecchino et al., 1991], long chain fatty alcohols may be used, from 12-18 carbon atoms. Abe et al. [1986] concludes that the role of the cosurfactant is to destroy liquid crystalline or gel

structures that form in place of a microemulsion phase. He also concludes that cosurfactant free microemulsions in most systems (they studied sulfonates) cannot be made except at high temperatures. To achieve a microemulsion phase in the 25-40°C range, cosurfactant must be used. Kahlweit et al. [1991] and Strey and Jonstroemer [1992] have investigated the effect of medium chain length alcohols in water/octane/POE octylether microemulsions. They characterize the role of the alcohol, and quantify its partitioning behavior between the oil, water, and interface phases. El-Nokaly et al. [1991] summarizes the role of a cosurfactant in the following table:

Table 3-2. Specific roles of cosurfactant in microemulsion formulation.

• decrease further the interfacial tension
• increase the fluidity of the interface
• destroy liquid crystalline and/or gel structures which would prevent the formation of microemulsions
• adjust HLB value and spontaneous curvature of the interface by changing surfactant partitioning characteristics
• decrease the sensitivity to composition fluctuations

Reference: [El-Nokaly et al., 1991]

Effect of oil phase. The nature of the oil phase is of great interest in the formulation of W/O microemulsions. Microemulsions are formed well using nonpolar oils such as the normal alkanes, but oils such as triglycerides are important because they are edible. The triglycerides are much more polar than the alkanes, and generally form poor microemulsions. For cosmetic applications, silicone oils such as cyclomethicone may be used, along with a triglyceride and/or squalane as moisturizing components (squalene is 2,6,10,15,19,23-hexamethyltetraeicos-2,6,10,14,18,22-hexene). El-Nokaly et al. [1991]

believes that a surfactant with a higher HLB must be used to compensate for this partial polar nature of the oil.

The choice of oil phase depends on the application. For cosmetic formulations, skin irritation is the most important factor. Zecchino et al. [1991] summarizes some oils that are generally acceptable. Hydrocarbons may be 12-18 carbon straight chain or 12-30 carbon branched alkyl compounds. Acceptable animal oils are cod liver oil, lanolin oil, mink oil, orange roughy oil, and shark liver oil. Acceptable vegetable oils include almond, apricot kernel, avocado, castor, coconut, corn, evening primrose, jojoba, olive, safflower, sesame, soybean, and wheat germ oils. Some silicone oils are acceptable, such as certain linear polysiloxanes and cyclic dimethyl polysiloxanes such as cyclomethicone. The solubility of lipophilic surfactants in the oil phase will influence the concentration of surfactant at the interface. Too high a solubility or too high a CMC in the oil phase will result in poor microemulsion solubilization. The CMC of a surfactant will decrease geometrically with molecular weight [Shinoda and Friberg, 1986, p.87].

The type of oil also has a significant effect on the PIT. Table 3-3 summarizes PIT for 10% POE (9.6) nonylphenyl ether in a volume ratio 1.0 water/oil emulsion system. Note that W/O is the state above the PIT and O/W is the state below the PIT [Shinoda and Friberg, p.97]. A lower PIT correlates well with the ability of the oil to dissolve the surfactant. For this case, benzene is the best solvent and hexadecane is the worst. The effect of mixing oils displays no nonlinear effects with respect to volume ratio, from observation of the change in PIT for mixtures of heptane with paraffin, cyclohexane, xylene, and benzene [Shinoda and Friberg, p. 109].

Table 3-3. The effect of oils on the PIT for volume ratio 1.0 water/oil emulsion containing 10% POE (9.6) nonylphenyl ether.

solvent	PIT (°C)
hexadecane	102
heptane	85
cyclohexane	68
m-xylene	50
toluene	40
benzene	32

Reference: [Shinoda and Friberg, 1986, p.97]

Experimental techniques for studying microemulsions. Droplet size measurements can be performed using QELS (quasi-elastic light scattering). QELS is a general technique for characterizing solutions of macromolecules or particles by studying the time dependent differences in laser light scattered from a sample solution. Droplet radius cannot be determined directly, but is derived from the diffusion coefficient, given certain assumptions, such as a monodisperse particle size distribution of spherical particles at infinite dilution (noninteracting particles). The Stokes-Einstein relationship is

$$R_H = kT/(6\pi\eta D_0)$$

where k is the Boltzmann's constant, η is the viscosity, T is the absolute temperature, and D_0 is the diffusion coefficient. The measured radius (R_H) is the hydrodynamic radius, not the precise radius of the particle, as it includes such things as the bound water or oil that moves with the particle.

Several researchers have investigated microemulsion droplet size using light scattering. Hou et al. [1987] reviewed the literature to date on QELS investigations of microemulsions, provided an overview of the theory and limitations of the technique, and

investigated water-in-oil microemulsions using AOT as a surfactant. The effect of additives such as NaCl, propanol, heptanol, Arlacel 20, as well as the effect of different alkanes as the oil phase were reviewed. Beckman and Smith [1990] investigated droplet size and diffusion coefficient of w/o microemulsions formed from a mixture of ethoxylated alcohols and acrylamide in a mixture of ethane and propane near the critical point. Aoudia et al. [1991] studied the effect of butanol as a cosurfactant on droplet size and interfacial fluidity for a O/W system of octane, NaCl, water, sodium dodecylbenzenesulfonate and butanol.

Design of Water-in-Oil Microemulsions

Surfactant structure studies. There have been several studies of the effect of surfactant molecular structure on microemulsion formation. It is well known that AOT (bis-2-ethylhexyl sodium sulfosuccinate) forms cosurfactant free W/O microemulsions. This is an anionic surfactant molecule with double branched hydrophobic tails. Because of its unusual shape, with its large two tailed hydrophobic domain, it forms reverse micelles, and thus W/O microemulsions.

Israelachvili [1992] described a packing parameter (R), which predicts the aggregate structure of a micellar solution. R is itself dependent on structural parameters of the surfactant. R is defined as $V_H/l_c a_0$, where V_H is the volume occupied by the hydrophobic groups in the micellar core, l_c is the length of the hydrophobic group in the core, and a_0 is the cross-sectional area occupied by the hydrophilic group at the micelle-solution interface. The following table shows the expected structure for different R values.

Table 3-4. Expected solution microstructures for different R values.

Value of R	Structure of the Micelle
0 to 1/3	spherical in aqueous media
1/3 to 1/2	cylindrical in aqueous media
1/2 to 1	lamellar in aqueous media
> 1	inverse micelles in nonpolar media

Reference: [Israelachvili, 1992]

The importance of double tailed surfactants was studied by Abe et al. [1986], using polyoxyethylenated alkanesulfonates. Their goal was to characterize the effect of different hydrophobic structures, both double tailed and branched, to produce cosurfactant free microemulsions at higher salinity and lower temperature than previously reported. They produced middle phase (Winsor III) microemulsions, which contain an equal amount of oil and water in a surfactant phase at equilibrium with an excess oil phase and an excess water phase. The phases used were hexadecane and aqueous NaCl solutions, along with polyoxyethylene sulfonates where the hydrophilic group was attached near the middle of a 12-20 carbon atom linear alkane. Their choice of a surfactant series allows for the alteration of the hydrophobic group, by changing the length of the group and the point of attachment of the hydrophilic group, as well as the alteration of the hydrophilic group by changing the length of the polyoxyethylene chain between the hydrophobic structure and the sulfonate. They concluded that alkane sulfonates with chain length of 14-18, and hydrophilic attachment at or near the middle carbon, can form microemulsions without cosurfactant. Microemulsions can be formed with an alkane chain length of 12, when three ethylene oxide units are added to the hydrophilic group. Lowering the surfactant molecular weight improves salt tolerance, but also lowers the solubilization parameter. An increase in NaCl

concentration acts to decrease solubilization, as does an increase in temperature. Adding two ethylene oxide units to the hydrophilic group increased tolerance to NaCl concentration as well as temperature. Note that ionic and nonionic surfactants have different partitioning behavior with temperature, ionic surfactants tend to be more hydrophilic with an increase in temperature, while nonionic surfactants tend to be more hydrophobic. It is estimated that $CaCl_2$ has 4-5 times the effect of NaCl in the aqueous phase.

Abe et al. [1986] concluded that there are three conflicting concepts that must be considered simultaneously when designing a cosolvent free microemulsion system. First, the surfactant must partition equally between the oil and water phases, through optimization of temperature, surfactant hydrophilic group structure, surfactant hydrophobic group structure, oil phase composition, and electrolyte composition in the aqueous phase. Choice of cosolvent and cosolvent concentration also effect partitioning when present. Second, the surfactant molecules must reach maximum linear extension, to produce high solubilization and low interfacial tension. Surfactant concentration must be above the critical micelle concentration. Third, net surfactant lateral interactions must be weak. The system must be above the melting point of all extended structures, such as liquid crystals and gels, so that the more disordered microemulsion state will be thermodynamically most stable. This can be accomplished by shortening the hydrophobe length, increasing hydrophobe branching, adding ethylene oxide units, increasing temperature, and decreasing electrolyte concentration. Adding cosolvent can also help when present. So, through optimization of the hydrophobe branching, surfactant molecular weight, and hydrophilic group, Abe was able to form cosurfactant free microemulsions, at lower temperatures than previously

reported, with good solubilization, and at NaCl concentrations from 0.1 M to 3.4 M without affecting microemulsion quality. Note that all surfactants used were ionic, with the polar group attached to the linear alkyl chain in middle carbon positions. Also, all surfactants studied had a limited molecular weight range, from 350 to 410. There was not much difference either in the fully extended length of the surfactant molecules, including the major tail, the ethylene oxide units and the sulfonate group. The best surfactants had three ethylene oxide units. These molecules are not available commercially, as they had all been synthesized for the study.

Table 3-5. Abe's microemulsion design rules.

- surfactant must partition equally between the oil and water phases
- surfactant molecules must reach maximum linear extension
- net surfactant lateral interactions must be weak (above M.P.)

Reference: [Abe et al., 1986]

Shinoda and Kunieda [1977] discussed formation of microemulsions using nonionic surfactant, with the goal of formulating microemulsions with less surfactant (equivalent to obtaining maximum solubilization with a given amount of surfactant). Hydrophilic nonionic surfactants generally have a long polyoxyethylene chain attached to the hydrophobic part of the molecule. This chain is attached by a polymerization reaction, and the number of monomer units per molecule cannot be controlled exactly. This results in surfactant which contains a distribution of POE chain lengths. The effect of the polyoxyethylene chain length distribution on the phase diagram of a microemulsion system was investigated.

Shinoda and Friberg [1986, p. 36] presents a phase diagram of temperature dependence vs. solvent oil fraction for the water/cyclohexane/5 wt% POE (7.4) nonyl-

phenylether system. A similar shaped phase diagram is given for POE chain length vs. solvent oil fraction, where the POE chain length variation is achieved by mixing n=7.4 and n=9.7 polyoxyethylene nonylphenylethers. Both of these graphs show W/O and O/W microemulsion regions, as well as a three phase region. The similarity between these two phase diagrams are an excellent example of the analogy between the change in HLB and a change in temperature for nonionic surfactant microemulsions. Shinoda also presents phase diagrams for other nonylphenylether surfactants, as well as for mixtures of these and ionic surfactants.

Surfactant mixture studies. Characterizing the effect of surfactant mixtures on the solubilization of water in oil is a more difficult problem than the solubilization using just one surfactant as described in the previous section. Since one is now working with at least a four phase system, triangular phase diagrams can no longer be used to represent the data. One way around this is to use a pseudophase diagram, where the vertices now represent a fixed ratio of two components. One can make one vertex water, another oil and one surfactant, and the last oil and the second surfactant. There has been no mention in the literature of enhanced solubilization by mixing surfactants, though several investigators have studied different proportions of cosurfactant to surfactant, where the cosurfactant is a small molecule, usually an alcohol.

It is important to point out that many commercially available surfactants, and especially nonionics, are mixtures. This is a direct result of their synthesis. The hydrophilic group of a nonionic surfactant is usually polyoxyethylene. This is formed by polymerization of ethylene oxide. The product of this reaction is not an exact number of monomers

attached to each surfactant molecule, but rather a distribution of chain lengths. The distribution has been analyzed for some commercial surfactant products, and an example is presented by Shinoda and Friberg [1986]. The distribution is usually a Poisson distribution. For block copolymers, there may be a distribution in the hydrophobic domain also. This often involves polymerization of propylene oxide. Some other surfactants may be a blend which has proven to be commercially successful. Neodol 23 (Shell) has a mixture of 12 and 13 carbon chains in its hydrophobic moiety. Arlacel 186 (ICI) is a mixture of glycerol oleate and propylene glycol. Arlacel 83 and Arlacel C (ICI) are mixtures of sorbitan mono- and dioleates. Atlas G1086 and G1096 (ICI) are POE versions of Arlacel 83.

Shinoda et al. [1984] stress the importance of selection of the size of the hydrophilic group of the surfactant, or selection of temperature, in order to adjust HLB and achieve high solubilization. Of course, another way to adjust HLB is to mix surfactants with different HLB numbers. Through the ability to continuously adjust HLB over a range of values, maximum solubilization for the system can be realized. As examples, he presents solubilization data for $C_{12}E_5$ in tetradecane, and also data for mixtures of water/ decane/ calcium dodecyl ethoxysulfate/ isooctyl monoglyceride, 3% NaCl aq./ decane/ SDS/C_8E_2, 3% NaCl aq./ decane/ SDS/ isooctyl monoglyceride, and 1% NaCl aq./ liquid paraffin/ sodium hexadecyl sulfate/ isooctyl monoglyceride. He found the mixtures of nonionic and anionic surfactants had high solubilization, both on the W/O and the O/W side of the phase diagram.

Shinoda et al. [1971] investigated the effect of the size and distribution of the oxyethylene chain on stability of emulsions using nonionic surfactants. He used POE

nonylphenylethers and POE dodecylethers, concluding that the stability of an emulsion increased when the hydrophilic groups are broadly distributed. It was also observed that the PIT became ambiguous and changed sensitively with concentration for surfactant mixtures containing of widely different HLB numbers. It is thus expected that mixing long and short oxyethylene chain homologs will increase the stability of emulsions.

Very few microemulsion studies exist in the literature involving cosurfactant-free formulations of nonionic surfactant mixtures. Only two were found, by Lissant [1974] and Shinoda and Friberg [1986], and these did not provide any insight into optimum mixing of surfactants. The following table summarizes relevant surfactant mixture studies found in the literature.

Table 3-6. Surfactant mixture studies. (ESO_4=ethoxysulfate, i-C_8MG=isooctyl monoglyceride, i-C_3OH=isopropanol)

WATER	OIL	SURFACTANT	REFERENCE
water	C_{14}	$C_{12}E_5$	Shinoda et al., 1984
water	C_{10}	Ca $C_{12}ESO_4$/i-C_8MG	Shinoda et al., 1984
3% NaCl	C_{10}	SDS/C_8E_2	Shinoda et al., 1984
3% NaCl	C_{10}	SDS/i-C_8MG	Shinoda et al., 1984
1% NaCl	paraffin	C_{16}DS/i-C_8MG	Shinoda et al., 1984
water	?	nonylphenyl ethers	Lissant, 1974
water	?	nonylphenyl ethers	Shinoda and Friberg, 1986
water	C_{16}	AOT/Arlacel 20	Johnson and Shah, 1985
var. NaCl	C_{16}	AOT/Arlacel 20	Johnson and Shah, 1985
water	various	AOT/Arlacel 20	Johnson and Shah, 1985
water	C_{10}	Brij 35/Arla 186/i-C_3OH	Jayakrishnan et al., 1983
water	various	Brij 35/Arla 186/i-C_3OH	Jayakrishnan et al., 1983

Water/Hexadecane/Sorbitan Ester Microemulsions

The goal of this effort is to discover a means to solubilize a maximum amount of water into an oil phase, in microemulsion form. Mixtures of surfactants will be used to achieve better results than possible with any single surfactant, taking advantage of synergism between the surfactants. By solubilization experiments the microemulsion region of the phase diagram can be mapped out for different surfactant mixtures. Confirmation of the existence of microemulsion droplets can be made with quasi-elastic light scattering, to estimate microemulsion droplet sizes, and using polarized filters, which allow detection of liquid crystal phases.

Solubilization experiments were performed by titrating water into mixtures of surfactant and hexadecane. Given a fixed surfactant to oil ratio and a specific oil phase, the only freedom remaining is the choice of surfactant. Single surfactants have been tested, along with binary mixtures of oil soluble and water soluble surfactants. For these binary mixtures, the oil soluble surfactant was a member of the Span or Arlacel family (sorbitan esters), and the water soluble surfactant was a Tween (polyoxyethylenated sorbitan esters).

Design rules for the choice of surfactants, as well as the optimum surfactant ratio, for maximum solubilization are sought. Of all previous work on microemulsions described in the introduction of this chapter, little exists on nonionic surfactant mixtures, and no design guidelines are apparent. Rules analogous to the guidelines for the use of surfactant HLB to select surfactants and mixture ratios for emulsification (*macro*emulsions) [Griffin, 1949; 1954], and the packing parameter of Israelachvili [1976; 1992] for determination of

surfactant aggregation structure, would be very useful in developing microemulsions for a variety of applications.

In this thesis clear examples of synergism in mixtures of nonionic surfactants are presented, and several design rules for formulating microemulsions are proposed.

Experimental Procedure

W/O solubilization. Solubilization is a very simple experimental technique. Surfactants are mixed with the oil phase and agitated. In most cases, the surfactants will dissolve in the oil. In some cases the mixture will separate, and continuous stirring may be necessary to achieve homogeneity before titration. Water or aqueous solution is added dropwise into the mixture until a permanent clear to cloudy phase transition is observed, which represents the maximum water solubilization for that particular oil and surfactant mixture. For the cases where the surfactant does not dissolve in the oil phase, the initial mixture will be cloudy and addition of water may result in a transition of cloudy to clear solution, representing the minimum solubilization for the surfactant mixture. The kinetics of solubilization vary, initially water is solubilized very fast, limited by the stirring speed. Near the end point, though, solubilization can be very slow, often taking hours for the cloudy (or hazy) solution to clear up. Solubilization was performed by titrating water dropwise into a prepared mixture of oil and surfactant, while stirring. 3.0 g of total surfactant were mixed 7.0 ml of hexadecane. This amounts to 42.9% w/v or 35.7 wt% initial surfactant. Water used was deionized and distilled. Experiments were performed at 25°C.

Liquid crystals. One complication is the potential formation of a liquid crystalline phase. Under certain conditions a combination of oil, water and surfactant will result in a

phase where there are orderly planes of oil and water separated by monomolecular layers of surfactant. Formation of these liquid crystals must be prevented if a microemulsion phase is desired. Several authors have addressed the factors necessary for the formation of liquid crystals. For the surfactant combinations studied in this dissertation, it is quite common for liquid crystals to form spontaneously for mixtures with an HLB of greater than 11. Israelachvili [1992] reports that liquid crystals (lamellar structures) will form for a certain range of R values (see Introduction of this Chapter). Liquid crystal formation can be detected by two methods; 1) a large increase in viscosity should be observed, and 2) checking with polarizing filters, one may see that the solution is birefringent, and thus has undergone a transition from an isotropic microemulsion solution to an ordered liquid phase.

Materials. Arlacel, Brij. Span and Tween families of surfactants were supplied by ICI Americas Inc. (Wilmington, DE). Several different oils were used in the investigations. The alkane series of decane, dodecane, tetradecane and hexadecane were purchased from Fisher Scientific (Fair Lawn, NJ). Water used was distilled and deionized.

Binary Mixture Results and Discussion

The intent of this series of experiments is to obtain high solubilization levels by mixing a more hydrophobic with a more hydrophilic surfactant. For the following examples, Tween 80 or Tween 85 are used as the more hydrophilic surfactant, and Span or Arlacel types are used as the more hydrophobic surfactant.

Synergistic mixtures of surfactants show increased solubilization capacity for many of the mixtures studied. A maximum value of solubilization is seen for most Span/Tween mixtures at a certain ratio. These solubilizations are much higher than any microemulsion

made with a single surfactant. Several mixtures can achieve solubilization of greater than 0.5 (v/v) water/oil, with the Arlacel 83/Tween 85 system achieving a maximum of 0.78 water/oil (see Table 3-7).

Cases with synergism. The binary surfactant mixture results are graphed with the Tween surfactant being the common factor, and the lines being defined by different Span surfactants. Figure 3-1 shows mixtures of Tween 85 with Arlacel 83, Span 20, 80 and 85. Figure 3-2 shows Tween 80 with the same Spans. Figure 3-3 shows Tween 20 with Span 20 and 80. Figure 3-4 shows Tween 21 with Span 20 and 80.

The Tween 85 systems show the greatest solubilization. The buildup to maximum solubilization with increasing HLB number is much more gradual than the sharp falloff after the maximum is achieved. This appears to be analogous to solubilization curves presented by Kon-No et al. [1971] who studied the effect of temperature on solubilization in W/O microemulsions. Though he used ionic surfactants, his graphs show multiple phase changes for a given temperature near the region of maximum solubilization. This could explain the extremely sharp drop-off that is seen, as the second microemulsion region that occurs when more water is added beyond the initial maximum solubilization region is not mapped out. For nonionic surfactants, the hydrophilicity of the surfactant is increased with decreasing temperature, so the temperature studies of Kon-No et al. [1971] may be qualitatively analogous to the mixture N_{HLB} excursions presented here.

Tween 80 showed maximum synergism with Span 20. Solubilization was also reasonable with Span 80. No synergism was observed with Span 85. As the HLB of Tween 80 is 15, higher HLB mixtures could be made than with Tween 85. This resulted in many

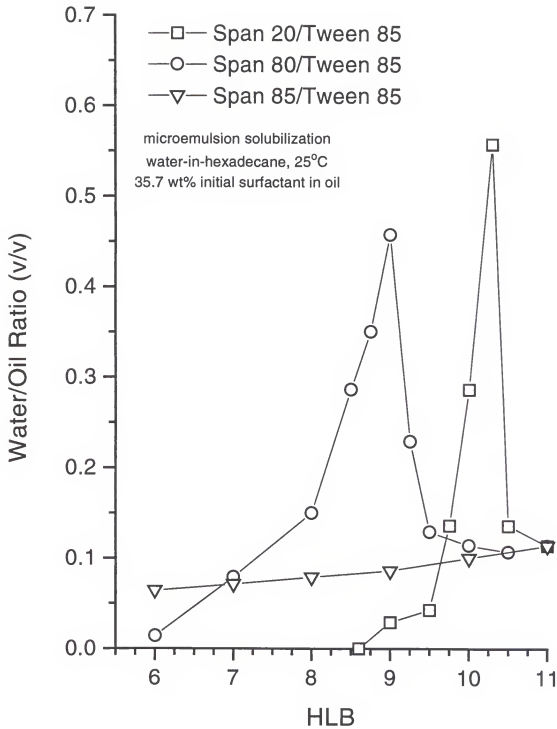

Figure 3-1. W/O solubilization, binary mixtures of Spans with Tween 85.

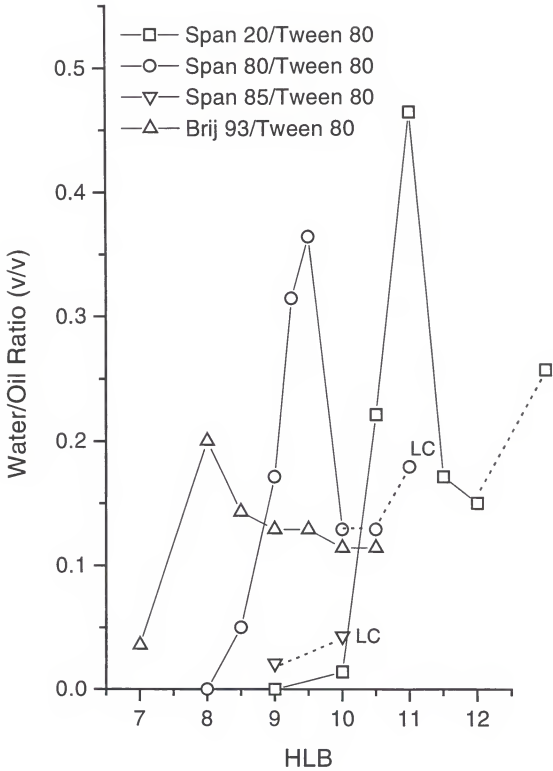

Figure 3-2. W/O solubilization, binary mixtures of Spans with Tween 80.

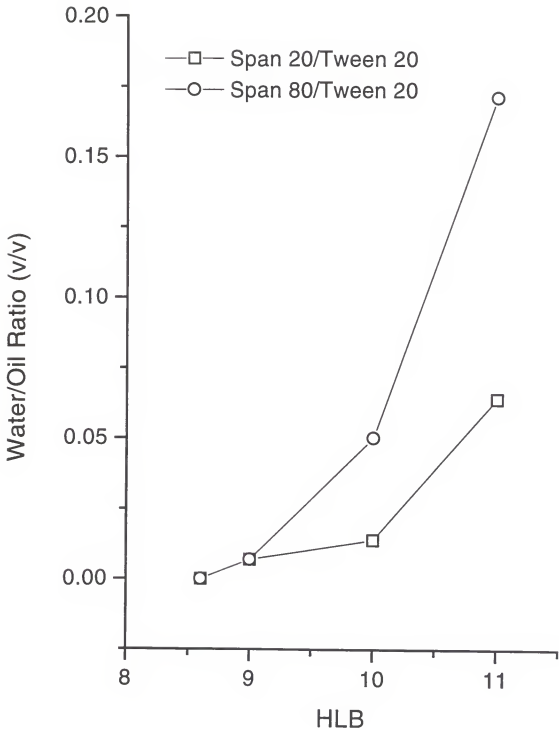

Figure 3-3. W/O solubilization, binary mixtures of Spans with Tween 20.

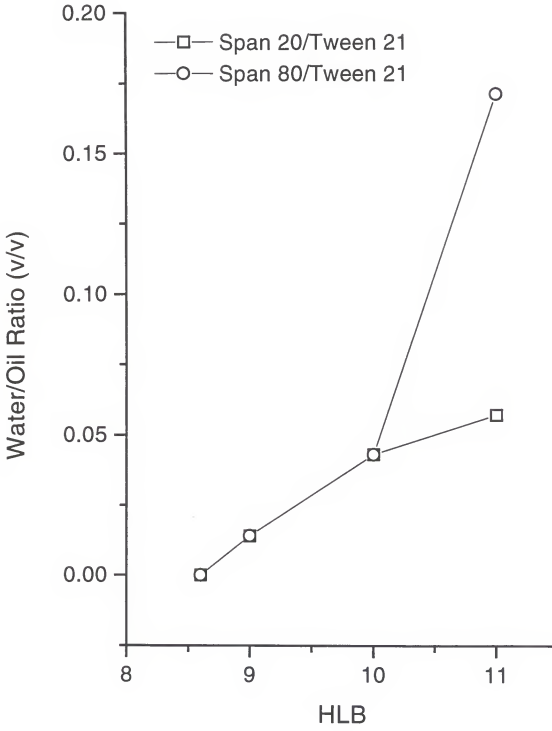

Figure 3-4. W/O solubilization, binary mixtures of Spans with Tween 21.

mixtures which solubilized significant water, but in the form of liquid crystals rather than microemulsions. Generally, liquid crystalline states were observed for mixtures with N_{HLB} greater than or equal to 12.

Synergism was less obvious with the other Tweens. Tween 20 and Tween 21 systems showed no maximum solubilization behavior. Solubilization was generally low, and increased with N_{HLB} until the onset of liquid crystalline states in the 10-11 range. It seems that much higher solubilization would be possible with these Tweens if the liquid crystal region occurred at higher HLB.

Cases without synergism. One of the exceptions showing no synergism is mixtures using Tween 81. This surfactant by itself displays an unusually high solubilization, and any mixture of Tween 81 with other Spans shows no improvement. Since Tween 81 has the lowest HLB (10) for any of the Tweens, mixtures with other Tweens were attempted to see if there was any improvement. No enhancement was seen with any of the Tween 81/Tween mixtures. Figure 3-5 shows Tween 81 with Span 20 and 80, as well as Tween 20, 80 and 85.

Another exception showing no synergism are mixtures involving Span 85. No enhancement in solubility is seen by mixing Span 85 with any Tween. As this is the most hydrophobic surfactant studied, with an HLB number of 1.8, it is possible that the majority of the Span 85 partitions into the oil phase and is not present to any appreciable extent at the interface. As seen in Figure 3-6, solubilization for mixtures of Span 85 and Tween 85 over the range studied corresponds quite well with the level predicted for hydration. This implies that the mixture may exist as a molecular mixture, with no formation of structure, such as

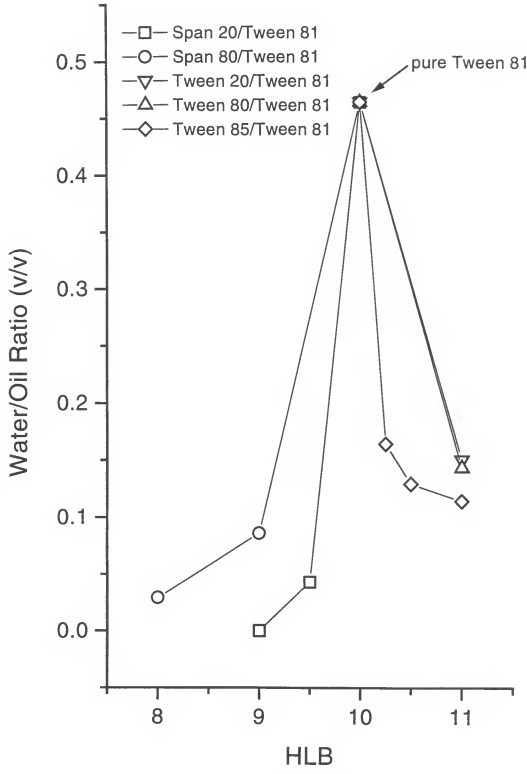

Figure 3-5. W/O solubilization, binary mixtures of Spans with Tween 81.

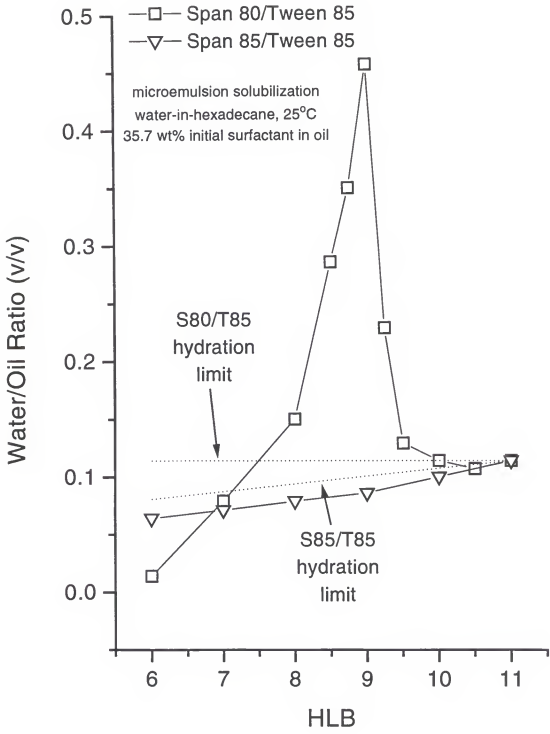

Figure 3-6. Solubilization assuming hydration, binary mixtures of Spans with Tween 85.

microemulsion droplets. Also, the QELS experiments on Span 85/Tween 85 mixtures showed little scattering. This would confirm the idea that this surfactant combination does not form microemulsion droplets, and the solubilization is only due to the hydration of the surfactant.

Hydration of the surfactant. Figure 3-6 shows solubilization curves for Span 80 and Span 85 with Tween 85, along with the estimated solubilization that would occur due to hydration, where only one water molecule per oxygen in the surfactant is solubilized. The graphs suggest that microemulsions may be formed for mixtures where excess solubilization occurs above the hydration line.

It may be assumed that the initial water added to a surfactant/oil mixture will result in hydration of the surfactant, and will not form microemulsion droplets. The solubilization by the Span 80/Tween 85 mixtures are mapped out in Figure 3-6, along with the hydration estimate. There are several regions of interest. It can be seen that for HLB values over 9.5, the solubilization tracks the hydration calculation quite well. No microemulsion droplets are formed here, as confirmed by QELS. An HLB of 11 is the upper limit for this mixture, as it is the HLB of Tween 85. Between HLB 8 and 9.5, there is a large excess of solubilization over the hydration limit. This is the region where a synergism between the surfactants is quite constructive in stabilizing the water droplets in the hexadecane. At HLB values of less than 8, one can see that the solubilization drops off to values below that predicted by hydration. In this regime, something must be preventing the surfactant from hydrating, as it does in the region from HLB of 9.5 to 11.

Formulation rules. HLB design rules may be found for microemulsions, analogous to the emulsion rules of Griffin [1949]. The optimum W/O microemulsion solubilization occurs in the HLB range of 8.5 to 11. This differs from the HLB range (3 to 6) that one would expect for W/O emulsions [ICI,1984]. Table 3-7 summarizes the maximum solubilization of water in hexadecane observed for various surfactants and binary combinations. Another HLB based rule is the onset of liquid crystallinity in the solution. Above an HLB of 12, apparently all formulations are liquid crystals.

Table 3-7. Maximum solubilization for Spans and Tweens.

Surfactant	HLB	max. solub. of water in oil (v/v)	wt% Tween in mixture
Single Surfactants			
Span 20	8.6	0.00	n/a
Tween 85	11	0.12	n/a
Tween 81	10	0.46	n/a
Surfactant Pairs			
Arlacel 83/Tween 85	8.5	0.78	66
Span 20/Tween 85	10.25	0.56	69
Span 80/Tween 85	9	0.46	70
Span 85/Tween 85	11*	0.11*	(100)
Span 20/Tween 80	11	0.48	38
Span 80/Tween 80	9.5	0.37	49
Span 85/Tween 80	--	(liq. crystal)	-
Span 20/Tween 20	--	(liq. crystal)	-
Span 20/Tween 80	--	(liq. crystal)	-
Span 20/Tween 81	10*	0.46*	(100)
Span 80/Tween 81	10*	0.46*	(100)
Tween 20/Tween 81	10*	0.46*	(100)
Tween 80/Tween 81	10*	0.46*	(100)
Tween 85/Tween 81	10*	0.46*	(100)

*No maximum observed, solubilization is for pure Tween surfactant.

Ternary Mixture Results and Discussion

Given the improvements seen with binary mixtures of surfactants, the possibility that ternary mixtures would lead to even greater solubilization was next to be explored. Having three components complicates the search for an optimum ratio of components, so initial attempts involved fixing the ratio of two of the surfactants, and mixing these two with the third.

The first ternary system studied was Span 20, Tween 80 and Tween 85. This system showed a sharp maximum in solubilization with respect to HLB, as can be seen in Figure 3-7. The peak is at a high HLB of 10.8. The surfactant ratio was x:1:1, so the relative amounts of the Tweens were equal, and only the ratio of Span 20 to the Tweens was changed to achieve a range of HLB values. Above N_{HLB}=11.5, liquid crystalline systems were formed.

The second system studied was Span 20, Span 80 and Tween 85. This system (Figure 3-7) had a peak and shape of the solubilization curve similar to that of the first. The surfactant ratio was 1:1:x, with equal amounts of Spans, and the ratio of Tween 85 to Spans changed to achieve different HLB values. The peak solubilization occurred at an HLB number which appears to be the average between the Span 20/Tween 85 peak and the Span 80/Tween 85 peak, suggesting that no synergism exists due to the Span/Span mixtures.

Effect of Surfactant/Oil Ratio on Solubilization

As all previous experiments were performed at a fixed surfactant/oil ratio (35.7 wt% surfactant), the dependence of solubilization on this parameter was not explored. Two systems were studied. The first was Tween 81, chosen because it had greatest water solubilization by itself, and the second was an N_{HLB}=10 Span 80/Tween 85 mixture.

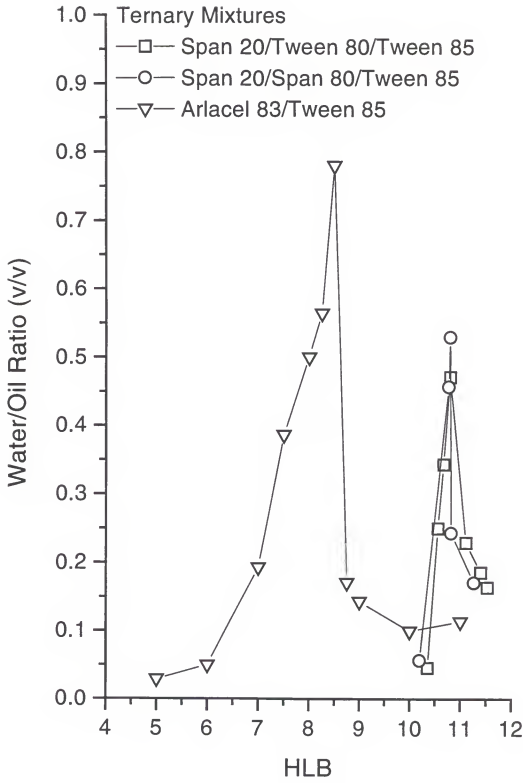

Figure 3-7. W/O solubilization in ternary Span/Tween mixtures.

Figure 3-8 shows water solubilization using Tween 81, and Figure 3-9 shows solubilization with the Span 80/Tween 85 mixture, vs. wt% surfactant. Additionally, water/surfactant ratio vs. water/oil ratio (Figure 3-10) is presented for the Span 80/Tween 85 mixture. Maximum solubilization vs. wt% surfactant was approximately linear for the Tween 81/water/hexadecane system. The Span 80/Tween 85 mixture showed an interesting deviation from this linear behavior. Above 20 wt% initial surfactant, the relationship appears linear. Below 20%, there is a region of excess solubilization, peaking at 10%. The peak at 10% is so high that solubilization is the same as the mixture with 30% surfactant.

Effect Of Oil Phase On Solubilization

Solubilization experiments were extended to alkane solvents other than hexadecane. Shorter linear alkanes were considered, as hexadecane is the longest chain alkane that is still a liquid at room temperature (MP=18.2 ^{o}C). Possibilities exist for synergistic effects between the oil and the surfactant (chain-length compatibility effect), as discussed in Shaio et al. [1996].

Experimental Procedure

Solubilization was performed as described in the previous section (Water/Hexadecane/Sorbitan Ester Microemulsions). Concern must be given to the evaporation of the oil, as the shortest alkane used, octane, has a boiling point of 125.7 ^{o}C.

Results and Discussion

Tween 81. In hexadecane, Tween 81 has the highest solubilization capacity of any of the surfactants. There is a drop-off in solubilization with the shorter alkanes, but the

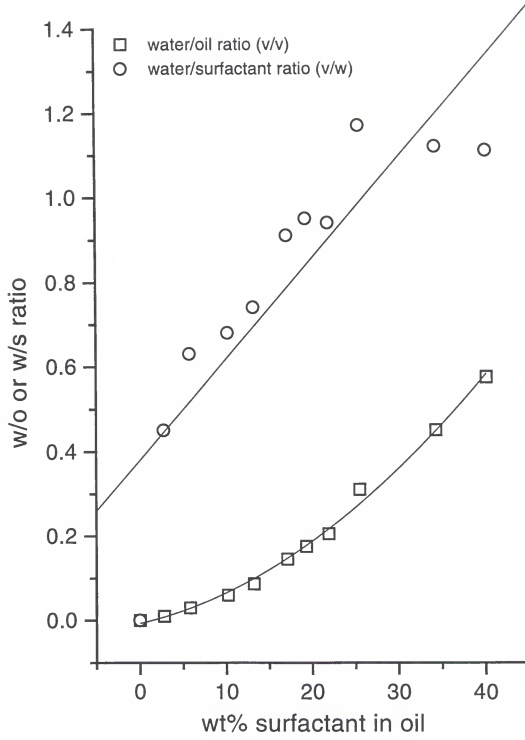

Figure 3-8. W/O solubilization, weight % excursion for Tween 81.

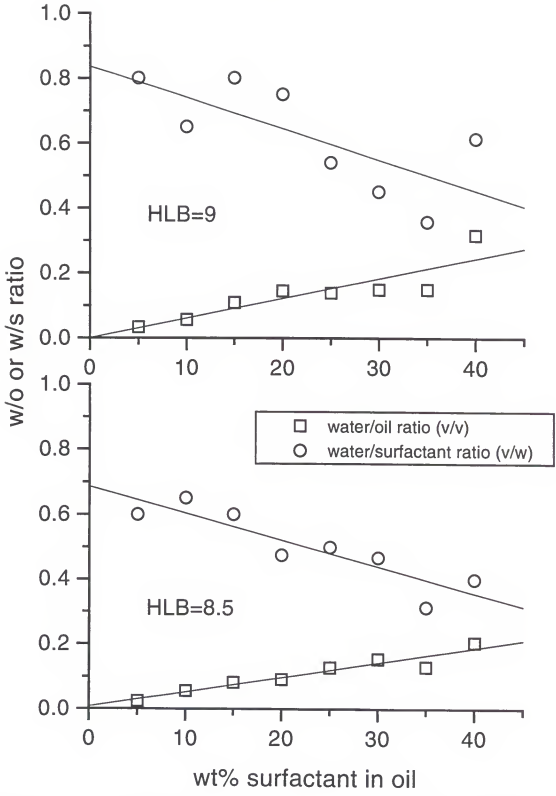

Figure 3-9. W/O solubilization, weight % excursion for Span 80/Tween 85 mixtures.

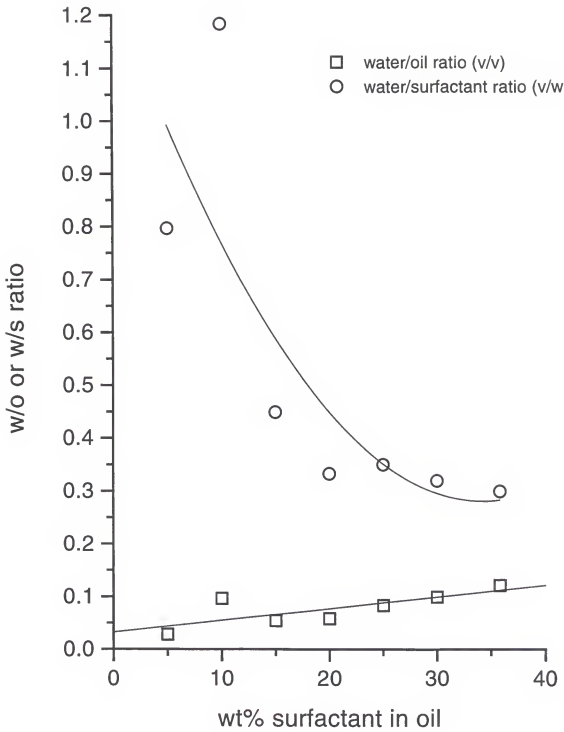

Figure 3-10. W/S ratio vs. S/O ratio, for Span 80/Tween 85 N_{HLB}=10 mixture.

decrease is not large. Figure 3-11 shows water solubilization vs. alkane carbon number for 20 wt% Tween 81 in the n-alkane series from decane to hexadecane. Solubilization of Tween 81 in corn oil was very poor. Several references mention the poor ability of triglycerides in forming W/O microemulsions.

Span/Tween mixtures. Figure 3-12 shows solubilization water in alkanes using Span 80/Tween 85, and Figure 3-13 shows solubilization water in alkanes using Span 20/Tween 85 mixtures, and Figure 3-14 shows solubilization water in alkanes different by four carbon atoms in length, using Span 20/Tween 85 mixtures. There is something unusual in the apparent solubilization maxima for C_8, C_{12} and C_{16}, as they seem significantly higher and more regularly spaced than the maxima for the other alkanes studied. There must be some explanation for this optimal four carbon step in the alkanes, perhaps there is some chain length compatibility argument that can be applied to explain this result.

Table 3-8. Maximum solubilization in different oils.

Surfactant	OIL	HLB	max. solubilization, water/oil, (v/v)
Tween 81	corn oil	10	0.02
Tween 81	diesel oil	10	0.02
Tween 81	cyclohexane	10	0.02
Igepal CO-430	cyclohexane	8.8	0.02
Igepal DM-430	cyclohexane	9.4	0.05
Arlacel 83/Tween 85	corn oil	10	0.05
Igepal CO 210/720	cyclohexane	9	0.33

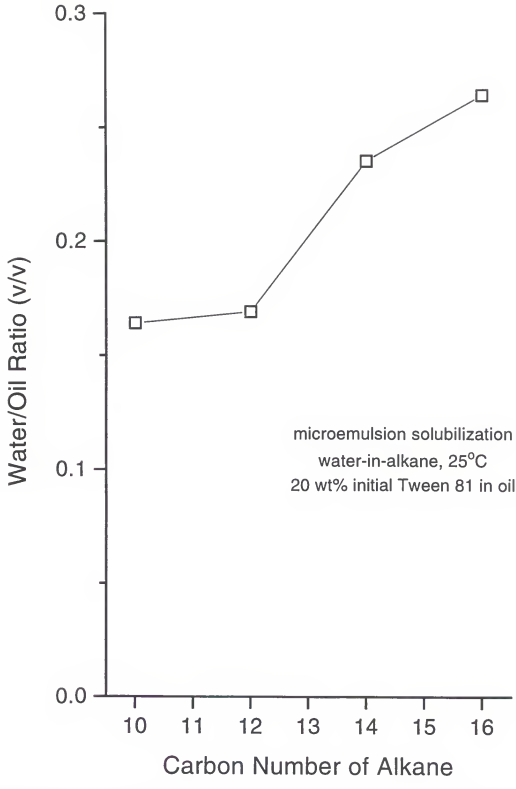

Figure 3-11. W/O solubilization in C_{10}-C_{16} n-alkane/Tween 81 microemulsions.

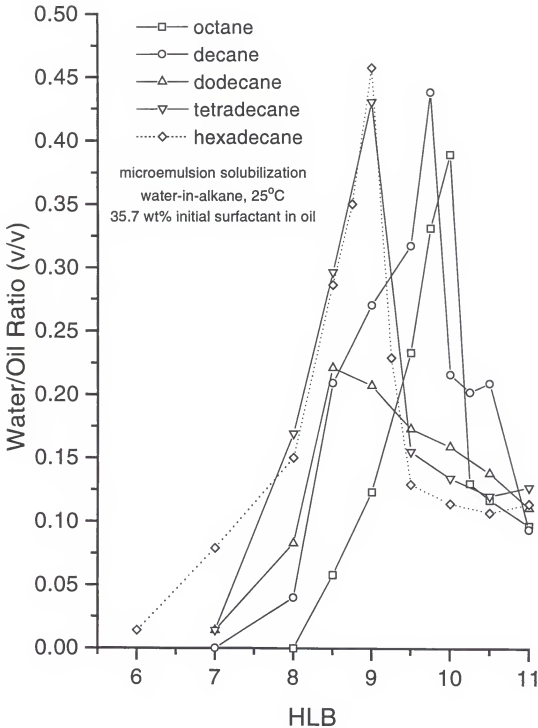

Figure 3-12. W/O solubilization in C_8-C_{16} n-alkane/Span 80/Tween 85 microemulsions.

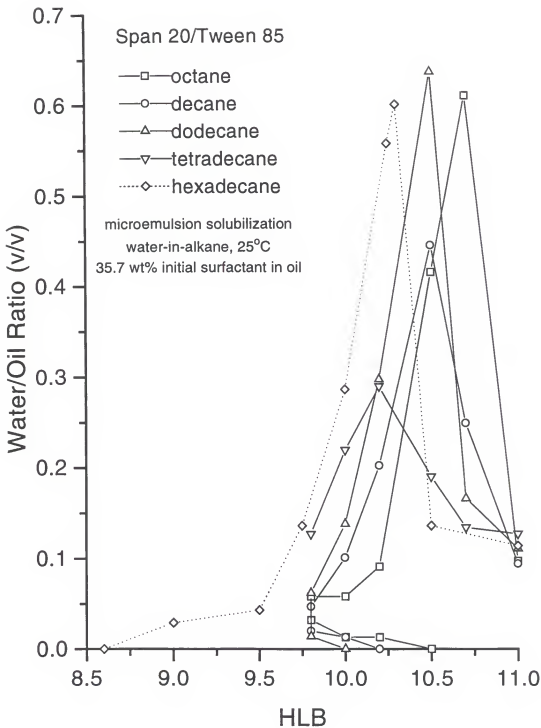

Figure 3-13. W/O solubilization in C_8-C_{16} n-alkane/Span 20/Tween 85 microemulsions.

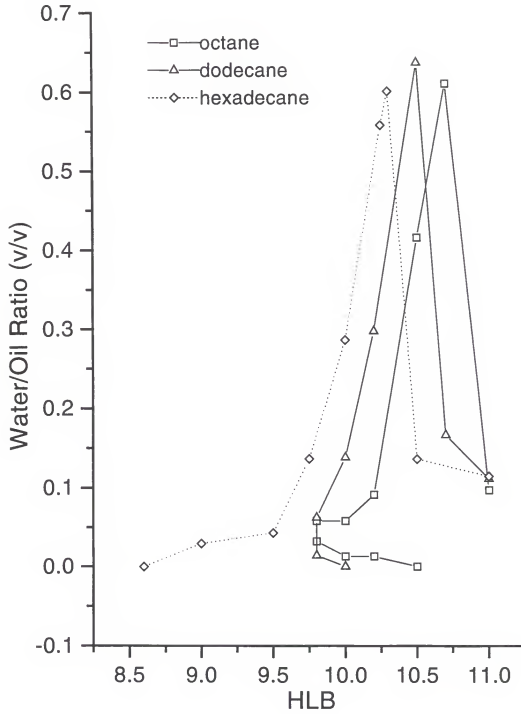

Figure 3-14. W/O solubilization in C_8, C_{12}, C_{16} n-alkane/Span 20/Tween 85 microemulsions.

Table 3-9. Mole fractions of Span and Tween 85 at the ratio of maximum water solubilization in different alkane oil phases.

Alkane	S20/T85 S20 mol%	S20/T85 T85 mol%	S80/T85 S80 mol%	S80/T85 T85 mol%
C_{16}	70	30	67	33
C_{12}	60	40	-	-
C_8	43	57	43	57

Interfacial curvature model. A possible explanation for the solubilization results in different alkanes can be made when one considers a model for the extent of oil penetration into the surfactant layer. One must consider the surfactant monolayer as being composed of a head group layer and a tail layer. When comparing a Span molecule (sorbitan alkylate) with Tween 85 (ethoxylated sorbitan trioleate), one sees that the Span has the much smaller head group relative to the size of the tail (Figure 3-15). If a monolayer were to be made entirely of Span, it would tend to curve towards the head group side (head group inside micelle or droplet) while Tween 85 would tend to curve the other way. At an oil/water interface, an excess of Span would cause a high interfacial curvature and thus small water-in-oil droplets. Adding Tween would tend to lower the curvature of the interface. A point is reached where sufficient Tween is added and the interface would be flat, and beyond this additional Tween at the interface would drive the curvature to flip the other way (Figure 3-15). This flat interface scenario is a reasonable model for the point of maximum solubilization, while the inversion of the direction of curvature is a possible explanation for the sudden collapse of solubilization when Tween is added just beyond the point of maximum solubilization. This can also be an explanation for the liquid crystal formation, which occurs when the interfacial curvature is optimally zero. This model

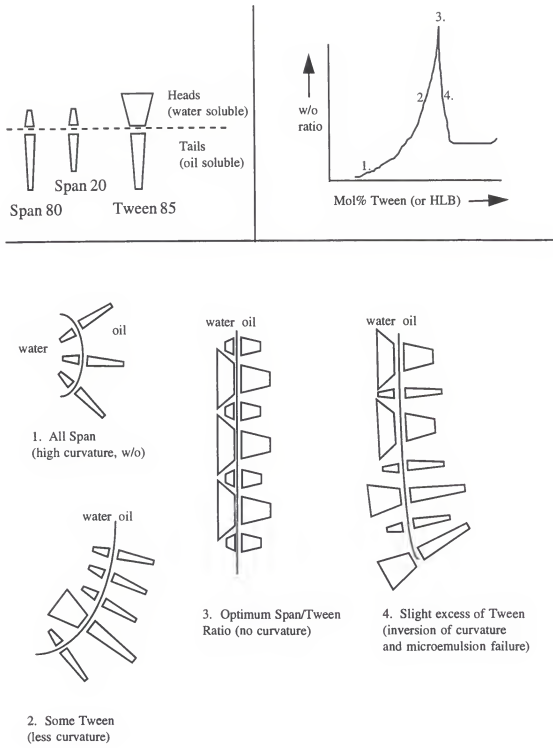

Figure 3-15. Curvature model for the solubilization behavior of Span/Tween W/O microemulsions.

of the curvature is related to the packing parameter developed by Israelachvili et al. [1976] and applied to the determination of aggregation structure.

The effect of the oil phase can also be explained by this model. It is reasonable to assume that a shorter alkane, such as octane, will penetrate into the tail layer of the interfacial film to a greater extent. Oil penetration will be in the tail side only, causing curvature to increase, resulting in smaller droplets, in favor of the W/O microemulsion (Figure 3-15). This expansion of the tail side of the interfacial film will thus allow more Tween to be present before the microemulsion fails. This is supported by the data in Figure 3-12 and 3-13, and summarized in Table 3-9, which show greater Tween present at microemulsion solubilization failure in the order octane > dodecane > hexadecane. The octane penetrates more into the tail layer than the other oils, and thus the Span/Tween/octane microemulsions have the greatest percentage of Tween at the point of maximum water solubilization.

Water/Cyclohexane/Nonylphenyl Ethoxylate Microemulsions

Given the success with the alkane/sorbitol ester mixtures, it was important to see if similar results would be found with oils and surfactants of different structure. Cyclohexane was studied as the oil phase, and POE nonylphenyl ethers as the surfactants (Igepal CO series). The different Igepals have varying amounts of polyoxyethylene. The POE number is an average, the distribution in POE numbers for a given average results from the lack of precision in the ethylene oxide polymerization reaction. The CO series has a nonylphenyl hydrophobic group. The nonyl- moiety is produced by polymerization of propylene, and

thus is a branched alkane structure. This microemulsion system was used by Kumar et al. [1993] for nanoparticle synthesis.

Experimental Procedure

Solubilization was performed as described in the previous section (Water/Hexadecane/Sorbitan Ester Microemulsions), but with different proportions. The Igepal CO and DM series, Emulphor and Alkamuls series of surfactants were supplied by Rhone-Poulenc, Inc. (Cranbury, NJ). The initial oil phase consisted of 1.5 g total of surfactant in 7.76 ml of hexadecane. Alternately, 1.2 g of total surfactant was dissolved in 6.23 ml cyclohexane (density=0.7791). These proportions result in 20 wt% initial surfactant in the oil phase. Cyclohexane (BP=80.7°C) is much more volatile than hexadecane (BP=287°C), so care must be taken to cap the sample vials during titration, if the sample is to be left stirring for extended periods.

Results and Discussion

Solubilization in cyclohexane. Table 3-10 shows mixtures of Igepal CO-430/CO-610, and CO-210/CO-720 in hexadecane. Figure 3-16 shows mixtures of CO-210/CO-720, as well as some single surfactants, in cyclohexane. The surfactant mixtures in cyclohexane performed fairly well. Surfactants were initially soluble in oil, unlike the hexadecane system. This Igepal/cyclohexane system is interesting, because it is the one used by Kumar [1993] for superconducting ceramic nanoparticle synthesis. CO-430 was used at 28 wt%. The results in Figure 3-16 clearly show the superiority in solubilization ability for mixtures of surfactants, over single surfactant systems. The mixture chosen was the most

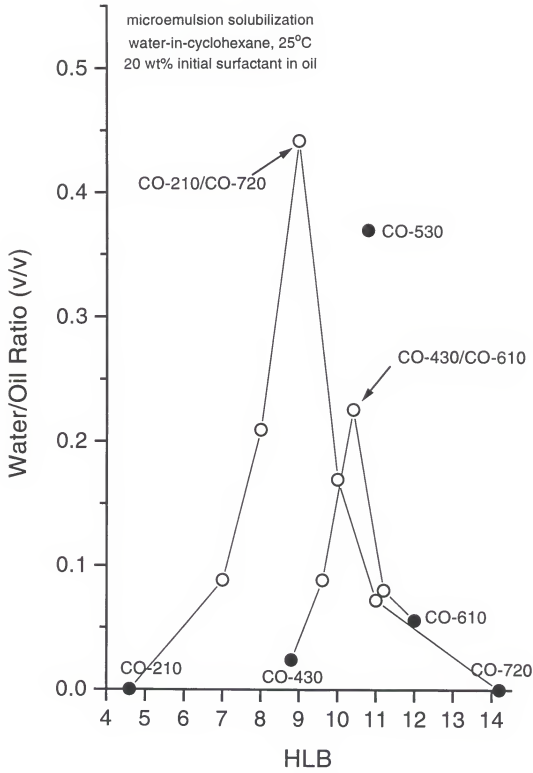

Figure 3-16. W/O solubilization, binary mixtures with Igepal CO series surfactants in cyclohexane.

hydrophobic Igepal CO, CO-210, with an N_{HLB} of 4.6, and the most hydrophilic that is still liquid at 25°C, CO-720, with an N_{HLB} of 14.2.

Table 3-10. Maximum water solubilization for Igepal CO mixtures in hexadecane and cyclohexane.

Surfactant	OIL	HLB	max. solubilization of water in oil, (v/v)
CO-430	hexadecane	8.8	0.14
CO-430/CO-610	hexadecane	9	0.026
CO-210/CO-720	hexadecane	7.74	0.097 (not max.)
CO-210/CO-720	hexadecane	8.72	0.23
CO-210	cyclohexane	4.6	0.0
CO-430	cyclohexane	8.8	0.016
CO-530	cyclohexane	10.8	0.37
CO-610	cyclohexane	12	0.056
Tween 81	cyclohexane	10	0.016
DM-430	cyclohexane	9.4	0.048
CO-430/CO-610	cyclohexane	10.4	0.23
CO-210/CO-720	cyclohexane	9	0.44

Solubilization in hexadecane. The solubilization results for the Igepal mixtures are not as impressive as for the Span/Tween mixtures in hexadecane, but much better in cyclohexane. Maximum solubilization is summarized in Table 3-10. The Igepal CO surfactant mixtures were not initially soluble in hexadecane. Only after the addition of an initial volume of water was a microemulsion state observed in hexadecane. Solubilization was observed in the N_{HLB} range of 7.7 to 9. At 9.5, no microemulsion phase was observed for the mixtures studied.

Possible explanations for the poor solubility in hexadecane may be the relative shortness of the hydrophobic moiety. All surfactants have the same nonylphenyl structure, which is short and multiply branched as compared to the long, linear lauryl and oleyl

structures in the Span and Tween surfactants. Poor steric hindrance of the nonylphenyl structures may cause poor microemulsion formation. The large difference in size between the hydrophobic moiety and the long POE chain of the hydrophilic moiety may result in poor packing of molecules at the interface, which may also disrupt microemulsion formation.

Electrolyte solubilization. One application of microemulsions is the preparation of nanoparticles, mixing w/o microemulsions prepared with different aqueous phases that will form an insoluble precipitate on contact. By mixing the microemulsions, collisions of microemulsion droplets cause the formation of nanoparticles of the precipitate material, much smaller in size than can be made by traditional methods. Figure 3-17 shows the solubilization of aqueous electrolyte solutions in Igepal CO-430 and cyclohexane. The applicability of microemulsion solubility studies with pure water to solubilization of electrolyte solutions is not obvious. The current effort examined solubilization of monovalent (NaCl) and divalent ($CaCl_2$) solutions in Igepal CO-430 in cyclohexane. This system has been used in several nanoparticle synthesis studies, with cations of up to tetravalent charge. The solubilization increases with ionic strength and valence for the solutions studied, up to 1 M concentration.

Conclusion. It appears that similar rules governing the formation of W/O microemulsions, based on HLB, are more general and can be applied to a variety of surfactant systems. These rules should help reduce the number of microemulsion systems screened in the development of new microemulsion applications.

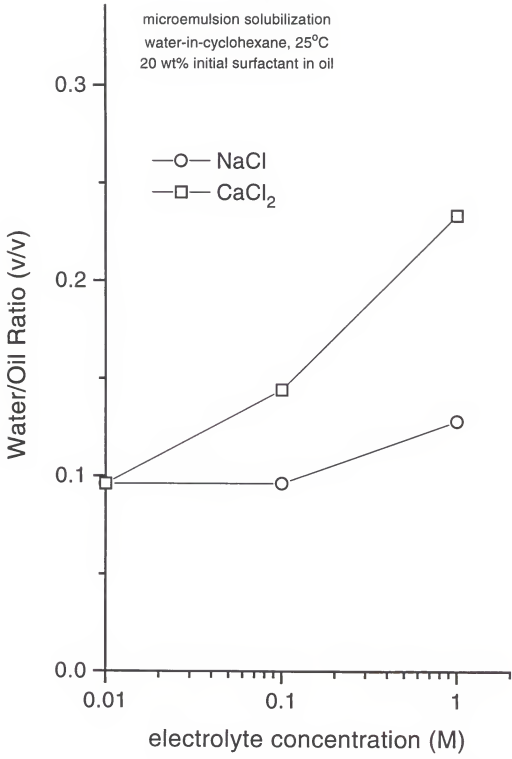

Figure 3-17. Solubilization of electrolyte solutions in Igepal/cyclohexane W/O microemulsions.

Other Solubilization Experiments

Solubilization in hexadecane with several other pure surfactants was tried, as well as a few other systems of binary mixtures, with the most successful being the Span/EL-719 mixtures (Figure 3-18). Solubilization in other oil phases was tried, including corn oil (a triglyceride) and diesel oil. Tables 3-11 and 3-12 summarize the surfactants and oils used in both successful and unsuccessful attempts at solubilization.

Experimental. ICI (Wilmington, DE) supplied the Span, Brij, and Alkamuls EL-719 surfactants. Corn oil, peanut oil and olive oil were commercial products available in any supermarket. Diesel fuel was purchased directly from an Exxon service station.

Results. Several O/W microemulsion solubilization experiments (the inverse of the previous W/O studies) were performed using water and hexadecane. Single surfactants were tried over a wide HLB range. No successful solubilization was achieved. Over the HLB range of 10 to 13.5, opaque gels were formed, while outside that range, two liquid phases were observed.

Table 3-11. Other successful maximum solubilization experiments.

Surfactant	**OIL**	**HLB**	**max. solubilization water/oil, (v/v)**
Span 20/EL-719	hexadecane	11	0.26
Span 80/EL-719	hexadecane	9	0.21
Span 20/Brij 98	hexadecane	11	0.13

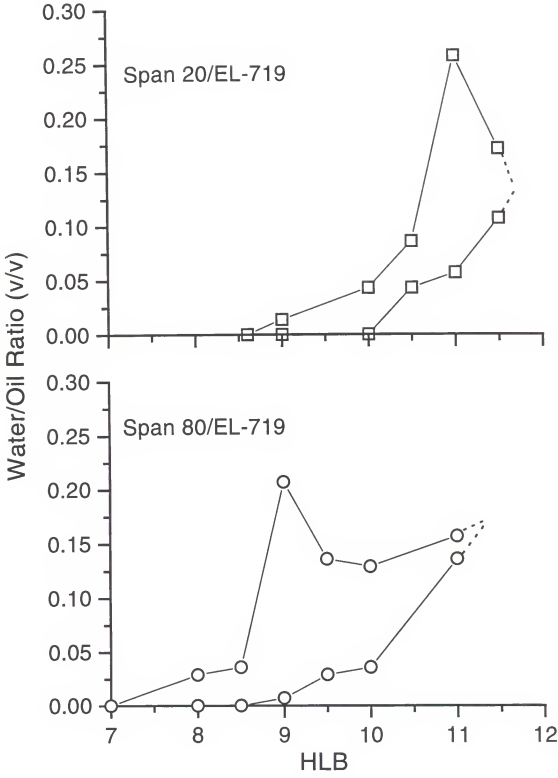

Figure 3-18. W/O solubilization in hexadecane/Span/ethoxylated castor oil microemulsions.

Table 3-12. Unsuccessful w/o maximum solubilization experiments.

Surfactant	POE #	OIL	HLB	max. solubilization water/oil, (v/v)
Igepal CO-610	7.5	hexadecane	12.2	never clear
Igepal DM-530	9	hexadecane	10.6	liquid crystal (LC)
Igepal DM-710	15	hexadecane	13.0	LC
G-1086	40	hexadecane	10.2	LC
G-1096	50	hexadecane	11.4	LC

Light Scattering Experiments

Quasi-elastic light scattering is a powerful technique for determination of macromolecular or particle size of these objects in a solution. Light scattering has been used in this research to determine the presence of microemulsion droplets, as well as to quantify the trend of droplet size with increasing surfactant/oil ratio.

Experimental. Dynamic light scattering measurements were performed using a Brookhaven Instruments Corp. (Holtsville, NY) model BI-2030 correlator, 200SM laser light scattering goniometer, and EMI-9865 photomultiplier cathode. Light scattering measurements were taken at a scattering angle of 90^{o}, using a Spectra Physics (Mountain View, CA) argon ion laser operating at a wavelength of 514.5 nm.

Samples were prepared at different volume fractions (ϕ), defined as:

$$\phi = (V_s + V_w)/V$$

where V is the total volume of the mixture, V_s is the volume of surfactant added and V_w the volume of water added. Extrapolation to zero volume fraction is done. Samples were filtered through a 0.2 micron PFT membrane and placed into a clean cylindrical cell. Samples were maintained at $25^{o}C$ during the measurements.

Data analysis involves an autocorrelation analysis of the time variation of the scattered signal. The Brookhaven Instruments software provides a particle size measurement and error, based on a monodisperse size distribution assumption required by the Stokes-Einstein relation. A cumulant analysis is also performed which assumes multiple exponential decay signals, and calculates the apparent mean particle size for a polydisperse mixture.

Results. Quasi-elastic light scattering measurements were taken on Span 85/Tween 85 samples, and on Tween 81 samples, in order to help elucidate the microstructure. A real analysis problem exists for these microemulsions, in that an absolute diffusion coefficient (and thus droplet hydrodynamic radius) cannot be absolutely measured, as the droplet size is found to be a relatively strong function of the light scattering sample time. This dependence suggests that one or more of the assumptions needed for QELS analysis is being violated (monodisperse, no interparticle interactions, sufficiently low particle density to avoid multiple light scatter).

Droplet size determination was done for Tween 81 surfactant in hexadecane, with initial surfactant/oil ratios of 20, 25 and 30%. Water is present at the maximum solubilization value, a water/oil ratio of 0.263, 0.327, and 0.389, respectively. This represents 2.0 ml water in 7.8 ml oil, 2.5 in 7.8, and 2.9 in 7.6 ml. Droplet size is shown to increase as surfactant/oil or water/oil increases. (see figure) Both the single exponential decay calculation (higher droplet radius value) and the polydisperse calculation (lower radius value) are presented.

The effect of sample time of the collection is also investigated. For the 30 wt% surfactant/oil sample, the sample time was varied from 1 to 50 microseconds. The change in measured droplet size is significant with the change in sample time. The droplet size is expected to increase with increasing water solubilized in the oil. The change in calculated particle diameter with a change in sample time is expected for a polydisperse sample. The error in the gamma value for the cumulant analysis is lower than the error in gamma for a single exponential, lending weight to the assumption that we have a polydisperse sample.

Conclusions

From the above experiments on W/O microemulsions, the following can be concluded:

1. Mixtures of surfactants generally lead to superior solubilization results for water-in-oil microemulsions. This has been for mixtures of sorbitan esters (Spans) and ethoxylated sorbitan esters (Tweens) in hexadecane, and mixtures of nonylphenyl ethoxylates in cyclohexane.
2. When synergism occurs, solubilization is greater than simple hydration of the surfactant molecules.
3. Mixtures do not always lead to improved solubilization. No synergism is seen for mixtures of Spans and Tweens with Tween 81. No synergism is also demonstrated for the Span 85/Tween 85 mixture.
4. The highest solubilization achieved for binary mixtures of Spans with Tween 85 is 0.55 water/oil ratio. The best solubilization for ternary mixtures is 0.78 water/oil.

5. Good nonionic water-in-oil microemulsions can be made without the use of cosurfactants.
6. Optimum water-in-oil microemulsions occur in the HLB range of 8 to 11.
7. The molar ratio of Span to Tween seems to be an important factor in selection of the best mixing ratio of surfactants, in addition to the optimum HLB range.
8. A curvature model has been developed to explain the shape of the solubilization vs. HLB curves for the Span/Tween mixtures, and the dependence of these curves on the oil phase, based on oil penetration into the tails of the surfactant interfacial layer.

CHAPTER 4
SURFACTANT MICELLAR LIFETIME

Introduction

Micellar lifetime, or stability, is a fundamental property of surfactants that can influence many of the processes where surfactants are used. Although micelles are drawn in textbooks as well defined, static aggregates, in reality most micelles have very short lives, completely disintegrating and reforming from surfactant monomers often in time scales of milliseconds.

The influence of micellar stability on technological processes has been an active area or research for the group of Professor Shah for a decade now, as reviewed in [Huibers et al., 1996a] (Figure 4-1). Following in the footsteps of several researchers before me, especially Dr. Seoung-Geun Oh, I have conducted a number of studies on the influence of certain additives on the micellar stability of sodium dodecylsulfate (SDS), as well as studies on the influence of micellar stability on processes of technological interest, such as foaming, solubilization, detergency, fabric wetting, and emulsification [Huibers et al., 1996a]. These micellar lifetime investigations were carried out using the pressure-jump technique with conductivity detection. We study micellar stability because of its potential to influence many such processes, and knowledge of the effects of certain types of additives on micellar stability helps make our understanding more complete.

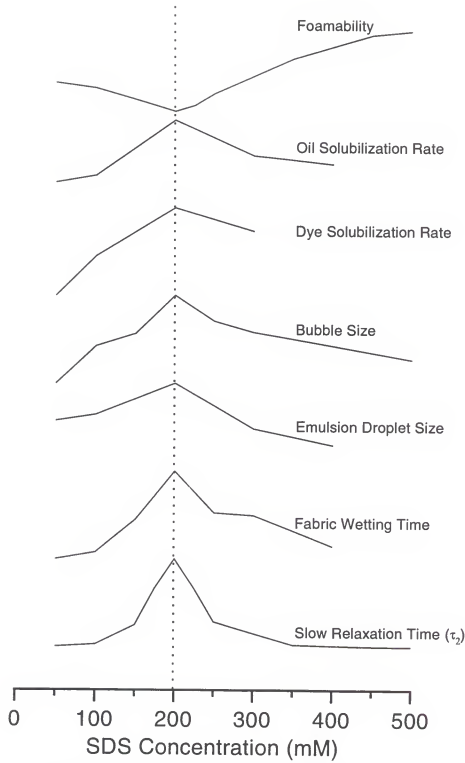

Figure 4-1. Effect of micellar lifetime (slow relaxation time) on technological processes.

Anionic Surfactants

All initial work on micellar lifetime was to establish the magnitude of the change in lifetime with the concentration of the surfactant. It was shown that lifetime could change by several orders of magnitude, depending on concentration. For several anionic surfactants, micellar lifetime was shown to increase by orders of magnitude up to a critical concentration (200 mM for SDS), and fall after that point [Huibers et al., 1996a; Lessner et al., 1981]. For several cationic surfactants, the increase in stability with concentration is more gradual, and then plateaus without displaying an obvious maximum stability value (see Cationic Surfactants section). Finally, for nonionic surfactants, micellar lifetime seems to drop with an increase in concentration [Lang et al., 1972a, b; Platz, 1981; Strey and Pakush, 1986]. Additionally, the influence of temperature has been studied, demonstrating a strong decrease in micellar lifetime with increasing temperature [Inoue et al., 1978; 1980].

Since all practical applications of surfactant involve the presence of other species besides surfactant and solvent, it is important to establish what the effect of these will be on micellar lifetime, in order to have a better understanding of the influence of these additives on the technological processes affected by micellar lifetime. Initial work by Leung and Shah [1986] studied the influences of short chain alcohols and water soluble polymer on SDS micellar stability, and Oh and Shah [1991] later studied SDS and some additional alcohols. Lessner et al. [1981a, b] studied the influence of salt on micellar lifetime, in this case $NaClO_4$ on SDS and sodium tetradecyl sulfate micelles.

I have extended these additive investigations, by studying the influence of longer chained alcohols (octanol through dodecanol), glycerol, large counterions of the tetraalkyl ammonium bromide class, nonionic surfactants (Tween 80) and electrolytes (NaCl, glycine, sodium octanoate) on SDS micellar lifetime.

Influence of Alcohol Cosurfactants on Micellar Lifetime

Earlier studies of the addition of alcohols to SDS micelles focused on the shorter alcohols. Generally, these shorter alcohols tend to destabilize the micelles. Leung and Shah [1986] added different concentrations of methanol through pentanol to 100 mM SDS micelles (Figure 4-2) [Huibers et al., 1996a]. Methanol, ethanol and propanol have a small effect on micellar lifetime, with τ_2 slowly decreasing with concentration. Given the solubility of the alcohols in water (Table 4-1), it appears that these alcohols do not partition extensively into the micelle, and the lower stability may be due to the nature of the solvent (water/alcohol) mixture. Butanol seems to have an effect of decreasing micellar lifetime, by over an order of magnitude for concentrations over 300 mM, but pentanol is the most interesting of the shorter alcohols, increasing micellar stability in 100 mM SDS by over a factor of two at 50 mM pentanol, but then sharply decreasing micellar lifetime for concentrations over 150 mM. Oh and Shah [1991] showed that hexanol increased the micellar stability of 50 mM SDS, up to a 70 mM hexanol concentration, and decreased τ_2 above that. From Table 4-1 it can be seen that the solubility of hexanol in water is 59 mM at 25°C, so it may be reasonable to assume that alcohol will stabilize the SDS micelles, as long as the alcohol will partition into the micelles (not the case for methanol through propanol),

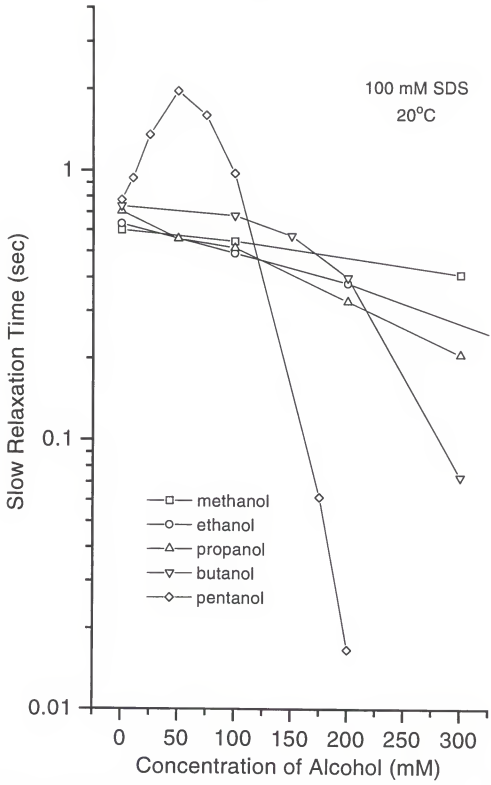

Figure 4-2. Variation of the slow relaxation time (τ_2) of 100 mM SDS as a function of alcohol concentration [Leung and Shah, 1986].

and as long as the ratio of alcohol to surfactant is not too high, as can happen when low alcohol solubility in water forces the alcohol to partition to a large extent into the micelles at higher alcohol concentrations.

Table 4-1. Solubility of n-aliphatic alcohols in water at 25°C [from Shinoda and Becher, 1978].

alcohol	solubility (mM)
butanol	970
pentanol	250
hexanol	59
heptanol	14.6
octanol	3.8
nonanol	0.97
decanol	0.234

Results. New measurements were taken of the micellar lifetime of SDS mixed with the higher alcohols, octanol, decanol, and dodecanol, were tested using the pressure jump technique. All were shown to increase the micellar lifetime of 100 mM solutions (alcohol + SDS concentration total of 100 mM). Due to the low solubility of decanol and dodecanol, it is expected that these alcohols will partition entirely into the micelles. Octanol has a low solubility of 3.8 mM, and this may partly explain the reason for the initial decrease in micellar lifetime of the mixture at 5 mM octanol + 95 mM SDS (Figure 4-3) [Huibers et al., 1996a]. From these results, combined with the previous work, some conclusions can be drawn about the influence of alcohol on micellar stability, as summarized in Table 4-2.

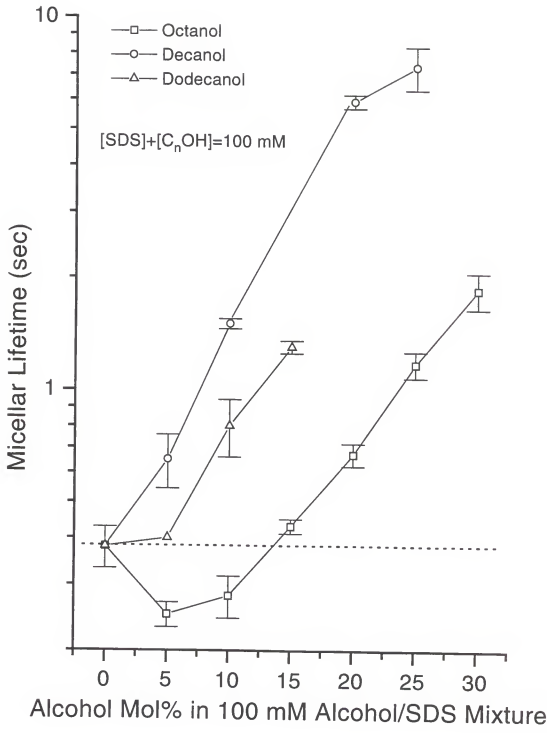

Figure 4-3. Slow relaxation time for mixtures of SDS and higher alcohols. The concentration of the mixtures remains constant at 100 mM (SDS+alcohol).

Table 4-2. Rules for alcohol influence on micellar stability.

1. alcohol initially increases the stability of micelles 2. micellar stability decreases for high alcohol/surfactant ratios *also:* • short chain alcohols do not partition into micelles • low aqueous solubility forces partitioning of alcohol into micelles

One issue in working with SDS solutions are questions about the apparent 'aging' of the solution. No satisfactory measurements have been published on the changes over time that have been seen in solution properties. It is interesting to note that the micellar lifetime of 5 mM dodecanol + 95 mM SDS is essentially the same as 100 mM SDS. The hydrolysis of SDS over time has been attributed to a change in observed properties over time, with SDS decaying into dodecanol and sulfate ions. This micellar lifetime result suggests that the decay of even a few percent of the SDS will not influence processes using SDS that are influenced by micellar lifetime.

Influence of Glycerol on Micellar Lifetime

The stability of SDS micelles, as measured by the slow relaxation time, has been well characterized [Huibers et al., 1996a; Oh et al., 1996]. Micelle stability increases with concentration above CMC to ?00 mM, then decreases. When glycerol/water mixtures are used as the solvent, one would expect changes due to the increased viscosity of the mixture, as well as the weaker solvent interaction as measured by a decrease in surface tension. The effect of additives on micellar properties has been well established for just one property, the CMC. van Os et al. [1993] has tabulated literature values of micellar properties, for pure

surfactants in aqueous solution, as well as for solutions with solvent and electrolyte additives. Such additives change the nature of the solvent, by changing the structure of water. Water normally forms a complex and dynamic hydrogen-bonding network, and additives modify this by requiring that some of these hydrogen bonds be broken, and new interactions formed with the additive. These changes have been accounted for in models by a change in the dielectric constant of solubility parameter of the solvent.

For a related compound, ethylene glycol, the solubilization parameter increases for glycol/water mixtures, resulting in increased solubility of the surfactant monomer and thus a higher CMC. This can also be determined from the surface tension of the solvent mixture, which is lower than that of pure water. This indicates that the solvent intermolecular forces are weaker, which will also allow an increased solubility of the surfactant.

As far as the author is aware, no previous work has been done on the effect of solvent mixtures on micellar stability. In this thesis the micellar stability of SDS at different concentrations is presented for 50/50 glycerol/water mixtures, and the effect of glycerol/water ratio is examined for 100 mM SDS.

Viscosity of glycerol/water mixtures. Glycerol is a solvent similar to water in that it engages in extensive hydrogen bonding with itself, resulting in a surface tension of 63 dyne/cm, comparable to 72 dyne/cm for water, and much higher than the 22-30 dyne/cm of a typical organic solvent. The addition of glycerol to water increases viscosity, but with a very nonlinear relationship to the volume fraction. Glycerol has a viscosity of 1000 cp at 25°C, and water has 0.89 cp. If the influence of adding glycerol to water on micellar

stability was only a viscosity effect, essentially slowing the transport of surfactant monomers to and from the micelle, then one would expect changes in micellar lifetime would be proportional to changes in viscosity. When measured, however, the change in micellar lifetime with the addition of glycerol is not so simple.

One can model the strong nonlinear nature of the viscosity of glycerol/water mixtures. The hyperbolic formula proposed by Waterman et al. [1960] for vapor-liquid equilibrium models provides an excellent fit to the data [CRC Press, 1980] when the log of the viscosity is considered. The resulting equation is

$$\log \eta_{mix} = x(1-x)/(-0.4722+0.31977x) + \log \eta_w + x(\log \eta_g - \log \eta_w)$$

where η_g is the viscosity of glycerol at 20°C (1412 cp), η_w is the viscosity of water (1.01 cp), and x is the weight fraction of water in the mixture. As can be seen in Figure 4-4, the fit to the data is quite good, and a sharp rise in viscosity is seen as the mixture approaches pure glycerol.

The addition of glycerol to the solvent causes a significant decrease in the conductivity of the micellar solution (Figure 4-5). One might expect that addition of a second solvent that lowers the intermolecular interactions in the solvent (as can be measured by glycerol/water surface tension) would cause an increase in CMC, and also an increase in conductivity. The viscosity also plays a role, with increasing viscosity causing a decrease in conductivity, and this must be the dominating factor.

Micellar lifetime. Addition of short chain alcohols such as methanol, ethanol and propanol, which are completely soluble in water, have been shown to decrease micellar

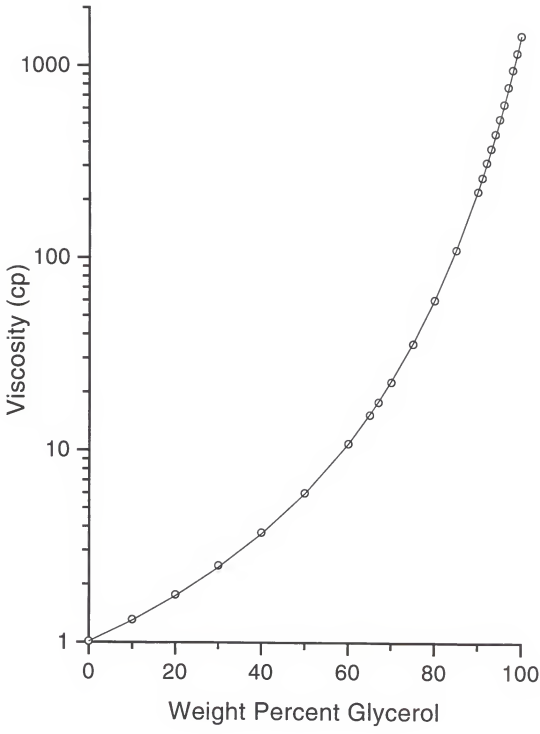

Figure 4-4. Viscosity of glycerol/water mixtures [CRC Press, 1980].

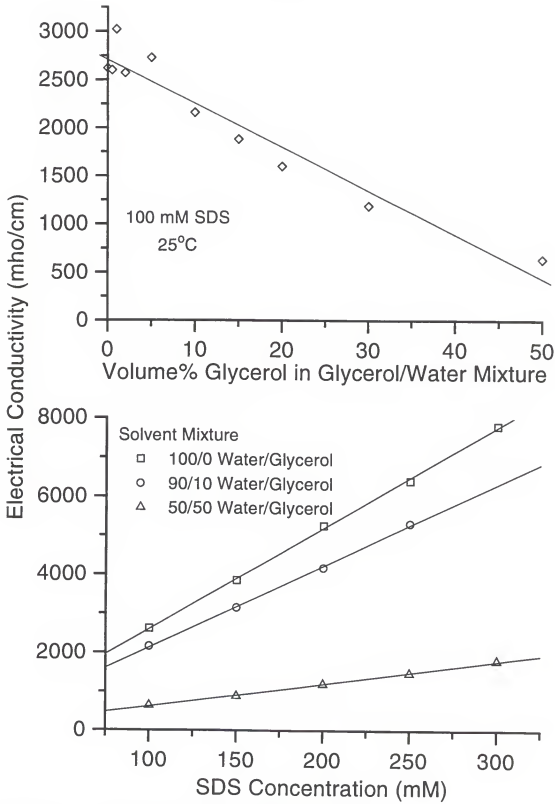

Figure 4-5. Conductivity of glycerol/water/SDS mixtures.

lifetime (Figure 4-2) [Huibers et al., 1996a]. It was expected that glycerol would do the same, and measurements at 1-10 wt% glycerol in water show the same trend (Figure 4-6). The micellar lifetime for 100 mM SDS is approximately 200 ms in water, falling to 30 ms for 10% glycerol in water as the solvent. The most unexpected result is the appearance of an apparent third lifetime, which appears above 10% glycerol. The initially observed decay time, which we will call τ_2, continues to decrease above 10% glycerol, with an apparent linear relationship between the glycerol weight fraction and the logarithm of the decay time. The τ_2 is too short to measure with more than 30% glycerol, as it falls below 1 millisecond. The new decay time, which we will call τ_3, rises slightly and appears to plateau at approximately 1.0 sec, and was not detected at concentrations below 10% glycerol.

At a constant 1:1 glycerol/water ratio, the micellar lifetime vs. SDS concentration also show some interesting features. When compared to SDS in pure water (Figure 4-7), the peak in micellar lifetime observed at 200 mM appears shifted to lower concentrations. This shift causes the glycerol/water τ_2 values to be higher than pure water in some cases, and to be lower in other concentrations, as seen in the Figure. The lifetime measured here for the glycerol/water mixtures is probably τ_3, as the τ_2 as measured for 100 mM SDS is probably too short to measure.

The physical meaning of τ_3 is not readily apparent. Some initial film stability tests for glycerol/water/SDS mixtures show that film stability greatly increases with the addition of glycerol. A micellar role in film stability has been established [Patel et al., 1996], with a decrease in micellar stability causing an increase in film stability. One would also

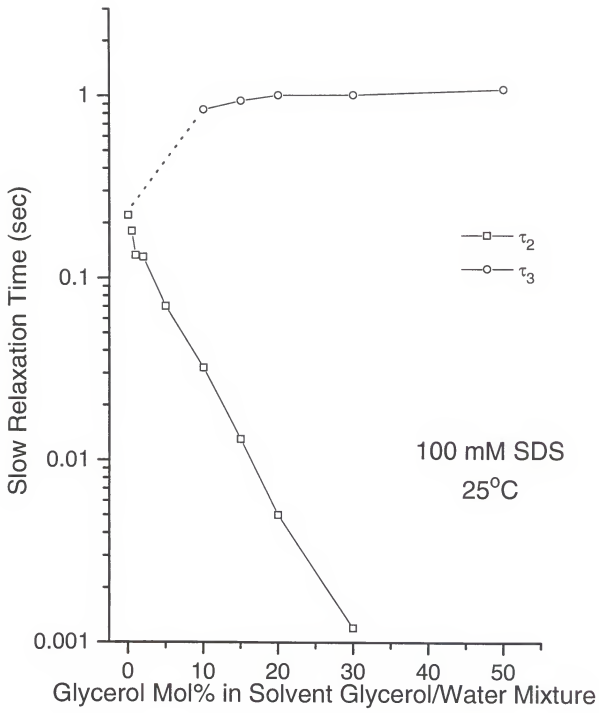

Figure 4-6. Slow relaxation time of 100 mM SDS with different glycerol/water ratios.

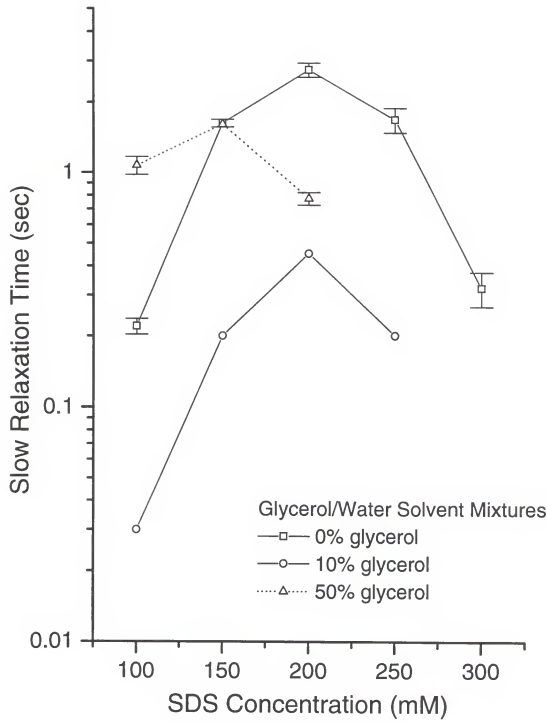

Figure 4-7. Slow relaxation time of SDS at a 1:1 glycerol/water ratio.

expect that an increase in the bulk viscosity of the film liquid by addition of glycerol would also act to increase film stability. Measurements of film stability suggest that the break time increases several times greater than the increase in viscosity, suggesting a role for micellar stability. As it is the τ_2 that decreases and not τ_3, this suggests that the former is the micellar lifetime as measured in previous studies, related to the time involved in complete formation or destruction of micelles from monomer, and thus the physical meaning of τ_3 is still unexplained. It is not surprising that this τ_3 has not been seen before, with no apparent solvent mixture data besides the short chain alcohols in the literature. It may be that τ_3 can be seen in alcohol/water mixtures, although the concentrations in previous studies were probably too low for it to become apparent. From Figure 4-2, alcohols were added at up to 300 mM, which amounts to 0.96, 1.38 and 1.80 wt% for methanol, ethanol and propanol, respectively, well below the 10 wt% where τ_3 was first observed in glycerol.

Influence of Counterion Size on Micellar Lifetime

The counterion plays a role in the micellar stability of ionic surfactants. Until recent years, little has been done to study this phenomenon. Oh and Shah [1993a] first measured the effect of counterions on SDS micelles. Blute et al. [1994] studied the influence of large counterions on foam stability, establishing that the tetraalkyl ammonium salts can be effective antifoaming agents for anionic surfactant solutions. We seek to explain this effect in terms of micellar stability.

Effect of antifoaming agents on micellar stability. The tetraalkyl ammonium salts have a demonstrated foam destabilizing ability. This has been attributed to their large size,

which alters the packing of surfactant head groups at the foam interface. If this change in packing serves to decrease the surface viscosity, foams will be less stable. The role of micellar stability on foamability has also been demonstrated, where more stable micelles result in less stable foams. The micelles act as a reservoir of surfactant, which may be drawn upon by thinning foam films. If the micelles are too stable, then the foam films do not receive the necessary surfactant and may break.

The effect of addition of tetraalkyl ammonium chloride (3, 30 mM) on the micellar stability of SDS micelles (150 mM) is investigated, with alkyl groups ranging from one to five carbons. These large cations act to destabilize micelles to a much greater extent than addition of an equivalent amount of sodium ions to solution. This can be attributed to the effect of their size on decreasing the packing density of the sulfate head groups at the micellar surface, and the resulting decrease in surface viscosity. Micellar stability thus has a less significant contribution to foam stability than surface viscosity.

Recent work has demonstrated that foam properties can be effected by micellar stability [Oh and Shah, 1991]. Blute et al. [1994] have demonstrated that large organic counterions can act as better antifoam agents than more traditional antifoamers such as tributyl phosphate and 2-ethylhexanol. They attribute the antifoaming ability of these large counterions to the decrease in packing density of the surfactant head groups, resulting in a less condensed film with lower surface viscosity.

Normally, addition of counterions leads to two counteracting effects: foam stability is decreased by addition of ions which reduce the electrical repulsion between the ionic

double layers on both sides of the liquid film, and is increased by the decrease in repulsion between adjacent surfactant head groups, causing a more condensed film of higher surface viscosity [Bikerman, 1973; Rosen, 1989].

To understand the impact of micellar stability on the action of antifoaming agents, we undertook a study of the effect of these large organic counterions on the micellar stability of SDS solutions. Micelles form a reservoir of surfactant in solution. When a foam film is thinned to the point where there is a depletion of surfactant at the interface, replenishment can occur from the micelles in solution. If the micelles are too stable, this process may be too slow, and the foam film can break. It would be expected that the addition of any species that stabilizes the micelles would contribute to less stable foam.

Experimental. Sodium dodecyl sulfate (99%, Sigma Chemical Co., St. Louis, MO), tetramethyl ammonium chloride (97%, Fisher Scientific, Fair Lawn, NJ), tetraethyl ammonium chloride, tetrabutyl ammonium chloride, and tetrapentyl ammonium chloride (Eastman Fine Chemicals, Rochester, NY) were used as received.

Pressure jump measurements were performed using an apparatus from Dia-Log GmbH, Düsseldorf, Germany. The surfactant/tetraalkyl ammonium chloride samples were pressurized to 130 bar for 30 seconds, allowing micellar equilibrium to be reached. The critical micellar concentration at this pressure should be higher, resulting in fewer micelles and more monomer surfactant than at one atmosphere pressure. After equilibrium is achieved, the pressure is released by overpressuring and bursting of a foil at one end of the pressure chamber. The conductivity of the surfactant solution held in a conductivity cell

attached to the pressure chamber is compared to a reference cell loaded with a KCl solution of the same conductivity. The change in the conductivity is monitored over time (Figure 1 in Huibers et al. [1996a]), and the observed exponential decay of the conductivity signal is related to the micellar stability. All measurements were taken at 25°C.

Results and discussion. To best understand the effect of the addition of tetraalkyl ammonium counterions to SDS micelles, one may compare the changes to that seen by the addition of an equivalent amount of sodium counterions. The effect of addition of Na^+ counterion to the stability of SDS micelles can be predicted. From the data of Lessner et al. [1981], the following relationships can be determined relating micellar stability as measured by the slow relaxation time constant, τ_2, to the counterion concentration, c_g, for the SDS/$NaClO_4$ system at 25°C.

$8 < c_g < 65$ mM: $\log(\tau_2^{-1}) = -4.41 \log(c_g) + 7.393$

$115 > c_g > 65$ mM: $\log(\tau_2^{-1}) = 3.64 \log(c_g) - 7.201$

$c_g = 0.325\, c_{SDS} + c_{NaClO4}$

These equations apply over a range of 25 to 350 mM SDS, given a salt free solution. Applying these equations to the 150 mM SDS cases studied here, the following estimates are given (Table 4-3):

Table 4-3. Slow relaxation time estimates for 150 mM SDS + salt ($NaClO_4$).

solution	**c_g (mM)**	**τ_2 (sec)**	**Δ**
150 mM SDS	48.8	1.12	(reference)
150 mM SDS + 3 mM Na^+	51.8	1.46	+30%
150 mM SDS + 30 mM Na^+	78.8	1.99	+78%

Addition of the tetraalkyl ammonium chloride salts to SDS micelles has two effects. The first is the compression of the electrical double layer and thus the reduction of the repulsion between the sulfate head groups at the micellar surface. The second is the substitution of tetraalkyl ammonium (TAA^+) ions for sodium ions, and the resulting change in packing of the sulfate groups, due to the difference in size between the Na^+ and the TAA^+ ions. Both of these phenomena will occur at the micellar interface as well as the foam film interface.

Pressure jump measurements with conductivity detection were performed on 150 mM SDS solutions, with the addition of 3 or 30 mM of tetraalkyl ammonium chloride (TAA^+). The alkyl groups studied were methyl, ethyl, butyl and pentyl. For 150 mM SDS alone, the micellar slow relaxation time, τ_2, was measured to be 1.38 sec.

On addition of 3 mM tetraalkyl ammonium ions, micellar stability increased for the methyl, ethyl and butyl cases, and no significant increase was observed for tetrapentyl ammonium chloride (Figure 4-8). One would expect an increase in micellar stability of approximately 30% for the addition of 3 mM Na^+, to a τ_2 value of 1.79 sec (Table 4-3). Thus, at a 50:1 Na^+:TAA^+ ratio, tetramethyl ammonium through tetrabutyl ammonium cations stabilize micelles better than the addition of an equivalent amount of Na^+.

On addition of 30 mM TAA^+, the situation is completely different. For all cases, a decrease in the micellar stability is observed. This decrease is greater for the larger counterions. For the tetrabutyl ammonium and tetrapentyl ammonium ions, the reduction in micellar lifetime is approximately three orders of magnitude. There are still many more

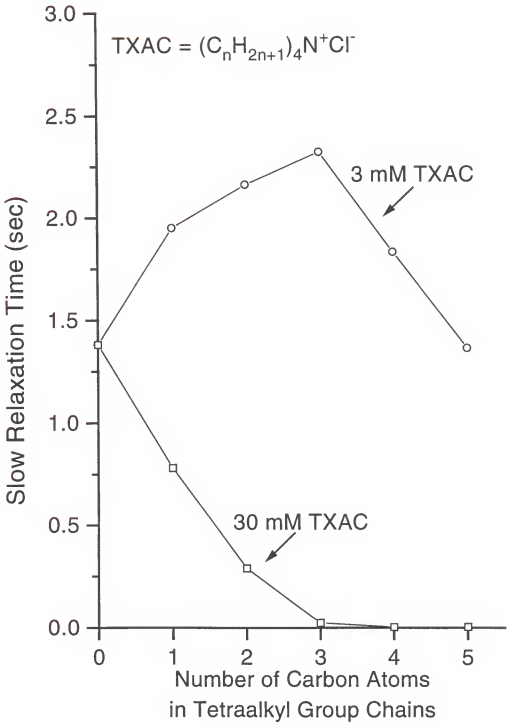

Figure 4-8. Slow relaxation time (τ_2) vs. size of counterion, for 3 and 30 mM concentrations of tetraalkyl-ammonium chloride salts, where the alkyl group varies from methyl to pentyl.

sodium ions present than TAA^+ ions, for this case the ratio is 5:1 Na^+:TAA^+. Sufficient amount of the TAA^+ counterions are present to affect the packing of the sulfate head groups at the micellar surface.

To establish more precisely what concentrations favor micellar stability, the effect of tetraethyl-ammonium chloride concentration was studied up to 50 mM (Figure 4-9) in 150 mM SDS. Concentrations up to 5 mM TEAC showed increasing τ_2, with τ_2 returning to the 0 mM level only above approximately 15 mM TEAC. In this case greater than 1:10 TEAC/SDS (molar basis) is required for micellar stability to be reduced. A comparison of molar ratio to micellar stability for different alkyl sizes shows that the smaller alkyl groups stabilize micelles to a greater extent (Figure 4-10).

One would expect that any addition leading to less stable micelles would result in a more stable foam. This is not the case with the addition of tetraalkyl ammonium ions, however. One may conclude that there are two counteracting changes taking place. The decrease in packing of the micelle sulfate head groups must also occur at the foam film interface. This destabilizing effect is overwhelming the foam stabilizing effect caused by the increase in micellar stability.

Conclusion. Addition of tetraalkyl ammonium counterions to SDS solutions in proportions as small as 5:1 SDS:TAA^+ causes a significant reduction of micellar stability, where an increase would be expected for the equivalent addition of Na^+ ions. This reduction of micellar stability is attributed to the decreased surface viscosity of the micelles due to the alteration of packing of the sulfate head groups by the bulky tetraalkyl ammonium

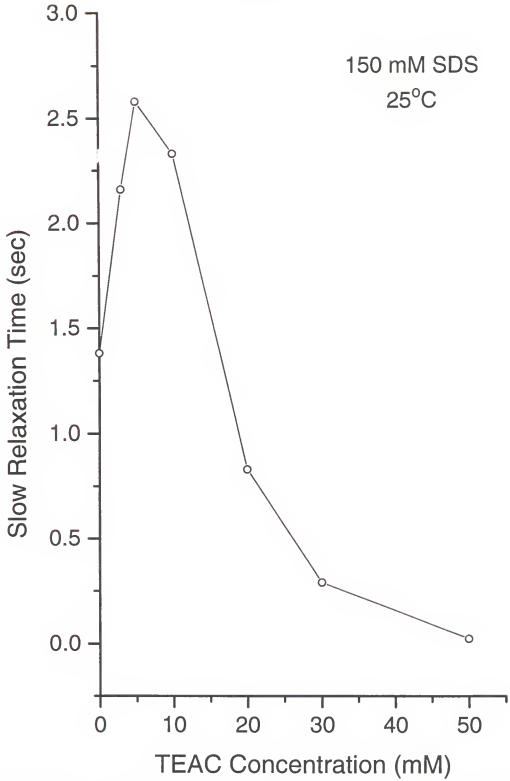

Figure 4-9. Slow relaxation time vs. concentration, for tetraethylammonium chloride in 150 mM SDS.

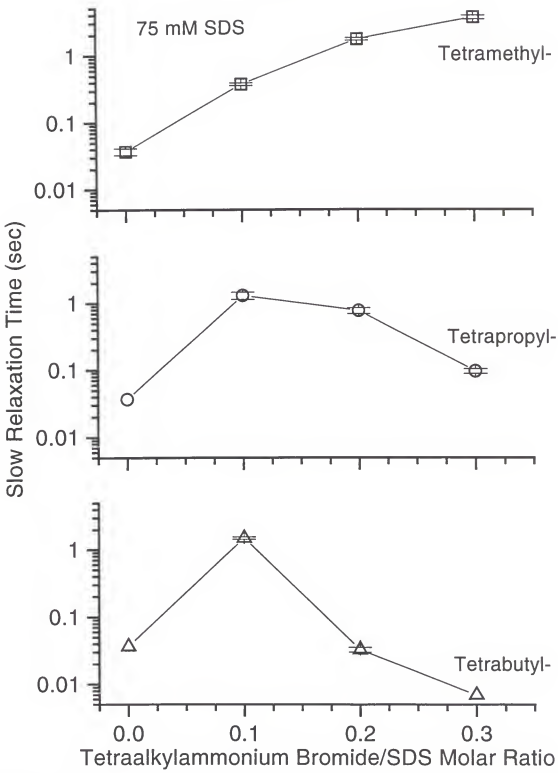

Figure 4-10. Slow relaxation time vs. concentration, for tetraethylammonium chloride in 75 mM SDS.

counterions. The large decrease in micellar stability achieved by the addition of these TAA^+ ions would normally be expected to stabilize foams. The foam destabilizing effect of a decrease in head group packing at the foam film interface appears to be the dominant factor over micellar stability.

Influence of Added Nonionic Surfactant on Micellar Lifetime

The pressure jump technique with electrical conductivity for the detection method is an ideal means for the measurement of ionic surfactant micellar stability, but is not suitable for the measurement of nonionic surfactant micellar stability due to the low conductivity (Table 4-4), and insignificant conductivity change with a change in CMC. The Dia-Log pressure jump apparatus is limited in the conductivity of the solutions that it can measure, from a minimum of 100 to a maximum of 10000 mho/cm. To explore the limits of studying nonionic surfactant micelles with pressure jump, I measured the micellar lifetimes of some mixed ionic/nonionic surfactants. The systems studied were SDS/Tween 80 and AOT/Arlacel 20.

Results. The effect of the nonionic surfactant, Tween 80 (polyoxyethylene 20 sorbitan monooleate), on SDS micellar lifetime was measured by substituting SDS by Tween 80 on an equimolar basis. The two surfactants couldn't be more different, especially in the hydrophilic domains. SDS has a dodecyl (C_{12}) alkyl tail, while Tween 80 has an oleate (C_{18} with a double bond at the 9th carbon) tail. SDS has a small, polar head group (SO_4^-), while the Tween has an extremely large head group, a sorbitan ring (cyclic six

carbon sorbitol carbohydrate), and 20 ethylene oxide residues (-C_2H_4O-) polymerized onto the hydroxyl groups of the sorbitan.

Table 4-4. Slow relaxation time (τ_2) and electrical conductivity for SDS micellar solutions with different concentrations of nonionic surfactants.

Additive	SDS [mM]	Conductivity	τ_2 (s)
(none)	200	5700	2.7
(none)	100	2800	0.22
5 mM Tween 80	95	2800	0.23
10 mM Tween 80	90	2800	3.2
20 mM Tween 80	80	2600	6.2
30 mM Tween 80	70	2500	6.6
3.7 mM Tween 80	0	10.5	n/a
3.7 mM Tween 80	0.75	58	n/a
1:3 AOT/Arlacel 20	n/a	163	0.10
3:1 AOT/Arlacel 20 (0.50 wt% surf.)	n/a	445	0.007

Starting with 100 mM SDS, τ_2 of mixtures were measured down to 70 mM SDS + 30 mM Tween 80. Initially, there appears to be no effect on τ_2, but above 5% (molar basis) Tween 80, the micellar lifetime of the mixtures greatly increases (Figure 4-11). This increase tails off at greater than 20% Tween. As the mixtures studied are equimolar, the stability increase can truly be attributed to synergism between the two surfactants. The stability of 80 mM SDS + 20 mM Tween 80 is even greater than the maximum for pure SDS at 200 mM.

The increase of SDS stability on the addition of Tween 80 is similar to the influence of long chain alcohols (Figure 4-3). The initial lack of increase with the addition of Tween is similar to octanol, and the magnitude of the increase at 25% is similar to that of

decanol. One clear advantage of Tween 80 over the long chain alcohols for enhancing micellar stability is the solubility of the Tween. Tween 80 has no apparent limit to its aqueous solubility, and forms micelles by itself. Contrarily, the long chain alcohols have extremely limited solubility, just 3.8 mM for octanol and 0.234 mM for decanol (Table 4-1), and in mixed micelles no more than 25 mM decanol and 15 mM octanol can be solubilized in a 100 mM SDS + alcohol mixture.

There are limits to the amount of nonionic surfactant added to SDS that can be studied using the pressure-jump technique. As the amount of Tween 80 is increased, the magnitude of the conductivity change with the change in CMC is diminished. Figure 4-12 shows typical traces seen from a pressure-jump experiment. The initially high conductivity level drops instantaneously after the bursting of the foil on overpressuring of the autoclave. The initial drop is due to the fast relaxation time (τ_1), and the time constant for this drop cannot be measured, as it is expected to be in the microsecond range. The second decay, due to the slow relaxation time (τ_2), is readily observable as an exponential decay and the time constant for this curve is easily obtainable. As the Tween 80 concentration is increased, the drop in amplitude of both the τ_1 and τ_2 signals are apparent. In Figure 4-12, the amplitudes drop from 10 mV to 2.5 mV for τ_1 going from 90/10 to 70/30 SDS/Tween (molar basis), and from 6 mV to 2.5 mV for τ_2. Below a 2 mV change in signal for τ_2 it is very difficult to determine the time constant. Although we know the conductivity of the solution is falling in this case with added Tween (Table 4-4), the same loss of signal results from the addition of electrolyte, such as NaCl, limiting the amount of added electrolyte that can be studied with

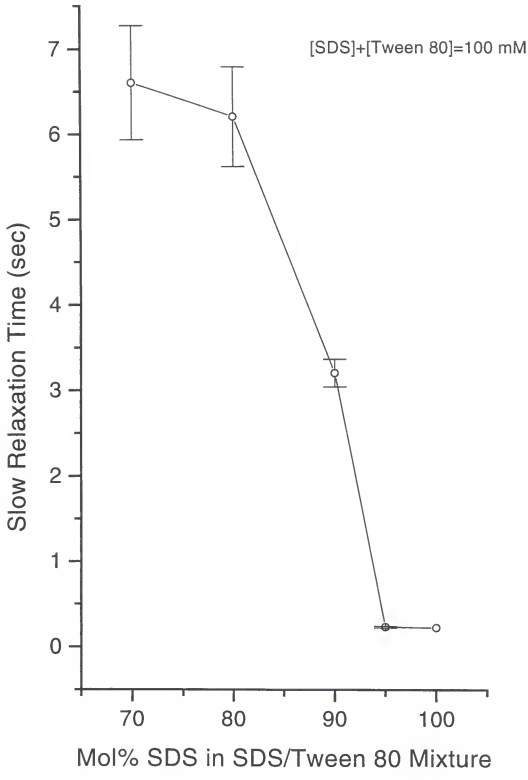

Figure 4-11. Slow relaxation time of mixed anionic and nonionic surfactants, for different mixtures of 100 mM combined SDS + Tween 80.

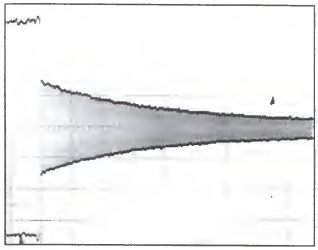

90 mM SDS + 10 mM Tween 80
5 mV/div, 1 sec/div

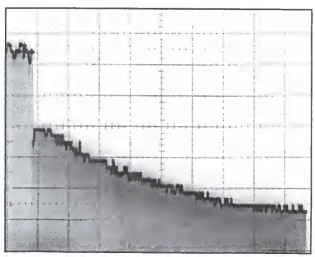

70 mM SDS + 30 mM Tween 80
1 mV/div, 2 sec/div

Figure 4-12. Typical electrical conductivity vs. time traces for pressure-jump experiments. These examples show the decrease in signal as the proportion of nonionic surfactant increases.

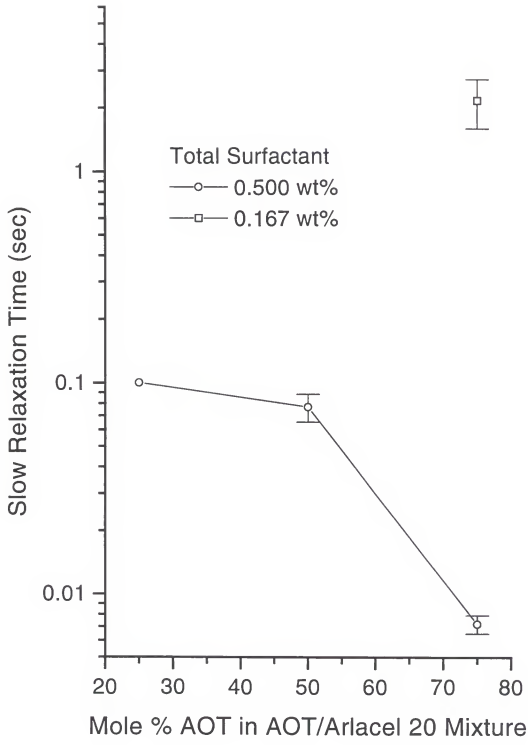

Figure 4-13. Slow relaxation time (τ_2) for mixed anionic and nonionic surfactants, for different mixtures of 0.5 wt% combined AOT + Arlacel 20.

the pressure jump technique. For 150 mM SDS, the signal levels had dropped to 2 mV for the addition of 30 mM NaCl.

Another anionic surfactant was studied, Aerosol OT (also known as AOT, sodium bis-2-ethylhexyl-sulfosuccinate), a twin tailed surfactant. AOT is most commonly used to make reverse micelles, because of its bulky hydrophobic group relative to its hydrophilic group. Normal micelles can be made by mixing with a surfactant with a bulky head group, such as Arlacel 20 (sorbitan laurate). The micellar lifetime of mixtures of these two surfactants in 0.5 wt% solutions has been measured for 1:3 and 3:1 AOT/Arlacel 20 mixtures. From Figure 4-13, the micellar stability is seen to be higher for mixtures with more Arlacel 20. One surprising result was the measurement of a 2 second micellar lifetime for 3:1 AOT/Arlacel 20 at 0.17 wt% surfactant. This is a very high τ_2 for such a low concentration of surfactant, which amounts to just 2.8 mM AOT (MW=444 g/mol) and 1.2 mM Arlacel 20 (MW=344).

Influence of Added Electrolyte on Micellar Lifetime

It has been demonstrated in this thesis that alcohols, glycerol, and tetraalkyl-ammonium chloride salts all influence micellar lifetime, with a variety of results. Considering other electrolytes, there is one study in the literature with a thorough study of the effect of $NaClO_4$ concentration on both SDS and sodium tetradecyl sulfate micellar solutions [Lessner et al., 1981a; b], where the maximum in the micellar stability was correlated to the counterion concentration (assuming some of the initial surfactant counterion is bound), resulting in a model where the micellar stability graphs for SDS with

different salt concentrations lie on top of each other. From this it appears that the reason for the decline in micellar stability after the maximum at 200 mM is caused by a change in the surfactant head group interactions, possibly due to the collapse of the electrical double layer with sufficient electrolyte in solution. It should be noted that the micellar lifetime vs. concentration for nonionics is always decreasing, which may be due to the lack of stabilizing ionic interactions.

Results. I have studied the effect of a few different counterions on micellar stability of 100 mM SDS, with the combined results for glycine, glycerol, and sodium octanoate in Figure 4-14, and the NaCl results in Table 4-5. All of the ionic species examined here act to increase micellar stability. The salt NaCl and the zwitterionic glycine increase micellar stability, but be less than a factor of two. The sodium octanoate, on the other hand, has a great stabilizing effect. It is itself a surfactant, although it has a very high CMC of 140 mM [Rosen, 1989] because of its short alkyl group (as confirmed in Figure 4-16). The initial increase, below 10 mM NaC_8OO is approximately 0.037 sec/mM, with τ_2 doubling on addition of 4.6 mM NaC_8OO. At the concentrations studied, sodium octanoate would not form micelles on its own.

Table 4-5. Slow relaxation time (τ_2) and electrical conductivity for SDS micellar solutions with different concentrations of electrolytes.

Additive	SDS [mM]	Conductivity	τ_2 (s)
(none)	150	4200	1.4
3 mM NaCl	150	4400	2.2
30 mM NaCl	150	6850	1.8
30 mM TMAC	150	7000	0.78
30 mM TPeAC	150	6500	0.004

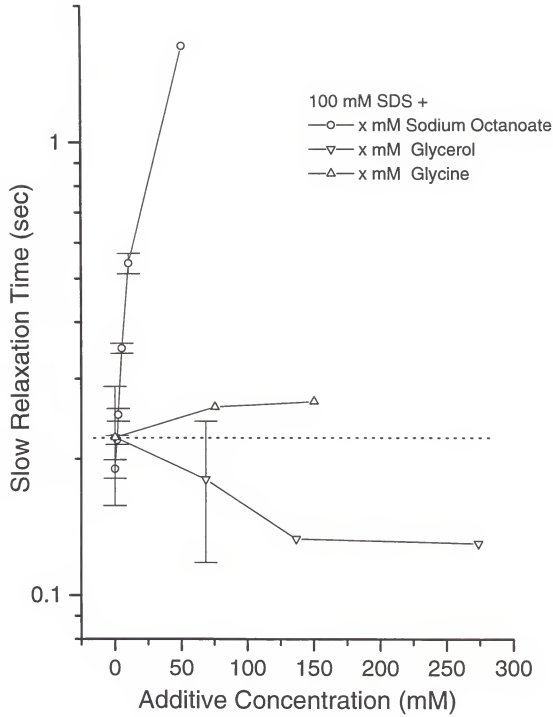

Figure 4-14. Slow relaxation time vs. additive concentration for 100 mM SDS with the additives glycerol, glycine and sodium octanoate.

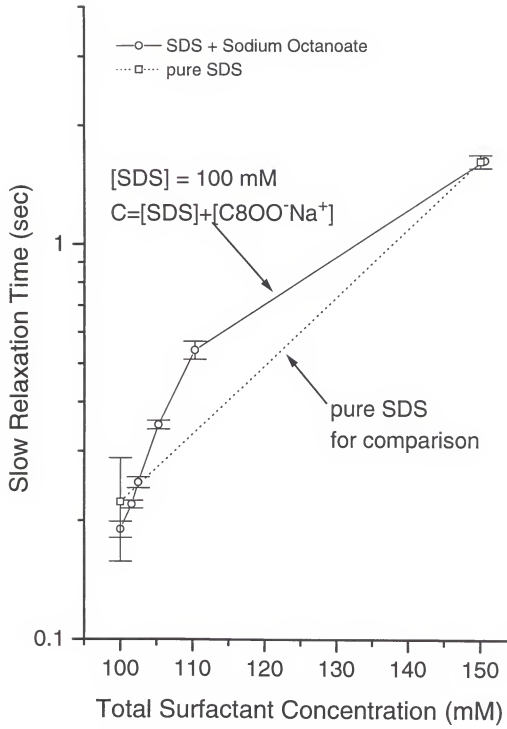

Figure 4-15. Slow relaxation time vs. concentration for mixed sodium octanoate/SDS micelles, compared with pure SDS micelles.

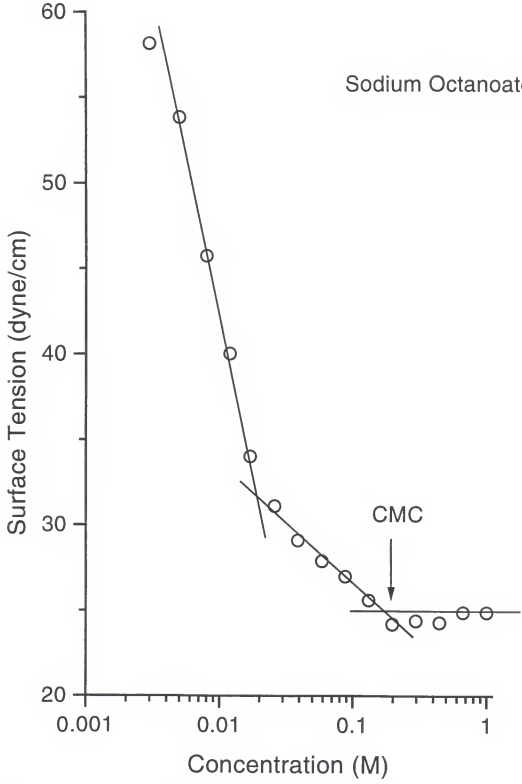

Figure 4-16. Surface tension vs. concentration for sodium octanoate.

The slight increase in micellar lifetime with the addition of electrolytes may be explained in the context of Lessner et al. [1981a; b], where the counterion concentration was shown to have a stabilizing influence at concentrations below the maximum, and destabilizing effects at concentrations above the maximum in micellar lifetime (200 mM for SDS). The stabilizing effect of the sodium octanoate may be explained by similar ionic considerations, as if it is ionic repulsion in the head groups that stabilizes micelles, then the surface active sodium octanoate will partition into the micelles and mixed micelles with two anionic components will be formed. This result is supported by the comparison in Figure 4-15, where the SDS/ NaC_8OO combination is compared with SDS, with a 1:1 substitution of SDS for NaC_8OO (ie. 100 mM SDS + 50 mM NaC_8OO is compared to 150 mM SDS). The resulting micellar lifetimes are very close, showing that the NaC_8OO essentially acts as additional SDS on an equimolar basis.

Effect of Molecular Structure on Dynamic Surface Tension

Besides these studies of the effects of various additives, I pursued the study of the SDS micellar system using several new techniques. Our goals were to find supporting evidence for the existence of a fundamental change in the micellar state at 200 mM, where SDS micellar lifetime is a maximum and a sphere to cylinder transition has been proposed [Oh and Shah, 1993b].

Equilibrium measurements of surface tension have been performed for many surfactant systems. The understanding of dynamic surface tension is of importance in any

technological application where a new gas/liquid interface is being created in the presence of a surfactant solution, because often the equilibrium surface tension value is never reached, and the actual dynamic surface tension value will be much higher. This effect is often more important for solutions containing large surfactants, which have a lower rate of diffusion to the interface. Measurements of dynamic properties are relevant to such technological processes as foaming and fabric wetting, as well as situations where surfactants diffuse to a new liquid/liquid interface, such as emulsification, or to a solid/liquid interface, such as detergency. The maximum bubble pressure technique was developed over a century ago as reviewed by Mysels [1990], although it became more useful only in recent decades with the availability of fast pressure transducers and the electronics necessary to monitor the varying pressure signal. It is the most common technique for the measurement of dynamic surface tension, and has been applied to a variety of surfactants (Table 1, [Huibers and Shah, 1996b]).

Two contributions to dynamic surface tension measurements are presented in this thesis. A new method of calibration using solvent mixtures is presented, addressing some important issues faced when dissimilar solvents are used in many cases cited in the literature. Second, measurements were performed on a family of commercial surfactants, the Brij 7x series of octadecyl ethoxylates, establishing cases where the traditional methods of analysis developed for maximum bubble pressure measurements cannot be applied satisfactorily [Huibers and Shah, 1996b]. Finally, some of the measurements are presented to establish the quality of the measurements taken with this homemade MBP instrument,

with comparisons to results in the literature for SDS and Triton X-100. This section also highlights the large variability found in the literature for identical or similar experiments.

Acetone/water mixtures for calibration of maximum bubble pressure instruments

Calibration of maximum bubble pressure instrumentation involves correlation of pressure transducer signals to surface tensions of various liquids. It is proposed that the use of acetone/water solvent mixtures can lead to more accurate measurements. The surface tensions of these calibration solvent mixtures can span the measurement range of 45 to 70 dyne/cm, where no pure solvent is available for calibration. Many surfactant solutions of interest have dynamic surface tension values in this range. Other considerations, such as solvent viscosity and wetting of the capillary material, may also make solvent mixtures a better choice.

The traditional method of calibration of maximum bubble pressure instrumentation for the measurement of dynamic surface tension involves correlation of the maximum voltage signal measured from a pressure transducer with the expected surface tension of a pure liquid. It is expected that this transducer signal will remain constant over the entire range of bubble rates for the instrument, as there should be no dynamic effect of the interface lifetime on surface tension for these liquids.

The primary limitation of this method is in the nature of the liquids used for calibration. Most organic solvents have surface tensions in the 20 to 30 dyne/cm range, and there are very few with higher values (see Table 4-7). There are only a handful of solvents with surface tensions in the 35 to 45 dyne/cm range, and then there is quite a large gap until

the surface tension of water of 72.75 dyne/cm is reached (at 20°C). In the literature, several references cite the use of either a two point [Woolfrey et al., 1986] or multiple point calibration [Tamura et al., 1995; Hua and Rosen, 1988]. A multiple point calibration was done, comparing surface tension values measured by the Wilhelmy plate method to transducer voltage levels. The solvents used are listed in Table 4-6. Voltage signals in the transducer are normalized by subtracting the baseline voltage at zero differential pressure. The measured values in the table result from a linear regression of the six solvent transducer readings to the literature values, using this equation to predict what the measured (MBP) value was.

Table 4-6. Surface tension values (dyne/cm) at 20°C.

solvent	**literature value**	**measured value**
water	72.75	74.4
methyl benzoate	37.6	38.9
tetrachloroethane	36.03	36.6
chloroform	27.14	27.7
cyclohexane	25.5	25.9
methanol	22.61	25.7

Materials and methods. Acetone was HPLC grade, purchased from Fisher Scientific (Fair Lawn, NJ). Water was distilled, deionized water. Static surface tension measurements were done using the Wilhelmy plate technique and a Rosano tensiometer. Dynamic surface tensions were done using a maximum bubble pressure apparatus. A differential pressure transducer (Model PX164-010D5V) covering the range 0" to 10" H_2O (2500 Pa) was purchased from OMEGA Engineering (Stamford, CT). A steel needle was used as a

capillary, with inner radius of 0.132 mm. A single capillary is used, submerged 1.0 cm into the sample solvent. The apparatus is capable of measuring interface lifetimes of 20 milliseconds to 10 seconds.

Discussion. One concern about the pure solvent calibration procedure is that for the investigation of dynamic surface tension of surfactant solutions at small interface lifetimes (high bubble rates), many measurements of interest will occur in the 45 to 70 dyne/cm range. This is especially true for the nonionic surfactants. For ethoxylated alkyl ethers, the equilibrium surface tension values for longer EO numbers ($n<15$ for $C_{12}E_n$) are greater than 40 dyne/cm and dynamic values approach 55 dyne/cm for short (20 millisecond) interface lifetimes, while shorter EO number surfactants may have equilibrium values as low as 30 dyne/cm, but approach 70 dyne/cm for short interface lifetimes [Tamura et al., 1995].

Another unknown factor in the use of many different pure solvents is the wetting characteristics of those solvents with the capillary material. Some organic solvents may wet the capillary in a different manner than water, depending on the hydrophobicity of the capillary material [Mysels, 1990]. This difference in wetting may affect bubble formation, and thus potentially affect the observed maximum bubble pressure for a given liquid surface tension.

Viscosity effect. Another potential problem with the use of a variety of solvents is the mismatch in viscosity. It can be demonstrated that the maximum bubble pressure apparatus can give higher apparent surface tension readings with viscous liquids. Figure 4-17 shows the dynamic surface tension of glycerol. It is expected that glycerol would have a

constant surface tension of 63.4 dyne/cm at all bubble rates. At higher bubble rates, however, the apparent surface tension is higher because the viscous resistance to the expansion of the bubble out of the capillary tip requires the inclusion of another pressure term in the calculation.

Another problem occurs when the bubble breakage process leaves behind a bubble attached to the capillary that has a larger radius than the capillary radius, rather than breaking off completely and leaving no bubble attached to the tip. This causes a problem because the maximum pressure is reached for a hemispherical bubble at the capillary tip that has a larger radius than the capillary radius, and will depend on gas flowrate. The assumption that the maximum pressure will occur due to the Laplace pressure of a hemispherical bubble at the capillary tip is violated. This obviously prevents the correlation of maximum bubble pressure with the surface tension of the liquid, because the radius of curvature at the maximum pressure is unknown. This process is demonstrated by Garrett and Ward [1989] for high gas flowrates in water.

Garrett and Ward [1989] also describe the inverse relationship between capillary radius and dead time. A larger radius is desirable to achieve a shorter dead time and thus a higher bubble rate, but there is a tradeoff because of the increased influence of the viscosity effect for larger capillaries. The viscosities of the solvents used for calibration are presented in Table 4-7.

Surface tension of solvent mixtures. The static and dynamic surface tension values of acetone/water mixtures were investigated. This pair was chosen because they are

completely miscible, the mixtures cover the surface tension range of interest, and the viscosities are relatively matched.

The static surface tension values for acetone/water mixtures are presented in Figure 4-18. For these mixtures there is no change as a function of interface lifetime for the entire dynamic range of the maximum bubble pressure instrument. This is critical to the use of these mixtures for the calibration of MBP equipment, as there should be no dynamic behavior of diffusion of one solvent to the interface, where it may change the surface tension over very short interface lifetimes. There may be a surface excess of one solvent, ie. one solvent prefers the interface to the bulk, but it must be that there is such a large fraction of that solvent that there is no diffusion limiting the transport of that solvent to newly formed interface, because of the large amount of that solvent in the bulk solvent mixture.

Conclusion. There appears to be no disadvantage to the use of acetone/water mixtures for calibration of maximum bubble pressure instrumentation, as opposed to using a number of pure solvents of varying surface tensions. The acetone/water mixtures show no dynamic behavior, and the dynamic and static values of surface tension correlate well. The mixtures have a definite advantage in allowing calibration of the instrumentation over the 45-70 dyne/cm surface tension range, where many measurements of interest are taken, but no suitable solvent is available for calibration. The mixtures may have an additional advantage over the use of several solvents, because of the close values of the viscosities and densities of the acetone/water mixtures, as well as a similarity in their wetting characteristics of capillary material.

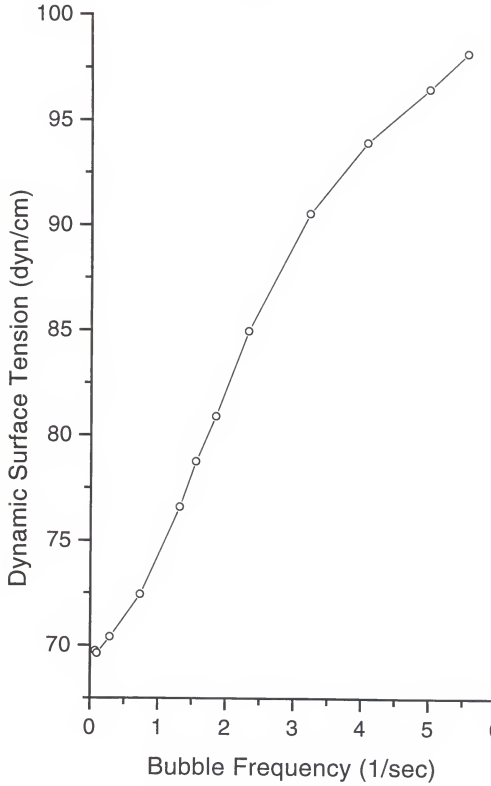

Figure 4-17. Apparent dynamic surface tension of glycerol.

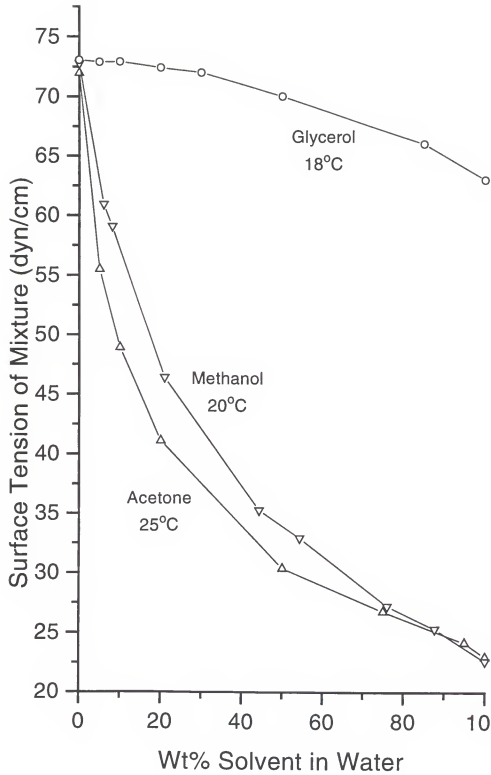

Figure 4-18. Equilibrium surface tension of methanol/water mixtures.

Table 4-7. Surface tension and viscosity values (20°C, unless otherwise marked).

solvent	S.T. (dyn/cm)	viscos. (cp)	density (g/cm^3)	references
water	72.75	1.002	0.998	(used by all)
glycerol	63.4	1490	1.261	(too viscous)
ethylene glycol	47.7	19.9	1.109	(too viscous)
nitrobenzene	43.9	2.03	1.204	Tamura, Hua
benzyl alcohol	39.0	5.8	1.072	Tamura
tetrachloroethane	36.03	1.844^{15}	1.553	
acetonitrile	29.3	0.345^{25}	0.786	Hua
benzene	28.85	0.652	0.879^{15}	Hua
1-octanol	27.53	-	0.827	Hua
chloroform	27.14	0.58	1.489	
cyclohexane	25.5	1.02^{17}	0.779	
acetone	23.70	0.316^{25}	0.792	Tamura, Hua
ethanol	22.75	1.200	0.789	(only denatured readily available)
methanol	22.61	0.597	0.791	Hua, Woolfrey
isopropanol	21.7	2.86^{15}	0.785	Tamura

Measurement of the dynamic surface tension of Brij 7x nonionic surfactants

Dynamic surface tension (DST) measurements using the maximum bubble pressure (MBP) technique were conducted on three nonionic surfactants, Brij 76 (polyethylene glycol 10 stearyl ether), Brij 78 (polyethylene glycol 20 stearyl ether) and Brij 700 (polyethylene glycol 100 stearyl ether), the latter (molecular weight of 4670 g/mol) being the largest surfactant examined to date with DST. Surface tension was measured for solution concentrations from 10^{-5} to 10^{-3} M, and for surface lifetimes from 20 milliseconds to 10 seconds, at 25°C. Due to the large size of these surfactants and their polydisperse nature, established analysis techniques to determine mesoequilibrium surface tension and surfactant diffusion coefficients cannot easily be applied over the time scales studied.

Results. There have been relatively few measurements of dynamic surface tension (using maximum bubble pressure) of nonionic surfactants. To this date, only the dodecyl ethoxylates, the nonylphenol polyglycol ethers, and the octylphenol polyglycol ethers (Triton X-100) have been studied (see Table 1, [Huibers and Shah, 1996b]). The quantity of dynamic surface tension data is greatly dwarfed by the body of literature on static surface tension measurements, which is a primary method of critical micelle concentration (CMC) determination. The contribution of this thesis is to demonstrate MBP measurements on surfactants that are larger than any studied to date (Brij 700), and to show that the established analysis techniques, both empirical formulas and diffusion coefficient determination, do not work for commercial surfactants, which are polydisperse mixtures by nature.

Effect of Micellar Structure on ^{23}Na NMR Measurements

Two distinct measurements come from NMR measurements, a shift and a decay lifetime. These are influenced by the environment of the nuclei probed. Both measurements are available for different nuclei, depending on the operation of the NMR apparatus. It is well known that the CMC can be measured using hydrogen NMR, as both the shift and the lifetime change with the chemical environment as some fraction of the surfactant molecules go from the monomer state (surrounded by water) to micellar aggregates, where they are in close association with other surfactant molecules. ^{23}Na NMR has been used for various biological studies, and some surfactant studies [Lindman et al., 1984; Yoshida et al., 1986; Soderman et al., 1987; Monduzzi et al., 1990; Ceglie et al., 1991; Romsted and Yoon,

1993], but not over the ranges of SDS concentrations that we were interested in. ^{1}H NMR has been used to show that a transition occurs in SDS micelles at 70-80 mM, which was attributed to a shape transition from spherical to cylindrical micelles [Zhao and Fung, 1993]. As it has been proposed that the maximum in micellar lifetime at 200 mM is due to this shape transition, we thought it could be productive to investigate ^{23}Na NMR measurements from premicellar to greater than 200 mM concentrations, to see what transitions were observable. It can be expected that counterion binding would change with the collapse of the electrical double layer, and the onset of the spherical-to-cylindrical micellar shape transition. This change of counterion binding, with a resulting change in the sodium environment, should be apparent in the ^{23}Na NMR measurements.

The definition of the second CMC is not very clear. The first CMC is well established, being the onset of micellization, and observed as a sharp change in slope in several solution properties, notably the surface tension [Rosen, 1989]. The presence of a second CMC implies that there is a second distinct change in slope in some properties at some higher concentration. Shah and coworkers have well established such a sharp change in the micellar lifetime of SDS at 200 mM, and corresponding technological processes that are influenced by micellar lifetime [Huibers et al., 1996a; Oh et al., 1996]. This inflection has also been designated the second CMC, and attributed to the transition of spherical to cylindrical micelles [Oh and Shah, 1993b].

It was believed that NMR measurements should support the existence of a transition at 200 mM for SDS, given the nature of the measurement, and clues from the literature.

^{23}Na nuclear magnetic resonance spectroscopy allows us to discover something of the dynamic state of the sodium ion in a micellar solution. The chemical shift (δ) provides information about the local environment of the sodium atom by the influence of the electron clouds of neighboring atoms in shielding the sodium atom signal. The spin-lattice relaxation time (T_1) will decrease with the corresponding decrease of the motion of the sodium ion, providing some dynamic information on the system. These NMR measurements provide information on the microenvironment of sodium ions, which exist both in solution as well as closely bound to monomers and micelles of SDS.

Evidence from the literature of some change at 200 mM is somewhat contradictory. Gustavsson and Lindman [1978] appeared to show an inflection in ^{23}Na NMR chemical shifts at approximately this concentration, though they do not discuss it in their text, as they were interested in changes near the first CMC. Zhao and Fung [1993] used ^{1}H NMR to study SDS, showing a 'second CMC' in the range of 70-84 mM using chemical shift data, and 50-67 mM using relaxation rate data. They did not perform measurements at sufficiently high concentrations to observe any inflections at 200 mM. Given these reports in the literature, it was judged useful to take careful measurements near 200 mM for SDS solutions, to establish whether any inflections were observable to lend support to the hypothesis that the second CMC lies there.

Experimental. Sodium dodecyl sulfate (99%) was purchased from Sigma Chemical Co. (St. Louis, MO) and used as received. The water used was deionized and distilled. ^{23}Na NMR spectra were obtained using a Varian XL spectrometer (300 MHz) under a deuterium

internal lock operating in the Fourier transform mode. The ^{23}Na spin-lattice relaxation time (T_1) was measured by the Inversion Recovery Fourier Transform method. All measurements were taken at 26°C.

Results and discussion. Measurements of ^{23}Na NMR chemical shifts (Figure 4-19) and relaxation times (Figure 4-20) were made at concentrations ranging from 2 mM to 400 mM. No obvious inflection in the data is seen in the vicinity of 200 mM. For the relaxation time data, the apparently significant measurement at 80 mM was not repeatable in a second set of NMR measurements, nor was any other change apparent from additional measurements in the 60-150 mM range.

When plotted vs. the inverse of concentration, as is common in NMR studies, the CMC is quite obvious, occurring near the third data point from the right (8 mM), in both chemical shift (Figure 4-21) and relaxation time (Figure 4-22). There also appears to be a change in slope between the 40 mM and 80 mM, which is gradual in the δ data but apparently more well defined in the T_1 data, although the T_1 data point at 80 mM is believed to be anomalous. This apparently supports the ^1H NMR evidence for some transition in the 50-90 mM range, although this may not be significant given the magnitude of the error in the ^{23}Na NMR measurements. Examining the NMR measurements vs. the inverse of concentration near 200 mM also shows some apparent change in slope near 200 mM and 250 mM, although again this may be insignificant when the error in the measurements is considered.

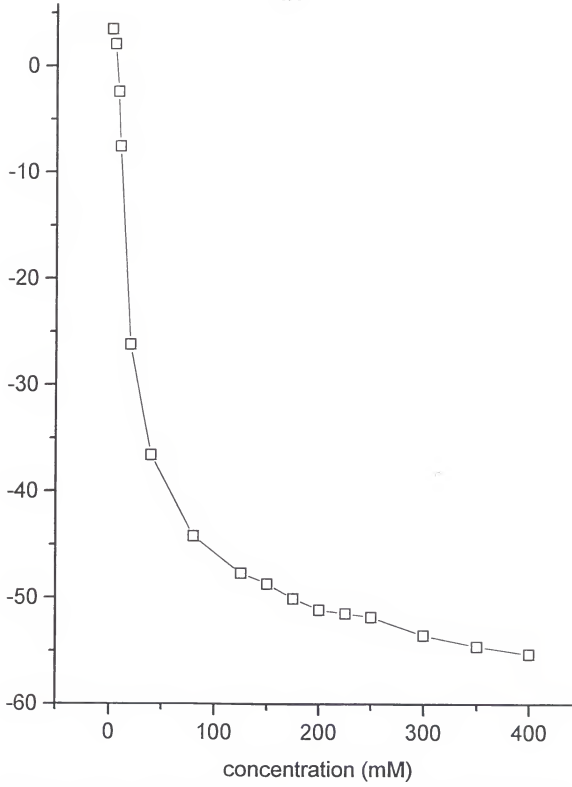

Figure 4-19. ^{23}Na chemical shift (d) vs. SDS concentration for the entire range from 2 to 400 mM.

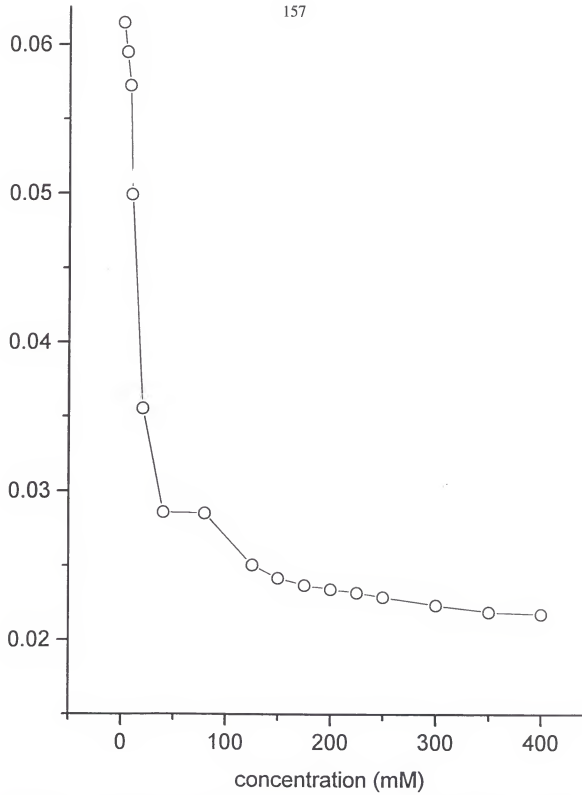

Figure 4-20. Spin-lattice relaxation time (T_1) vs. SDS concentration for the entire range from 2 to 400 mM.

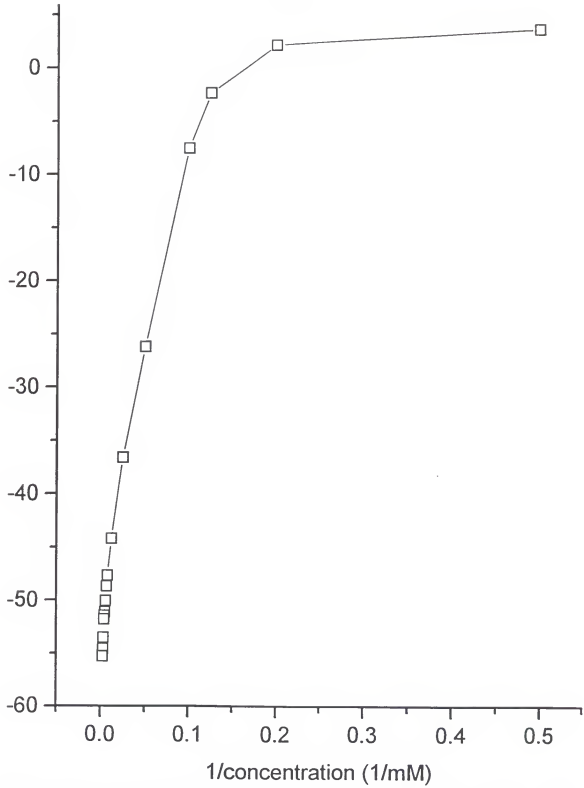

Figure 4-21. ^{23}Na chemical shift (δ) vs. the inverse of the SDS concentration for the entire range from 2 to 400 mM.

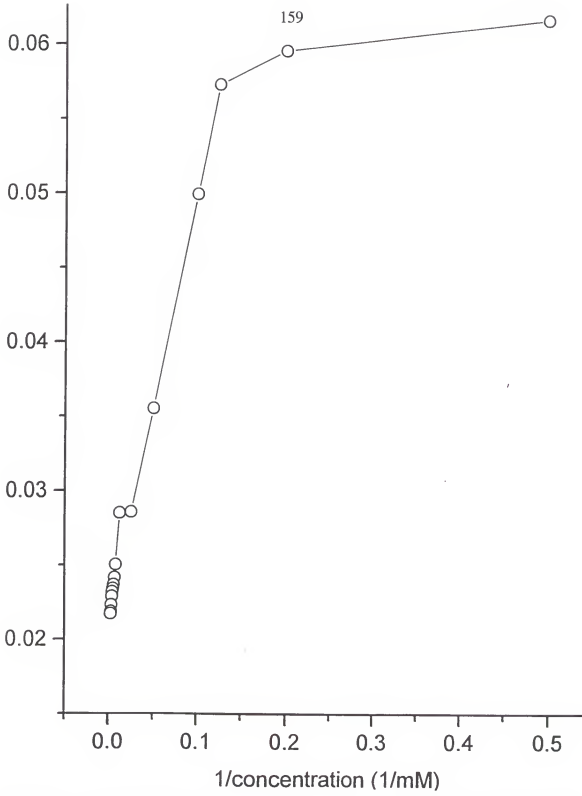

Figure 4-22. Spin-lattice relaxation time (T_1) vs. the inverse of the SDS concentration for the entire range from 2 to 400 mM, showing linear relationship of T_1 to 1/[SDS] over certain concentration ranges.

Conclusion. I am reluctant to draw a conclusion that there are no changes above CMC apparent in ^{23}Na NMR δ and T_1 data. The application of ^{23}Na NMR to micellar systems continues in the literature and I believe that additional careful studies may show some evidence for transitions in SDS micellar systems above 8 mM.

Cationic Surfactants

In order to extend the work of this group beyond studies of SDS, I undertook some measurements of the micellar lifetime of cationic micelles, including cetyltrimethyl ammonium bromide (CTAB), myristyltrimethyl ammonium chloride (MTAB), and cetyl pyridinium chloride (CPC). It was expected that a similar situation to SDS would be seen - an increase in lifetime with concentration up to some maximum, and then a decrease. For the three systems studied, this is not the case, as a much slower rise in τ_2 was observed with concentration, followed by a plateau, and no apparent drop. Investigations were also made into the correlation between micellar lifetime and two technological processes, foamability for MTAB and fabric wetting for both MTAB and CTAB.

Micellar Lifetime

Using the pressure-jump technique, I measured the micellar lifetime of several cationic surfactants. There are literature references for such studies in the review articles mentioned at the beginning of this chapter, although these focus only on the concentrations near CMC. My goal was to go to much higher concentrations, and determine whether a

maximum micellar stability was observable, as with the SDS system. I studied three common cationic surfactants, CPC, MTAB and CTAB.

The concentrations studied were all well above CMC, as can be determined from surface tension measurements (Figure 4-23) or from the literature. The CMC values for these three surfactants are 0.9, 3.6 and 0.9 mM respectively at 25°C. Care must be taken when working with CTAB, as its Krafft point is reported in the literature as 25°C [van Os et al., 1993] or 26°C [Rosen, 1989], and can crystallize out of solution if the temperature is lowered below this point. If the surfactant crystallizes out of solution in the pressure-jump sample cell, then the surfactant concentration of the measurements would be much lower than expected. The conductivity of these solutions increases with concentration in a linear manner, as can be seen with MTAB (Figure 4-24), which follows a formula $C = a + b$ [MTAB].

Results. Micellar lifetime is plotted for CPC (Figure 4-25), MTAB (Figure 4-26) and CTAB (Figure 4-27). As can be seen in these figures, the micellar lifetime increases with concentration, and then plateaus, with no clear maximum. The MTAB case is the most unusual, with lifetimes of 25 sec at 75 mM. Concentrations were tested up to 300 mM, but no decrease was seen. This long τ_2 of 25 sec approaches the upper limit of what can be measured with the digital storage oscilloscope used at the pressure-jump recording device. Results could not be determined at higher concentrations, as the amplitude of the conductivity signal difference as seen by the pressure-jump bridge circuit drops with the increase in ionic strength of the solution (Figure 4-28). The concentration where the signal

drops to a minimum observable value happens at a lower surfactant concentration and a lower conductivity than the SDS solutions.

Discussion. These cationic systems have certain clear differences from the SDS system. First, the rise in micellar lifetime with concentration is not as large. Second, there is no clearly defined maximum, but rather a large plateau region. What does this tell us about these cationic micelles? Certainly the influence of surfactant head group charge is a factor in stabilizing the micelles as concentration increases, similar to the anionic SDS, but to a lesser extent, and opposed to the nonionic surfactants, where micellar lifetime drops with increasing concentration. The plateau is reached at a concentration of the order of 100 mM, well below the ionic strength of the SDS solutions (200 mM) where the maximum is found. If the SDS maximum is due to the collapse of the electrical double layer, and the onset of cylindrical micelles, then there is still roughly 100 mM more surfactant needed to bring about a double layer collapse in the cationic systems. Why then would there be a plateau, instead of the steady rise seen in the SDS system? The only possible explanations for this are either a fundamental difference in repulsion between positive charges in aqueous solutions vs. negative charges (this seems unlikely to be significant) or the influence of the size of the head group. The sulfate head group in SDS is smaller and more highly charged than the head groups of trimethylammonium or pyridinium. It is possible that this distributed head group charge plays a strong role on the magnitude of the interactions between micelles, and thus the slope of the micellar lifetime with concentration.

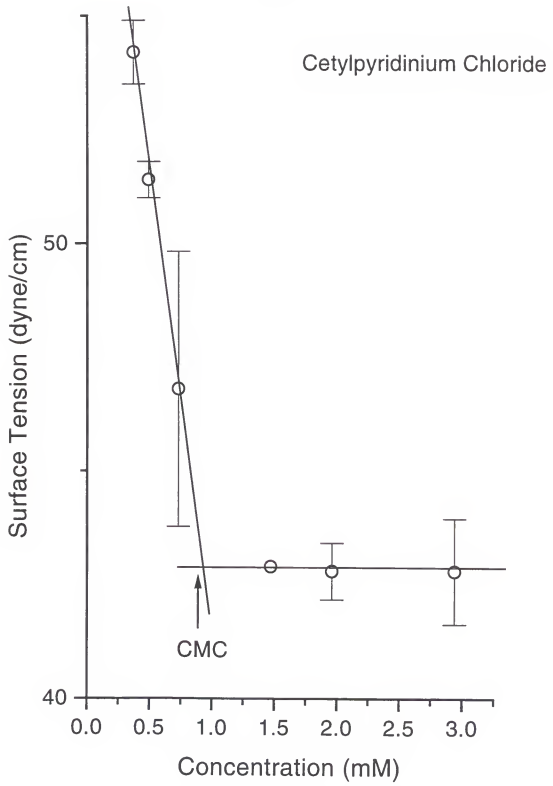

Figure 4-23. Surface tension vs. concentration for CPC, establishing a CMC of 0.9 mM.

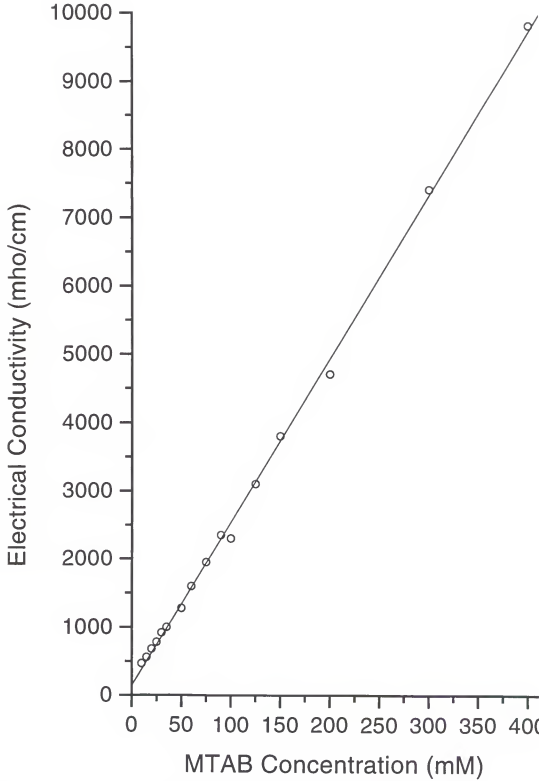

Figure 4-24. Electrical conductivity vs. concentration for MTAB.

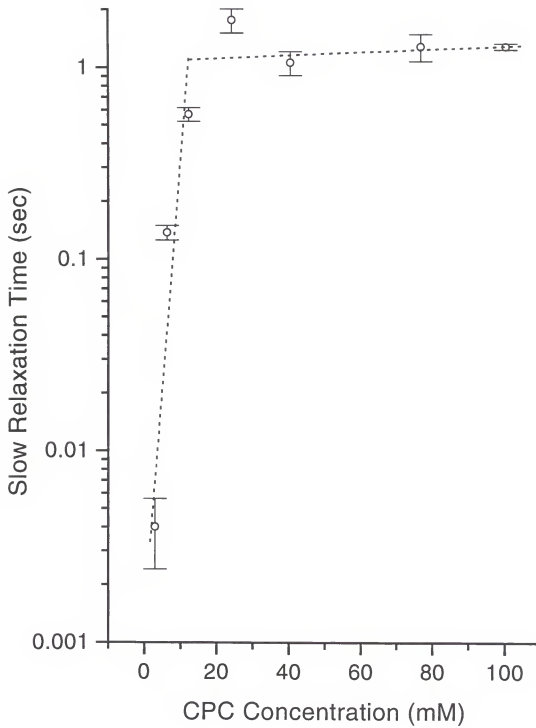

Figure 4-25. Slow relaxation time (τ_2) vs. concentration for CPC.

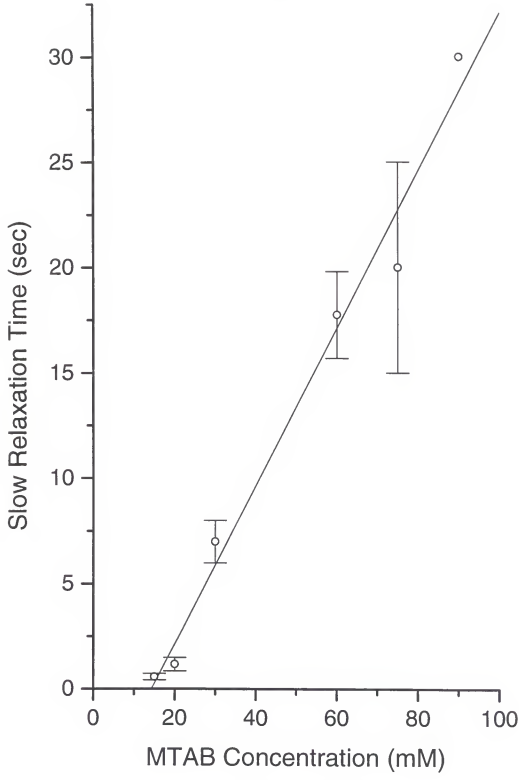

Figure 4-26. Slow relaxation time vs. concentration for MTAB.

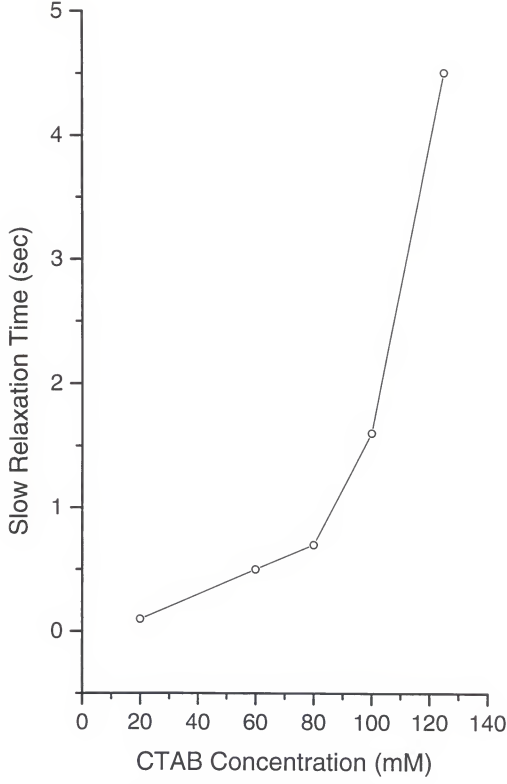

Figure 4-27. Slow relaxation time vs. concentration for CTAB.

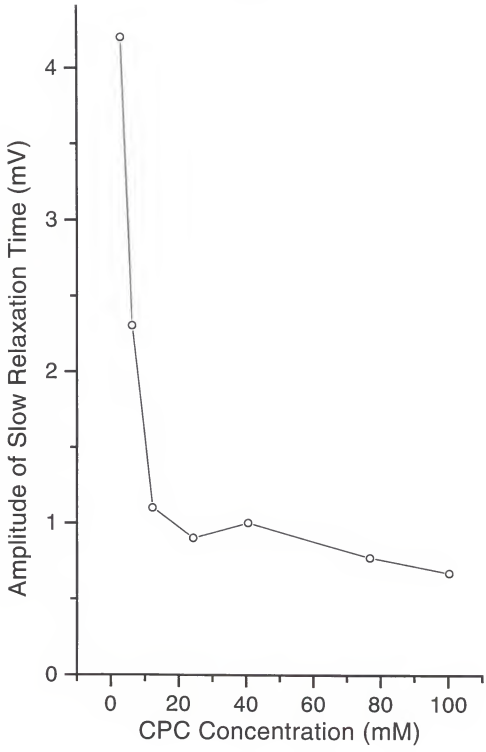

Figure 4-28. Slow relaxation time conductivity signal amplitude vs. concentration for CPC.

For further studies of this system, it would be interesting to see the effect of added electrolyte on these cationic micellar systems, as they may show a maximum at 100 mM or below given enough electrolyte added. Of course, there are limits to the amount of electrolyte that can be added and still have an observable signal using the conductivity detection method with the pressure-jump apparatus. It should also prove useful to study shorter chained surfactants. Especially for the CTAB studies, it would be better to take measurements at higher temperatures, as the literature value for the Krafft point of CTAB is 25-26°C, and the CTAB solutions will often spontaneously crystallize out of solution (and potentially in the pressure-jump cells) even hours after the solution has been prepared and appears stable. These measurements could be done at higher temperatures, but one must be aware that the micellar lifetime falls sharply with temperature [Inoue et al., 1980]. Another option is to use the chloride, as I have observed that CTAC has a lower Krafft point and is thus more soluble.

Effect of Micellar Lifetime on Processes

Investigations were made into the correlation between micellar lifetime and two technological processes, foamability for MTAB and fabric wetting for both MTAB and CTAB. For SDS solutions, fabric wetting time was shown to increase with concentration up to a maximum at 200 mM, and then fall (Figure 5.9 in Oh et al. [1996]). Foamability was shown to decrease to 200 mM SDS, then increase (Figure 5.5 in Oh et al. [1996]). An analogous correlation for cationic surfactants would lead to much more general conclusions about the influence of micellar stability on such technological processes.

Fabric wetting time. The fabric wetting experiments were conducted by dropping a 1 cm x 1 cm square of cotton fabric onto the surface of a micellar solution. The wetting time is the time it takes for the fabric to break below the surface of the liquid. As a piece of fabric has a large surface area and many small pores, one can imagine that the dynamic surface tension of the liquid plays an important role in the wetting of this large new surface area and in the penetration of the liquid into small pores.

Fabric wetting results show a decrease in wetting time with an increase of concentration, both for MTAB (Figure 4-29) and CTAB (Figure 4-30). These results are contrary to the SDS results (Figure 5.9 in [Oh et al., 1996]), where the wetting time increased initially with increasing concentration. This leads to the conclusion that a correlation cannot generally be drawn between this process of decreased fabric wetting time and an increase in micellar stability. It may be possible that the comparison between cationic and anionic surfactant binding to the fabric may not be valid, due to differences in the specific molecular interactions between the surfactant and the fabric. One assumes that the cotton fabric is essentially 'nonionic', having a carbon backbone and exposed hydroxyl groups. A positively charged cationic surfactant or a negatively charged anionic surfactant may be expected to have approximately the same charge-dipole interaction with these hydroxyl groups, so no obvious difference in the two surfactants can be seen.

Foamability. Foamability experiments are conducted by blowing air through a glass frit at the bottom of a long tube, containing a sample of surfactant solution. The air passes through the solution and foam is formed. By maintaining a constant air flowrate from

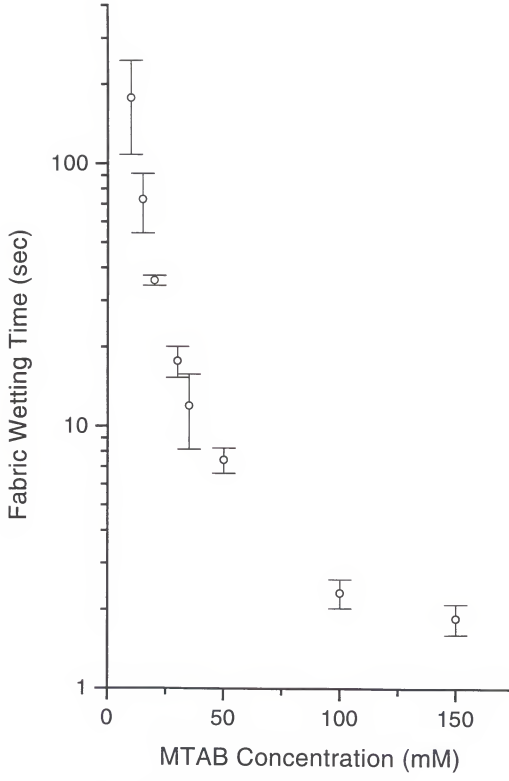

Figure 4-29. Fabric wetting time vs. concentration for MTAB.

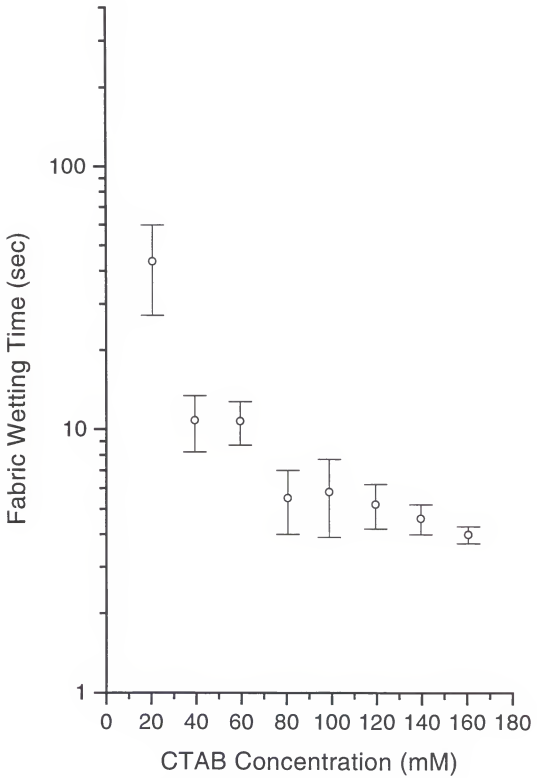

Figure 4-30. Fabric wetting time vs. concentration for CTAB.

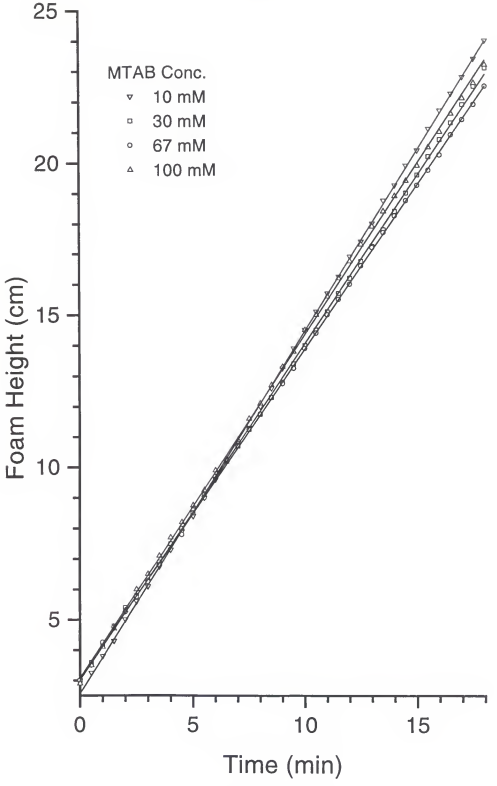

Figure 4-31. Foam height vs. concentration for MTAB.

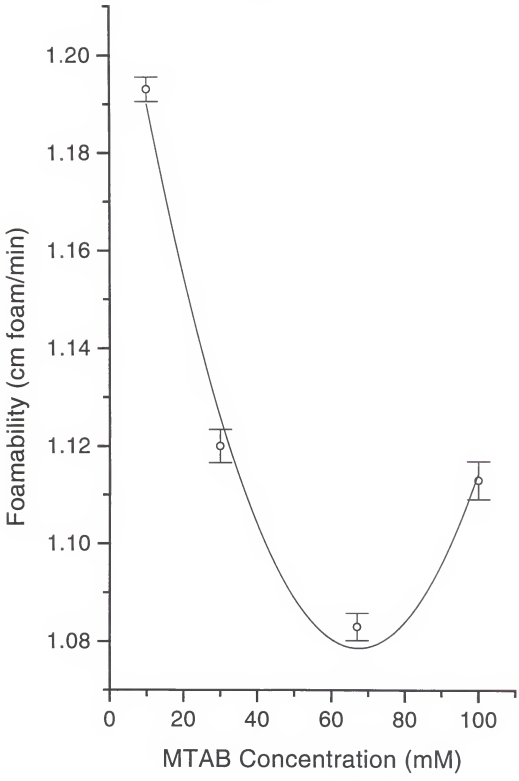

Figure 4-32. Foamability vs. concentration for MTAB.

sample to sample, foamability can be measured by determining the foam height as a function of time for the initial foam formation. It is important to measure the initial foam creation rate, since as the foam ages, drainage and collapse start to take place and the foam height increases more slowly, eventually reaching an equilibrium height.

Foamability was measured for MTAB solutions, over the concentration range of 10 to 100 mM. The foam height increased linearly with time (Figure 4-31), with very little difference between the different concentrations. When the slope (foamability) is plotted vs. concentration (Figure 4-32), small changes are seen between the solutions, with an apparent minimum in foamability in the 30 to 70 mM range. As with the fabric wetting experiments, the results are contrary to SDS (Figure 5.5 in [Oh et al., 1996]), where a decrease in the foamability is seen with increase in concentration (increase in micellar stability). In this experiment no such complicating factors are present such as the possibility of the different surfactants interacting differently with the fabric material, as in this case the newly formed interface is an air/solution surface. Again, no clear conclusion can be drawn from these experiments with cationic surfactants that the micellar lifetime has a dominant influence on these processes.

Nonionic Surfactants

Nonionic surfactant micellar lifetime cannot be measured with the same apparatus as the ionic surfactants (pressure-jump with electrical conductivity detection) simply because the nonionics are nonconducting in comparison to the ionics, and thus conductivity changes cannot be measured with a change in micellar state. New methods must be

developed, and the most promising is temperature-jump with ultraviolet light absorbance as the detection method. Since nonionic surfactant aggregation number is so temperature dependent, a small change in temperature will cause a detectable change in aggregation number (Figure 4-33). In the UV, absorption due to losses from Rayleigh scattering should be detectable. In the visible, if a solvatochromic dye is present, a shift in absorbance peak may be detectable with a change in the micellar shape. Both of these detection methods for nonionic surfactant micellar stability determination are investigated in the following sections.

Solvatochromism in Nonionic Surfactants

It has been established decades ago that certain dyes have shifts in their UV/visible absorbance spectral peaks with the polarity of their environment [Zollinger, 1987]. Thus, such dyes have been used as an empirical means to quantify the polarity of solvents, one of the applications being solvent selection for organic synthesis. Two popular indices are the Kosower [1958] index, based on the dye 1-ethyl-4-methoxycarbonyl-pyridinium iodide, and the $E_T(30)$ index, based on Reichardt's dye, 2,6-diphenyl-4-(2,4,6-triphenyl-1-pyridinium)-phenoxide [Reichardt, 1994]. A large number of compounds exhibiting solvatochromism are tabulated by Reichardt [1994].

Dyes have been used for several micellar core polarity studies; for example Zhu and Schelly [1992] studied the interior of Triton X-100 reverse micelles in cyclohexane with Methyl Orange, Ueda and Schelly [1989] studied AOT reverse micelles in benzene using the dye 1-methyl-8-oxyquinolinium betaine. Several studies used Reichardt's dye as a

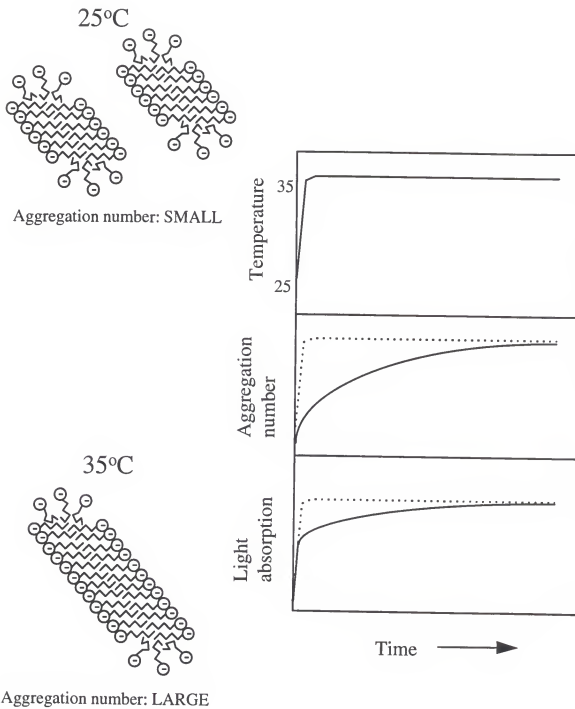

Figure 4-33. Nonionic surfactant micellar kinetics via temperature-jump.

probe; Varadaraj et al. [1993] studied the interior of SDS/acrylamide polymer micelles, Varadaraj et al. [1990] and Warr and Evans [1988] studied micelles from several different surfactant types, Zachariasse et al. [1981] studied micelles, microemulsions and bilayers made from several different surfactants, and Lay et al. [1989] studied W/O microemulsion interfaces. Several other studies using Reichardt's dye on organized media besides micelles are tabulated in his review [Reichardt, 1994].

Results. A number of oil soluble dyes were screened for possible solvatochromism by measuring the wavelength of the primary absorption peaks in isobutanol and decane, thus covering a range of solvent polarities. From Table 4-8, it can be seen that Sudan Black B had the largest shift in pure solvents. Dyes Sudan II and Orange OT are interesting, as they show multiple peaks, which shift differently (and also change in height) with solvent polarity. Aniline Blue is interesting, being insoluble in water and oil (decane), but soluble in an intermediate solvent, isobutanol, and also shows potential for solvatochromism in micellar solutions.

Table 4-8. Absorbance peaks and solvatochromic shift of selected dyes in organic solvents.

Dye	Isobutanol Peak (nm)	Decane Peak (nm)	Shift $\Delta\lambda$ (nm)
Sudan II (peak 1)	500	478	+22
Sudan II (peak 2)	421	431	-10
Sudan III	513	503	+10
Sudan IV	523	515	+8
Sudan Orange G	384	382	+2
Sudan Black B	603	558	+45
Aniline Blue	595	(insol)	n/a
Orange OT	495	485	+10

To see whether this dye would be sensitive to the polarity of the micellar interior, the maximum absorbance peak in several different micelles with different hydrophobic tail structures was measured (Table 4-9). The maximum shift of 10 nm between the micelles sampled here indicates that this dye has potential as a micellar probe. The absorbance peaks for Sudan Black B were higher than for the isobutanol, indicating a more polar environment in the micellar core than in the alcohol.

Table 4-9. Absorbance peaks of Sudan Black B in selected micelles.

Surfactant	Tail Structure	Peak (nm)
Tween 80	oleyl	622
Brij 78	stearyl	630
Tween 20	lauryl	632

Conclusions. Several commonly available oil soluble dyes have demonstrable solvatochromism. The dye with the greatest spectral shift among those studied, Sudan II, also shows spectral shift from one type of nonionic micelle to another, suggesting that a shift may be observable for aggregation number changes in a given micelle.

Determination of Aggregation Number by UV Rayleigh Scattering

The aggregation number, or mean number of surfactant molecules in a micelle, has been determined by several means. The primary methods include dye fluorescence and micellar diffusion measurements.

The standard method of using fluorescence involves solubilizing pyrene into the micellar solution [Zana, 1987; Lianos and Zana, 1981]. Pyrene is a fused ring aromatic hydrocarbon, water insoluble, and partitions into the micellar interior. Given a number of

pyrene molecules roughly of the same order as the number of micelles, the pyrene will partition among the micelles, with some having no pyrene, some having one molecule per micelle, some having two, etc. in a Poisson population distribution. It has been established that the ratio between two fluorescent (vibronic) peaks in the spectrum depend on whether the fluorescing pyrene is isolated, or closely associated with another pyrene molecule, probably through pi-electron overlap. Through the ratio of these two peaks it can be determined what fraction exists as monomer, and from the Poisson statistics it can then be determined, knowing the pyrene to surfactant molar ratio, what the aggregation number is. This method has been applied to many surfactant systems. One question with any dye method is whether the dye itself influences the micellar property that we are interested in measuring, and Tondre et al. [1975] have addressed this by establishing the minimum surfactant/dye ratio allowable for the dye to have no influence on the system, for a variety of surfactants. A disadvantage of this method is the need to maintain a high purity of the sample, as many compounds act to quench the fluorescence, resulting in too weak or erroneous readings. One quencher is oxygen, so the prepared samples must be purged with nitrogen and nitrogen must be maintained as the head space gas of the cuvette during the measurement.

The standard method using micellar diffusion involves the examination of a micellar solution using quasi-elastic (dynamic) light scattering. Using this technique, the diffusion of light scattering objects in solution (micelles in this case) can be directly measured. Applying the Stokes-Einstein equation, the particle size can be determined, assuming that the objects

are spheres, are not interacting with neighboring spheres, and the size distribution of the scatterers is uniform. These requirements are not strictly met for micellar solutions, but it is often assumed that they are true. Another factor causing this to be a less than ideal method is that the hydrodynamic radius of the diffusing micelle includes whatever water is entrained or closely associated with the hydrophilic domains of the surfactants, and the extent of this water is not known.

Both of these methods for aggregation number determination require expensive instrumentation. I have come across a means for determining aggregation number accidentally by studies of nonionic micellar solutions using a relatively more common and inexpensive UV/vis spectrophotometer.

All micellar solutions appear clear and colorless, thus absorbing no visible light. Assuming that no UV chromophore is present, such as a phenyl ring or double bonds, one might assume that the solution will be transparent in the ultraviolet spectrum also. This is not the case if light scattering objects, such as the micelles in solution, are large enough, as they will scatter light through the Rayleigh scattering mechanism. This mechanism is interesting, as the scattering intensity has an inverse fourth power with wavelength, so if scattering will occur it will be seen most prominently in the UV. This mechanism is more commonly thought of as molecular scattering, and is the reason why the sky is blue (blue light scatters from the atmospheric gas molecules much more than red) and sunsets are red. Using a UV/vis spectrophotometer, an apparent absorption can be measured with a sensitive instrument. This absorption will not be due to actual molecular absorption, which is

responsible for most colors, but actually is due to scattering losses (Figure 4-34). I have established that this absorption loss can be determined for nonionic micelles, as two size factors are in our favor - the micelles have a quite large aggregation number, and the individual surfactant molecules are also large. This method of aggregation number determination is more appropriate for relative determinations, such as what the effect of an additive or temperature change will do to the micelles, unless a calibration can be performed. Calculations of the scattering intensity from first principles are possible, but require an estimate for the index of refraction of the micelle, which at best can only be estimated assuming an oil-drop model for the micellar interior.

Results. Figure 4-35 is an example of the absorbance spectrum of a typical (Brij 78) nonionic surfactant micellar solution. When plotted as log absorbance vs. log wavelength (Figure 4-36), the slope of approximately -4 strongly suggests that the absorbance is due to Rayleigh scattering. The same absorbance spectrum for SDS (Figure 4-37), whose aggregation has been well established as approximately 64, shows a much weaker scattering signal. This is expected, as the micelles are much smaller than nonionic micelles, and the SDS molecules themselves are small compared to most nonionic surfactants. In the UV region, water starts to absorb as well (Figure 4-38). To determine the absolute amount of light attributed to Rayleigh scattering, this baseline water absorption must be subtracted.

For surfactants with strong absorbing features, such as alkylphenyl ethoxylates (Figure 4-39), the UV absorption band of the phenyl ring at 245-290 nm is a complicating feature of the spectrum. Other molecular features can also cause UV absorption, such as

individual double bonds (Figure 4-40). It may be possible to see changes in the aggregation number from Rayleigh scattering by considering regions above 290 nm, if the scattering signal is strong enough. It may be possible to extend this to lower wavelengths, by precisely measuring the molar absorptivity of the surfactant, and correcting the absorption measured for the micelles by the molecular absorption from the surfactant.

This method of aggregation number determination holds out a possibility for a detection method for nonionic surfactant micellar lifetime measurements using temperature-jump. Since it has been well established that aggregation number for the nonionics increases so strongly with temperature (Table 4-10), an increase in the UV absorbance due to Rayleigh scattering should be measurable after a temperature-jump, and the kinetics of this change should be related to the micellar kinetics, as the micelles must rearrange from more smaller micelles at the original temperature to fewer, larger micelles at the higher temperature.

Table 4-10. Aggregation number of some typical nonionic surfactants as a function of temperature [van Os et al., 1993].

Surfactant	T (°C)	Agg. No.		
C_8E_6	18	30		
	30	41		
	40	51		
	60	210		
$C_{12}E_6$	15		140	
	25		400	
	35		1400	
	45		4000	
$C_{16}E_6$	25			2430
	34			16600

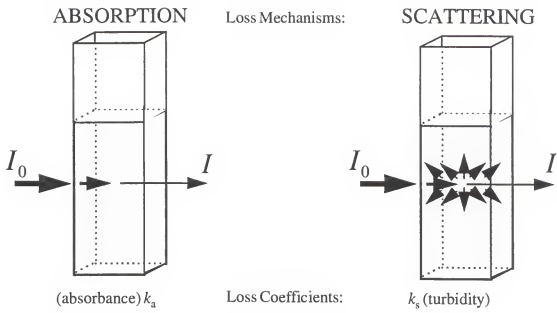

The two mechanisms are indistinguishable to the absorbance spectrophotometer!

Rayleigh Scattering

$$k_s = \frac{24\pi^3}{\lambda^4}\left(\frac{n^2-1}{n^2+2}\right)^2 V^2 c$$

Observed Absorbance

$$A = -\log\left(\frac{I}{I_0}\right) = \left(k_a + k_s\right)L$$

λ=wavelength of light
n=rel. ind. of refraction
V=volume of scatterer
c=conc. of scatterer
A=absorbance
L=path length

Figure 4-34. Measuring light scattering with absorbance spectroscopy.

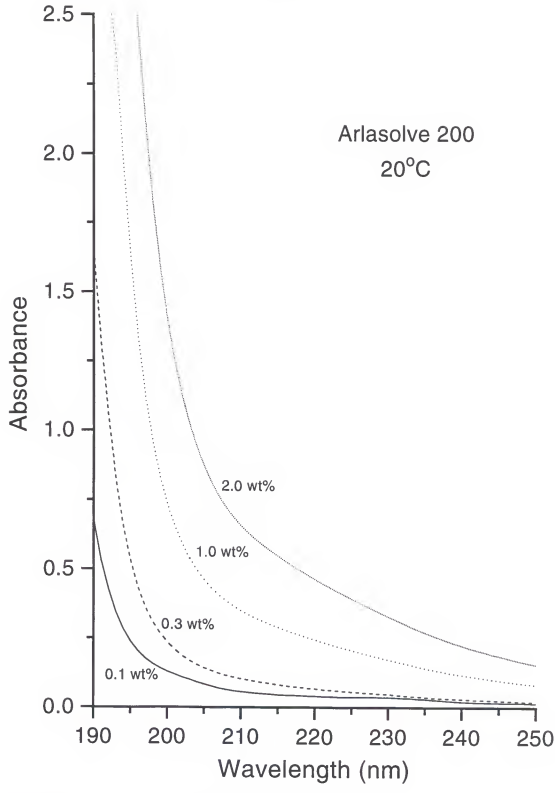

Figure 4-35. Absorbance spectrum of Arlasolve 200.

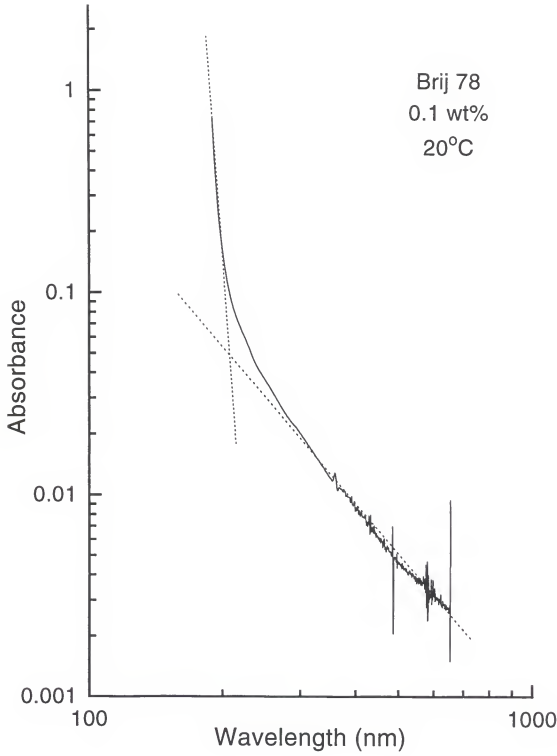

Figure 4-36. Log absorbance vs log wavelength for Brij 78.

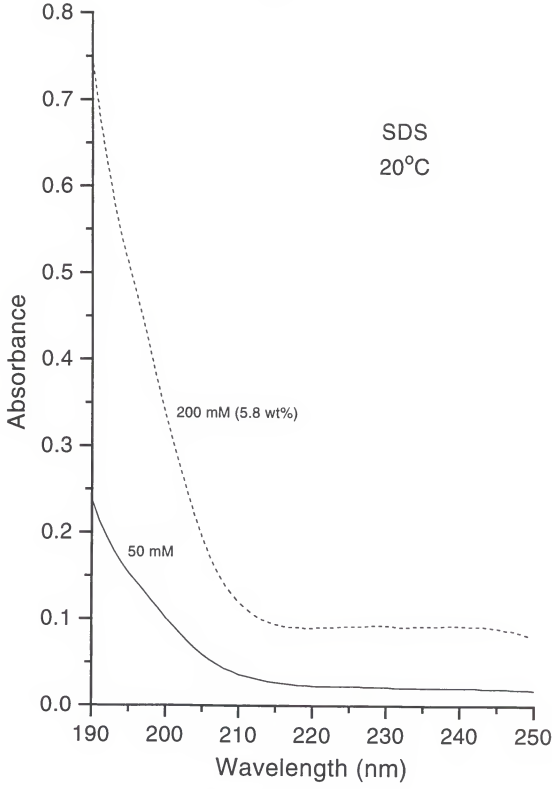

Figure 4-37. Absorbance spectrum of SDS.

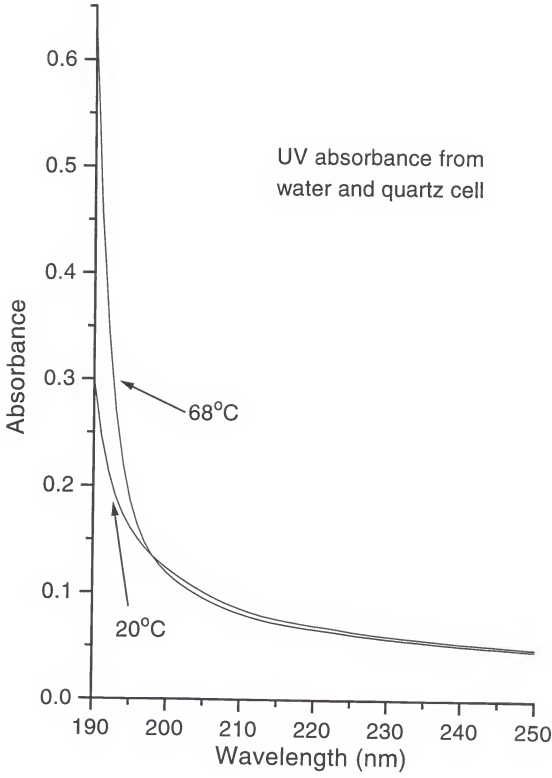

Figure 4-38. Ultraviolet absorbance spectrum of water vs. temperature.

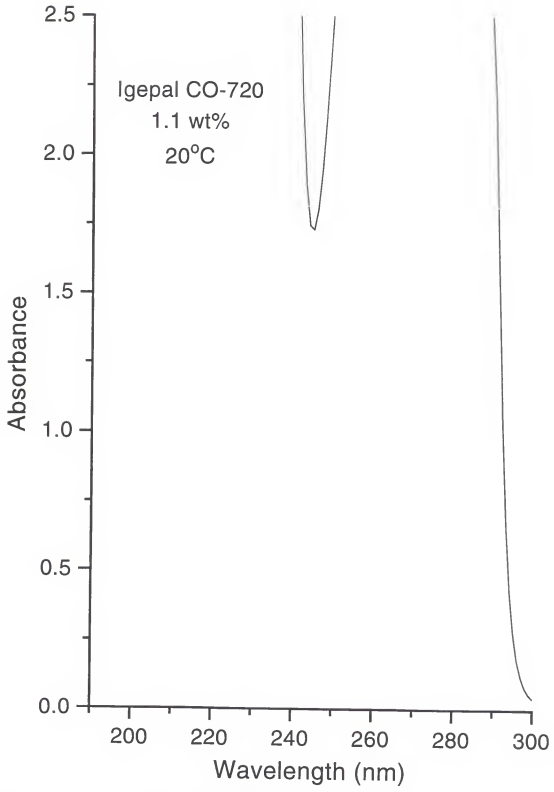

Figure 4-39. Absorbance spectrum of Igepal CO-720.

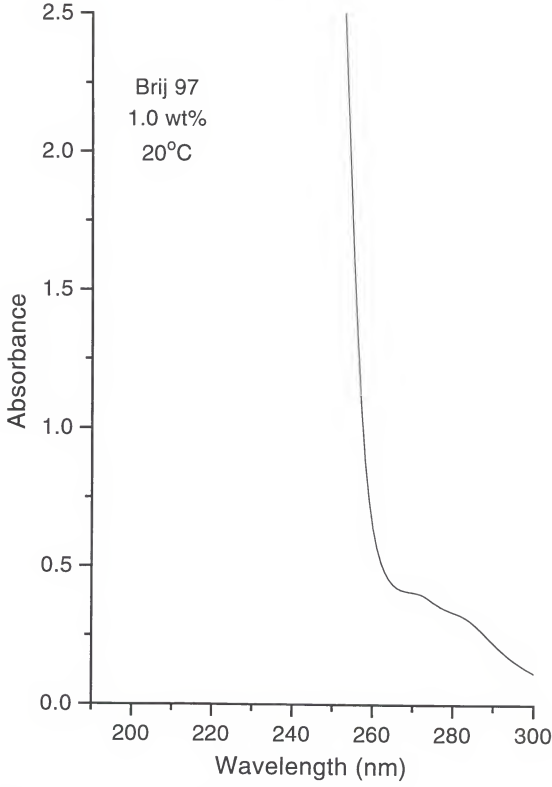

Figure 4-40. Absorbance spectrum of Brij 97.

Conclusion. There are clearly observable changes in UV absorption with temperature, which appear to be Rayleigh scattering from the functional dependence of absorption on wavelength. As the Rayleigh scattering signal should be proportional to the size of the micelle, and scattering is readily measured in the 190-230 nm region, UV absorption appears to be an ideal, unobtrusive method for the measurement of changes in micellar aggregation number with temperature-jump perturbations.

Conclusions

The following comments are the conclusions from this research on micellar stability:

1. Short chain alcohols (methanol through propanol) do not seem to be very surface active, and probably reduce micellar lifetime by increasing the solubility of the surfactant in the solvent (water and alcohol mixture). This solvent effect causes the system to be closer to CMC and thus have a lower micellar lifetime.
2. Longer chain alcohols have little solubility in water and must partition into the micelles, where they act as additional surfactant and increase the micellar stability for the 100 mM SDS case.
3. Nonionic surfactant behaves in a very similar way to the long chain alcohols, increasing micellar stability by acting as additional surfactant. The advantage of the nonionic surfactant over the alcohols is that it is much more soluble in water, thus there is no limit to the amount that can be added to the SDS (the nonionic surfactant may itself micellize with a very low CMC).

4. Glycerol has a similar effect on micellar lifetime as the short chain alcohols, decreasing micellar lifetime by increasing the solubility of the surfactant, thus lowering the concentration/CMC ratio.
5. High proportions of glycerol (>10 vol%) causes the appearance of a third relaxation time, not observed before in micellar systems, and not yet explained.
6. The antifoaming agents of the tetraalkylammonium halide (TAA) class will actually cause increased foamability if the antifoam/surfactant ratio is not sufficiently high.
7. The correlations between micellar stability and foamability for the mixtures of SDS with TAA are opposite of pure SDS cases; increased micellar stability in these systems leads to increased foamability.
8. Longer chain TAA compounds are more efficient at reducing micellar stability, but have lower solubility, limiting their use.
9. Micellar lifetime for certain AOT/Arlacel 20 mixtures seem to behave as nonionic micelles, in that the micellar stability decreases with concentration, contrary to all ionic surfactants and other ionic/nonionic surfactant mixtures studied to date.
10. Ionic species such as NaCl and glycine act to increase micellar lifetime, this can be explained by the salting-out effect - the surfactant becomes less soluble in the electrolyte solution, and it appears as if the concentration is higher, increasing micellar lifetime.
11. The anionic surfactant sodium octanoate added to SDS increases CMC, appearing to behave with equal effect as would additional SDS.

12. Cationic surfactants do not display the same micellar lifetime vs. concentration relationship as anionic surfactants (SDS).
13. The correlation between micellar lifetime and processes such as foamability and fabric wetting do not seem to hold for cationic surfactants in the same way as anionic surfactants (SDS).
14. Rayleigh scattering is clearly observed from nonionic micellar solutions. An increase in scattering with temperature is also observed, as would be expected from scattering from larger micelles. It is well established that nonionic micelles increase in size with temperature. UV absorption measurements of Rayleigh scattering coupled with temperature-jump appear to be the best method for measuring the micellar lifetime of nonionic surfactants that contain no UV chromophore (double bond or phenyl ring).

CHAPTER 5
SUMMARY AND CONCLUSIONS

The following section summarizes the key contributions of the research presented in this thesis, in the areas of surfactant property prediction, microemulsion formulation, and micellar stability. More specific conclusions can be found at the end of chapters 2-4 for the above subjects, respectively.

Surfactant property prediction. The ability to predict properties from molecular structure alone can be a powerful tool, both for prediction of properties of compounds not yet synthesized, and for tailoring molecules to achieve certain properties. The descriptors chosen in such quantitative relationships also may reveal the aspects of molecular structure influencing the property of interest. Over the last 20 years, hundreds of molecular descriptors have been developed for predicting various chemical and physical properties. In this thesis, these descriptors have been applied to the prediction of predicting surfractant properties, for the first time. Excellent results were achieved for the prediction of CMC, cloud point and Krafft point for diverse sets of surfactants.

Microemulsion formulation. Microemulsions have wide application in industry and consumer products. The microemulsions considered here are special, as they are made from mixtures of nonionic surfactants, using no cosurfactant that may not be suitable for cosmetic applications, thus increasing the difficulty of the formulation work. Presently the means of designing new microemulsions for a specific purpose is a trial and error process of

surfactant selection for given oil and aqueous phases. In this thesis, rules are developed to narrow the trial and error search process, by providing some guidelines for the design of water-in-oil microemulsions. The utility of HLB is demonstrated for the first time, as a tool for w/o microemulsion design.

Micellar stability. Micelles are aggregates of surfactants in aqueous solution. They are essential for most of the processes that use surfactants, as they allow the creation of a hydrophobic domain in an otherwise aqueous environment. Micelles are not static structures, but rather are dynamic, constantly disintegrating and reforming. In this thesis, new research progress has been made on several related fronts. The influence of additives (electrolyte, nonionic surfactant, alcohols, cosolvents) on anionic surfactant micellar stability is investigated. The influence of micellar lifetime on processes is studied. The stability of cationic micelles is studied at higher concentrations than previously reported. A comparison between some technological processes (fabric wetting, foamability) and cationic surfactant micellar stability show that the relationships drawn from anionic surfactant studies may not apply to cationic surfactants. Finally, methods for measuring the micellar stability of nonionic surfactants are investigated. The detection method used in ionic surfactant lifetime studies, namely solution electrical conductivity, cannot be used for nonionic surfactants. Alternative detection methods, such as the use of solvatochromic dyes to probe the polarity of the micellar interior, coupled with light absorption detection, are potentially usable. A light absorption method without dye is possible, if absorption measurements are made in the ultraviolet region of the spectrum, where size changes in the

micelles can be detected by changes in the Rayleigh scattering losses. Either of these techniques, coupled with a rapid temperature-jump of the sample, should allow the measurement of nonionic surfactant micellar lifetime.

Suggestions for Future Studies

The following research ideas are possible future projects that are a direct continuation of the work performed in this thesis.

Surfactant property prediction. 1) A new set of descriptors has been developed by Kier and Hall, called the electrotopological indices, which were designed to better handle polar interactions. The surfactant structure-property correlations should be tried with these new descriptors. 2) Data is available for cationic and zwitterionic surfactant CMC, and these should be investigated. 3) By examining possible groupings of surfactant classes for CMC prediction, it may be possible to make more general equations than those limited to each of the classes. 4) Additional surfactant property data can be gathered and analysed using the QSPR approach. 5) It would be interesting to analyse the results obtained with correlations developed using a training set consisting of most of the compounds, testing the errors in a test set to see how general the regressions are. 6) It would be interesting to study the development of rules for surfactant mixture properties. The nonlinear nature of such mixture properties may be predictable.

Microemulsions. Several interesting microemulsion formulation problems exist, that remain unsolved. 1) Microemulsions with triglyceride oils are poorly understood, and no

examples of highly solubilizing microemulsions exist. Such microemulsions would be valuable for pharmaceutical applications. 2) Microemulsions formed with lecithin as a surfactant are of interest, also with pharmaceutical applications. 3) More work can be done to map out the mixture phase diagrams beyond the microemulsion phase region. 4) The temperature dependence of nonionic microemulsion solubilization should be studied.

Micellar stability. There is still relatively little research done on micellar stability, and many opportunities for projects exist. 1) Additional work on the relationship between micellar lifetime and technological processes for cationic surfactants needs to be done to address the differences between these relationships and those seen for anionic surfactants. 2) It would be very interesting to build an apparatus to measure nonionic temperature-jump using absorption detection, as nonionic micellar lifetime is essentially unmeasured. 3) Solvatochromism in micellar solutions should be investigated, as certain dyes are potentially useful probes of micellar changes.

APPENDIX
SURFACTANTS USED IN THIS RESEARCH

Abbreviation or Trade Name	Full Name	HLB	MW (g/mol)
	Anionic Surfactants		
SDS	sodium dodecylsulfate	n/a	288.4
AOT	sodium bis-2-ethylhexylsulfosuccinate	n/a	444.6
	Cationic Surfactants		
CPC	cetylpyridinium chloride	n/a	358.0
MTAB	myristyltrimethylammonium bromide	n/a	336.4
CTAB	cetyltrimethylammonium bromide	n/a	364.5
	Nonionic Surfactants		
Span 20	sorbitan monolaurate	8.6	346
Span 80	sorbitan mono-oleate	4.3	428
Arlacel 83	sorbitan sesquioleate	3.7	560
Span 85	sorbitan trioleate	1.8	956
Tween 20	POE 20 sorbitan monolaurate	16.7	1226
Tween 21	POE 4 sorbitan monolaurate	13.3	522
Tween 80	POE 20 sorbitan mono-oleate	15.0	1308
Tween 81	POE 5 sorbitan mono-oleate	10.0	648
Tween 85	POE 20 sorbitan trioleate	11.0	1836
Brij 76	POE 10 stearyl ether	12.4	710
Brij 78	POE 20 stearyl ether	15.3	1150
Brij 700	POE 100 stearyl ether	18.8	4670
Brij 93	POE 2 oleyl ether	4.9	356
Alkamuls EL-719	POE 40 castor oil^{+}	13.6	2692
Igepal CO-210	POE 1.5 nonylphenyl ether	4.6	286
Igepal CO-430	POE 4 nonylphenyl ether	8.8	396
Igepal CO-530	POE 6 nonylphenyl ether	10.8	484
Igepal CO-610	POE 7.5 nonylphenyl ether	12.2	550
Igepal CO-630	POE 9 nonylphenyl ether	13.0	616
Igepal CO-720	POE 12 nonylphenyl ether	14.2	748
Igepal DM-430	POE 7 dinonylphenyl ether	9.4	650

Table A-1. Surfactants used in this thesis, names, structures, HLB and est. molecular weight. *POE {polyoxyethylene} (#) is the average number of ethylene oxide repeats. $^{+}$Castor oil is triricinoleoyl glycerol. Ricinoleic acid is a C_{18} fatty acid, $C_{18}H_{34}O_3$, whose structure is $CH_3(CH_2)_5CH(OH)CH_2CH{=}CH(CH_2)_7COOH$.

Nonionic Surfactants Used in This Thesis

Table A-1 summarizes the surfactants used in this dissertation. For the microemulsion studies, nonionic surfactant structures covered include sorbitan esters, POE sorbitan esters, nonylphenyl POE ethers, other alkyl POE ethers, and POE triglycerides. Surfactants were chosen for the range of structures available for analogous compounds, allowing excursions on small variations of molecular structure to be performed in order to elucidate the effect of surfactant structure on solubilization.

Sorbitan esters and alkyl ethers are provided by ICI Americas, Inc., Wilmington, Delaware, and alkylphenyl ethers are provided by Rhone-Poulenc, Inc., Atlanta, Georgia. We are indebted to these companies for their generous support in providing samples.

Structural Variation and Polydispersity of the Nonionic Surfactants

It should be noted that all commercial surfactants used are not isomerically pure, but rather a diverse collection homologous surfactant molecules. This results from the synthesis reactions used in creating the surfactants, where the extent of reaction cannot be controlled completely.

For studies of the influence of surfactant structure on properties, one must consider structural variability in both the hydrophilic and the hydrophobic domains of the surfactant molecule. For the hydrophobic domain, variation occurs in alkyl chain length, saturation, and ring structures. Many surfactants are created by reacting a hydrophilic structure with a fatty acid, to create an ester. The purity of the fatty acid used will clearly effect the homogeneity of the resulting surfactant. Some surfactants use relatively pure fatty acids and

will have only a few percent of impurities. Commonly, an oleate ($C_{18:1}$, one double bond) will have a small amount of stearate (C_{18}) and linoleate ($C_{18:2}$) as impurities. A linear saturated fatty acid will usually be contaminated with the saturated fatty acids with two more and two less carbons.

In the hydrophobic group, variation is seen in different lengths of polyethylene oxide (PEO) polymer, and in the presence of other hydrophilic structures such as sorbitan. Variation in PEO chain length results when there are multiple reaction sites (hydroxy groups) possible for the esterification (sorbitan esters have multiple sites). Sorbitan ester surfactants are available as monoesters, triesters, and sesquiesters. The monoesters will have some di- and triesters present, and the triesters will have some mono- and diesters. The sesquiesters, such as Arlacel 83, sorbitan sesquioleate, is really a mixture of sorbitan mono- and dioleates, with an average of 1.5 oleic acid residues per sorbitan.

The most common variability is found in the hydrophilic component of the surfactants. The hydrophilic domain in most nonionic surfactants is a polymer created by reacting ethylene oxide. The polymerization reaction cannot be controlled precisely, so the final product is not a homogeneous, monomolecular product. These polyoxyethylene compounds are assigned a number for the number of repeats of ethylene oxide residues. This number can be considered either an average, or the most probable (peak) number of ethylene oxide residues per molecule. The distribution of POE lengths for a given average may be quite wide, and some investigators [Shinoda et al., 1971] have studied the effect of

the width of the distribution on surfactant properties by distilling the surfactants and narrowing the distribution.

Another variability present in the hydrophilic component of the sorbitan esters is also due to a reaction whose extent cannot be controlled precisely. Sorbitan (a ring) is produced by dehydration of sorbitol, where the two end hydroxyl groups of the six carbon molecules react. A fraction of the sorbitan rings will react further, with an additional dehydration leading to a isosorbide, which is a multiple ring type structure. This sorbide should be less hydrophilic, as it has fewer oxygens available to hydrogen bond.

LIST OF REFERENCES

Abe, M., Schechter, D., Schechter, R. S., Wade, W. H., Weerasooriya, U., Yiv, S. "Microemulsion Formation with Branched Tail Polyoxyethylene Sulfonate Surfactants," *J. Colloid Interface Sci.* **114**, 342-356 (1986).

Aoudia, M., Rodgers, M. A. J., Wade, W. H. "Light Scattering and Fluorescence Studies of o/w Microemulsion: The Sodium 4-Dodecylbenzenesulfonate-Butanol-Water-NaCl-Octane System," *J. Colloid Interface Sci.* **144**, 353 (1991).

Bansal, V. K., Chinnaswamy, K., Ramachandran, C., Shah, D. O. "Structural Aspects of Microemulsions Using Dielectric Relaxation and Spin Label Techniques," *J. Colloid Interface Sci.* **72**, 524-537 (1979).

Becher, P. "Hydrophile-Lipophile Balance: History and Recent Developments. Langmuir Lecture - 1983," *J. Disp. Sci. Tech.* **5**, 81-96 (1984).

Beckman, E. J., Smith, R. D. "Microemulsions Formed from Nonionic Surfactants in Near-Critical and Supercritical Alkanes: Quasi-Elastic Light Scattering Investigations," *J. Phys. Chem.* **94**, 3729 (1990).

Bikerman, J.J. Foams, Springer Verlag, New York, 1973.

Blute, I., Jansson, M., Oh, S.G , Shah, D.O. "The Molecular Mechanism for Destabilization of Foams by Organic Ions," *J. Am. Oil Chem. Soc.* **71**, 41-46 (1994).

Brookhaven Instruments Corp. Instruction Manual for Model BI-2030 Digital Correlator, Holtsville, NY, 1983.

Brookhaven Instruments Corp. Instruction Manual for Laser Light Scattering Goniometers, Holtsville, NY, 1984.

Ceglie, A., Colafemmina, G., Monica, M.D., Burlamacchi, L., Monduzzi, M. "^{23}Na NMR Relaxation Study of Sodium Dodecyl Sulphate in Some Aqueous and Nonaqueous Systems," *J. Colloid Interface Sci.* **146**, 363-372 (1991).

CRC Handbook of Chemistry and Physics, 61st Edition, CRC Press, Boca Raton, FL, 1980.

Edward, J.T., Farrell, P.G., Shahidi, F. "Partial Molal Volumes of Organic Compounds in Carbon Tetrachloride. 1. Alkanes. Conformational Effects," *J. Phys. Chem.* **82**, 2310-2313 (1978).

El-Nokaly, M., Hiler, G., McGrady, J. "Solubilization of Water and Water-Soluble Compounds in Triglycerides," in Microemulsions and Emulsions in Foods, (M. El-Nokaly, D. Cornell, Eds.), ACS Press, Washington, DC, 1991.

Garrett, P.R., and Ward, D.R. "A Reexamination of the Measurement of Dynamic Surface Tensions Using the Maximum Bubble Pressure Apparatus," *J. Colloid Interface Sci.* **132**, 475-490 (1989).

Griffin, W.C. "Classification of Surface-Active Agents by HLB," *J. Soc. Cosmet. Chem.* **1**, 311-326 (1949).

Griffin, W.C. "Calculation of HLB Values of Non-Ionic Surfactants," *J. Soc. Cosmet. Chem.* **5**, 249-256 (1954).

Gu, T., Sjöblom, J. "Empirical Relationships between the Krafft Points and the Structural Units in Surfactants," *Acta Scand. Chem.* **45**, 762-765 (1991).

Gu, T., Sjöblom, J. "Surfactant Structure and its Relation to the Krafft Point, Cloud Point and Micellization; Some Empirical Relationships," *Colloids Surf.* **64**, 39-46 (1992).

Gustavsson, H., Lindman, B. "Alkali Ion Binding to Aggregates of Amphiphilic Compounds Studied by Nuclear Magnetic Resonance Chemical Shifts," *J. Am. Chem. Soc.* **100**, 4647-4654 (1978).

Hou, M. J., Kim, M., Shah, D. O. "A Light Scattering Study on the Droplet Size and Interdroplet Interaction in Microemulsions of AOT-Oil-Water System," *J. Colloid Interface Sci.* **123**, 398-412 (1987).

Hua, X.Y., and Rosen, M.J. "Dynamic Surface Tension of Aqueous Surfactant Solutions. I. Basic Parameters," *J. Colloid Interface Sci.* **124**, 652-659 (1988).

Huibers, P.D.T., Shah, D.O., "Enhanced Solubilization in Water-in-Oil Microemulsions Using Mixtures of Nonionic Surfactants," in Dynamic Properties of Interfaces and Association Structures, V. Pillai, D.O. Shah, Eds., AOCS Press; Champaign, IL, 1996a.

Huibers, P.D.T., Shah, D.O. "Dynamic Surface Tension of Octadecyl Ethoxylate Surfactants" submitted to *J. Colloid Interface Sci.* (1996b).

Huibers, P.D.T., Shah, D.O. "Evidence for Synergism in Nonionic Surfactant Mixtures: Enhancement of Microemulsion Solubilization" submitted to *Langmuir* (1996c).

Huibers, P.D.T., Oh, S.G., Shah, D.O., "Pressure-Jump Studies on Micellar Relaxation Time and its Effect on Various Technological Processes," in Surfactants in Solution, A.K. Chattopadhyay, K.L. Mittal, Editors, Marcel Dekker; New York, 1996a.

Huibers, P.D.T., Lobanov, V.S., Katritzky, A.R., Shah, D.O., Karelson, M., "Prediction of Critical Micelle Concentration Using a Quantitative Structure-Property Relationship Approach. 1. Nonionic Surfactants," *Langmuir* **12**, 1462-1470 (1996b).

Huibers, P.D.T., Lobanov, V.S., Katritzky, A.R., Shah, D.O., Karelson, M., "Prediction of Critical Micelle Concentration Using a Quantitative Structure-Property Relationship Approach. 2. Anionic Surfactants," *J. Colloid Interface Sci.*, in press (1996c).

Huibers, P.D.T., Shah, D.O., Katritzky, A.R., "Predicting Surfactant Cloud Point from Molecular Structure" submitted to *J. Colloid Interface Sci.* (1996d).

ICI Americas, Inc. The HLB System: A Time Saving Guide to Emulsifier Selection, ICI, Wilmington, DE, 1984.

Inoue, T., Shibuya, Y., Shimozawa, R. "Chemical Relaxation Studies in Micellar Solutions of Sodium Alkyl Sulfates," *J. Colloid Interface Sci.* **65**, 370-379 (1978).

Inoue, T., Tashiro, R., Shibuya, Y., Shimozawa, R. "Kinetic Study on Micelle Formation of Tetradecylpyridinium Salts," *J. Colloid Interface Sci.* **73**, 105-114 (1980).

Israelachvili, J.N. Intermolecular & Surface Forces, 2nd Ed., Academic Press, New York, 1992.

Israelachvili, J.N., Mitchell, D.J., Ninham, B.W. "Theory of Self-Assembly of Hydrocarbon Amphiphiles into Micelles and Bilayers," *J. Chem. Soc. Faraday Trans. I* **72**, 1525-1568 (1976).

Jayakrishnan, A., Kalaiarasi, K., Shah, D. O. "Microemulsions: Evolving Technology for Cosmetic Applications," *J. Soc. Cosmet. Chem.* **34**, 335-350 (1983).

Johnson, K. A., Shah, D. O. "Effect of Oil Chain Length and Electrolytes on Water Solubilization in Alcohol-Free Pharmaceutical Microemulsions," *J. Colloid Interface Sci.* **107**, 269-271 (1985).

Kahlweit, M., Strey, R., Busse, G. "Effect of Alcohols on the Phase Behavior of Microemulsions," *J. Phys. Chem.* **95**, 5344-5352 (1991).

Katritzky, A.R., Lobanov, V.S., Karelson, M., CODESSA software, University of Florida, Gainesville, ©1994. CODESSA is distributed by SemiChem, Inc., 7128 Summit, Shawnee, KS 66216.

Katritzky, A.R., Lobanov, V.S., Karelson, M. "QSPR: The Correlation and Quantitative Prediction of Chemical and Physical Properties from Structure," *Chem. Soc. Rev.* **24**, 279-284 (1995).

Kier, L.B. "Computational Aspects of Molecular Connectivity and its Role in Structure-Property Modeling," *in* Computational Chemical Graph Theory, (D.H. Rouvray, Ed.), Chap. 6, Nova Science Publishers, New York, 1990, Chap. 8.

Kier, L.B., Hall, L.H. Molecular Connectivity in Chemistry and Drug Research, Academic Press, New York, 1976.

Kier, L.B., Hall, L.H. Molecular Connectivity in Structure-Activity Analysis, Wiley, New York, 1986.

Klevens, H.B. "Critical Micelle Concentrations as Determined by Refraction," *J. Phys. Colloid Chem.* **52**, 130-148 (1948).

Klevens, H.B., *J. Am. Oil Chem. Soc.* **30**, 74 (1953).

Kon-No, K., Kitahara, A. "Solubility Behavior of Water in Nonaqueous Solutions of Oil-Soluble Surfactants: Effect of Molecular Structure of Surfactants and Solvents," *J. Colloid Interface Sci.* **37**, 469 (1971).

Kosower, E.M. *J. Am. Chem. Soc.* **80**, 3253-3270 (1958).

Krafft, F., Wiglow, H. *Ber. Dtsch. Chem. Ges.* **28**, 2566 (1895).

Kumar, P., Pillai, V., Shah, D.O. "Preparation of Bi-Pb-Sr-Ca-Cu-O Oxide Superconductors by Coprecipitation of Nanosize Oxalate Precursor Powders in the Aqueous Core of Water-in-Oil Microemulsions," *Appl. Phys. Lett.* **62**, 765-767 (1993).

Lang, J., Auburn, J.J., Eyring, E.M. "Kinetics of Octylphenyl Polyoxyethylene Alcohol Micelle Dissociation by a Stopped-Flow Technique," *J. Colloid Interface Sci.* **41**, 484-490 (1972a).

Lang, J., Eyring, E.M. "Kinetics of the Dissociation of Nonionic Detergent Micelles by a Temperature-Jump Technique," *J. Polymer Sci. A-2* **10**, 89-99 (1972b).

Lay, M.B., Drummond, C.J., Thistlethwaite, P.J., Grieser, F. "$E_T(30)$ as a Probe for the Interfacial Microenvironment of Water-in-Oil Microemulsions," *J. Colloid Interface Sci.* **128**, 602-604 (1989).

Lessner, E., Teubner, M., Kahlweit, M. "Relaxation Experiments in Aqueous Solutions of Ionic Micelles. 1. Theory and Experiments on the System H_2O-Sodium Tetradecyl Sulfate-$NaClO_4$," *J. Phys. Chem.* **85**, 1529-1536 (1981a).

Lessner, E., Teubner, M., Kahlweit, M. "Relaxation Experiments in Aqueous Solutions of Ionic Micelles. 2. Experiments on the System H_2O-NaDS-$NaClO_4$ and Their Theoretical Interpretation," *J. Phys. Chem.* **85**, 3167-3175 (1981b).

Leung, R., Shah, D.O. "Dynamic Properties of Micellar Solutions. I. Effects of Short-Chain Alcohols and Polymers on Micellar Stability," *J. Colloid Interface Sci.* **113**, 484 (1986).

Lianos, P., Zana, R. "Fluorescence Probe Studies of the Effect of Concentration on the State of Aggregation of Surfactants in Aqueous Solution," *J. Colloid Interface Sci.* **84**, 100-107 (1981).

Lindgren, Å. "Multivariate Structure-Property-Relationships of Non-Ionic Surfactants," Ph.D. Thesis, Research Group for Chemometrics, Dept. of Organic Chemistry, Umeå University, Umeå, Sweden, 1995.

Lindgren, Å., Sjöström, M. "Multivariate Physicochemical Characterization of Some Technical Non-Ionic Surfactants," *Chemometrics and Intelligent Lab. Sys.* **23**, 179-189 (1994).

Lindgren, Å., Sjöström, M., Hellsten, M., Lif, A. "Modeling of the Detergency Performance for Some Technical Non-Ionic Surfactants," *Tenside Surf. Det.* **32**, 300-309 (1995).

Lindman, B., Soderman, O., Stilbs, P. "Microstructure and Molecular Dynamics of Surfactant Solutions: An Overview of NMR Self-Diffusion and Relaxation Studies," in Surfactants in Solution, Volume 7, (K.L. Mittal, Ed.), Plenum Press, New York (1984).

Lissant, K.J., in Emulsions and Emulsion Technology, (K.J. Lissant, Ed.), Marcel Dekker, New York, 1974, p. 363, 390.

Lobanov, V. "Quantitative Structure-Property Relationships in Large Descriptor Spaces," Ph.D. Thesis, Tartu University, Tartu, Estonia, 1996.

Matsuki, H., Ichikawa, R., Kaneshina, S., Kamaya, H., Ueda, I. "Differential Scanning Calorimetric Study on the Krafft Phenomenon of Local Anesthetics," *J. Colloid Interface Sci.* **181**, 362-369 (1996).

Monduzzi, M., Ceglie, A., Lindman, B., Soderman, O. "A ^2H and ^{13}C NMR Multifield Relaxation Study of Aqueous Aggregate Systems of Sodium Dodecyl Sulfate," *J. Colloid Interface Sci.* **136**, 113-123 (1990).

Moroi, Y., Nishikido, N., Uehara, H., Matuura, R. "An Interrelationship Between Heat of Micelle Formation and Critical Micelle Concentration," *J. Colloid Interface Sci.* **50**, 254-264 (1975).

Mukerjee, P., Mysels, K.J. Critical Micelle Concentrations of Aqueous Surfactant Systems, NSRDS-NBS 36, U.S. Dept. of Commerce, Washington DC, 1971.

Mysels, K.J. "The Maximum Bubble Pressure Method of Measuring Surface Tension, Revisited," *Colloids Surf.* **43**, 241-262, (1990).

Nagarajan, R., Ruckenstein, E. "Theory of Surfactant Self-Assembly: A Predictive Molecular Thermodynamic Approach," *Langmuir* **7**, 2934-2969 (1991).

Oh, S.G., Shah, D.O. "Relationship between Micellar Lifetime and Foamability of Sodium Dodecyl Sulfate and Sodium Dodecyl Sulfate/1-Hexanol Mixtures," *Langmuir* **7**, 1316-1318 (1991).

Oh, S.G., Shah, D.O. "Effect of Counterions on the Interfacial Tension and Emulsion Droplet Size in the Oil/Water/Dodecyl Sulfate System," *J. Phys. Chem.* **97**, 284-286 (1993a).

Oh, S.G., Shah, D.O. "The Effect of Micellar Lifetime on the Rate of Solubilization and Detergency in Sodium Dodecyl Sulfate Solutions," *J. Am. Oil Chem. Soc.* **70**, 673-678 (1993b).

Oh, S.G., Huibers, P.D.T., Shah, D.O., "The Influence of Micellar Stability on Technological Processes," in Dynamic Properties of Interfaces and Association Structures, V. Pillai, D.O. Shah, Eds., AOCS Press; Champaign, IL, 1996.

Patel, S.S., Kumar, K., Shah, D.O., Delfino, J.J. "Effect of Surfactant Concentration and Film Area on the Stability of Films of Surfactant Solutions," *J. Colloid Interface Sci.* **183**, 603-606 (1996).

Platz, G. "Untersuchung von Trübungserscheinungen im Einphasengebiet wäßriger Lösungen nichtionogener Tenside," *Ber. Bunsenges. Phys. Chem.* **85**, 1155-1163 (1981).

Püschel, F., Todorov, O. "Zusammenhänge Zwischen der Konstitution und Einigen Eigenschaften von Grenzflächenactiven Benzolsulfonaten mit Heteroatomen in der Aliphatischen Seitenkette. 1. Löslichkeit, Grenzflächenaktivität, Kritische Micellbildungskonzentration und Papierchromatographie der Sulfonate," *Tenside* **5**, 193-198 (1968).

Puvvada, S., Blankschtein, D. "Molecular-Thermodynamic Approach to Predict Micellization, Phase Behavior and Phase Separation of Micellar Solutions. I. Application to Nonionic Surfactants," *J. Chem. Phys.* **92**, 3710-3724 (1990).

Randic, M. "On Characterization of Molecular Branching," *J. Am. Chem. Soc.* **97**, 6609-6615 (1975).

Rassing, J., Sams, P.J., Wyn-Jones, E. "Temperature Dependence of the Rate of Micellization Determined from Ultrasonic Relaxation Data," *J. Chem. Soc. Faraday Trans II* **69**, 180-185 (1973).

Ravey, J.C., Gherbi, A., Stebe, M.J. "Comparative Study of Fluorinated and Hydrogenated Nonionic Surfactants. I. Surface Activity Properties and Critical Concentrations," *Progr. Colloid Polym. Sci.* **76**, 234-241 (1988).

Reichardt, C. "Solvochromic Dyes as Solvent Polarity Indicators," *Chem. Rev.* **94**, 2319-2358 (1994).

Richter, R.R., Bluhm, Th., Krusmann, H. "Struktur-Aktivitatsbeziehungen zwischen Tensidstruktur und Waschleistung," *Tenside Surf. Det.* **33**, 42-45 (1996).

Romsted, L.S., Yoon, C.O. "Counterion Affinity Orders in Aqueous Micellar Solutions of Sodium Dodecyl Phosphate and Sodium Dodecyl Sulfate Determined by Changes in ^{23}Na NMR Relaxation Rates: A Surprising Dependence on Head Group Charge," *J. Am. Chem. Soc.* **115**, 989-994 (1993).

Rosen, M.J. "The Relationship of Structure to Properties in Surfactants. IV. Effectiveness in Surface or Interfacial Tension Reduction," *J. Colloid Interface Sci.* **56**, 320-327 (1976).

Rosen, M.J. Surfactants and Interfacial Phenomena, 2nd Ed., Wiley, New York, 1989.

Rosen, M.J. "Synergism in Binary Mixtures of Surfactants at Various Interfaces," in Mixed Surfactant Systems, (P.M. Holland, D.N. Rubingh, Eds.), ACS, Washington, DC, 1992.

Rouviere, J., Faucompre, B., Lindheimer, M., Partyka, S., Brun, B. "Proprietes Physico-Chimiques de N-Alkyl P-Benzene Sulfonates Alcalins: Temperature de Krafft et Concentration Critique Micellaire," *J. Chim. Phys.* **80**, 309-314 (1983).

Rouvray, D.H. "Predicting Chemistry from Topology," *Scientific American* **254**, 40-47 (1986).

Sakurai, M., Nakamura, K., Nitta, K. "Volumetric Properties of Dilute Aqueous Alcohol Solutions at Different Temperatures," *Bull. Chem. Soc. Japan* **67**, 1580-1587 (1994).

Shiao, S.Y., Patist, A., Free, M.L., Chhabra, V., Huibers, P.D.T., Gregory, A., Patel, S., Shah, D.O. "The Importance of Sub-Angstrom Distances in Mixed Surfactant Systems for Technological Processes," *Colloids Surf. A*, in press, 1996.

Shinoda, K., Becher, P. Principles of Solution and Solubility, Marcel Dekker, New York, 1978.

Shinoda, K., Friberg, S. Emulsions and Solubilization, Wiley, New York, 1986.

Shinoda, K., Kunieda, H. "How to Formulate Microemulsions with Less Surfactant," in Microemulsions: Theory and Practice (L. M. Prince, Ed.), Academic Press, New York, 1977, Chap. 4.

Shinoda, K., Kunieda, H., Arai, T., Saijo, H. "Principles of Attaining Very Large Solubilization (Microemulsion): Inclusive Understanding of the Solubilization of Oil and Water in Aqueous and Hydrocarbon Media," *J. Phys. Chem.* **88**, 5126 (1984).

Shinoda, K., Saito, H., Arai, H. "The Effect of the Size and the Distribution of the Oxyethylene Chain Lengths of Nonionic Emulsifiers on the Stability of Emulsions," *J. Colloid Interface Sci.* **35**, 624 (1971).

Soderman, O., Canet, D., Carnali, J., Henriksson, U., Nery, H., Walderhaug, H., Warnheim, T. "The Interpretation of Nuclear Magnetic Resonance Relaxation Data from Micellar and Microemulsion Systems," in Microemulsion Systems (H.L. Rosano, M. Clausse, Eds.), Marcel Dekker, New York, 1987.

Stanton, D.T., Jurs, P.C. "Development and Use of Charged Partial Surface Area Structural Descriptors in Computer-Assisted Quantitative Structure-Property Relationship Studies," *Anal. Chem.* **62**, 2323-2329 (1990).

Strey, R., Jonstroemer, M. "Role of Medium-Chain Alcohols in Interfacial Films of Nonionic Microemulsions," *J. Phys. Chem.* **96**, 4537 (1992).

Strey, R., Pakush, A. "Critical Fluctuations, Micelle Kinetics and Phase Diagram of Water - Nonionic Surfactant, H_2O - $C_{12}E_6$" in Surfactants in Solution, Vol. 4 (K.L. Mittal, P. Bothorel, Eds.), Plenum Press, New York, 1986.

Tamura, T., Kaneko, Y., Ohyama, M. "Dynamic Surface Tension and Foaming Properties of Aqueous Polyoxyethylene n-Dodecyl Ether Solutions," *J. Colloid Interface Sci.* **173**, 493-499 (1995).

Tanford, C. "Micelle Shape and Size," *J. Phys. Chem.* **76**, 3020-3024 (1972).

Tanford, C. The Hydrophobic Effect, 2nd Ed., Wiley, New York, 1980.

Tondre, C., Lang, J., Zana, R. "On the Use of Dyes for the Kinetic Study of Micellar Equilibria," *J. Colloid Interface Sci.* **52**, 372-379 (1975).

Traube, J. *Samml. Chem. Vortr.* **4**, 255 (1899).

Ueda, M., Schelly, Z.A. "Reverse Micelles of Aerosol-OT in Benzene. 4. Investigation of the Micropolarity Using 1-Methyl-8-oxyquinolinium Betaine as a Probe," *Langmuir* **5**, 1005-1008 (1989).

van Krevelen, D.W. Properties of Polymers, 3rd Ed., Elsevier, New York, 1990.

van Os, N.M., Daane, G.J., Bolsman, T.A.B.M. "The Effect of Chemical Structure upon the Thermodynamics of Micellization of Model Alkylarenesulfonates. I. Sodium p-(x-decyl)benzenesulfonate Isomers," *J. Colloid Interface Sci.* **115**, 402-409 (1987).

van Os, N.M., Daane, G.J., Bolsman, T.A.B.M. "The Effect of Chemical Structure upon the Thermodynamics of Micellization of Model Alkylarenesulfonates. II. Sodium p-(3-alkyl)benzenesulfonate Homologs," *J. Colloid Interface Sci.* **123**, 267-274 (1988).

van Os, N.M., Haak, J.R., Rupert, L.A.M. Physico-Chemical Properties of Selected Anionic, Cationic and Nonionic Surfactants, Elsevier, Amsterdam, 1993.

Varadaraj, R., Bock, J., Valint, P., Brons, N. "Micropolarity and Water Penetration in Micellar Aggregates of Linear and Branched Hydrocarbon Surfactants," *Langmuir* **6**, 1376-1378 (1990).

Varadaraj, R., Bock, J., Brons, N., Pace, S. "Probing Hydrophobic Microdomains of Hydrophobically Associating Acrylamide-N-Alkylacrylamide Copolymers in Solution Using a Solvatochromic Absorption Dye Probe," *J. Phys. Chem.* **97**, 12991-12994 (1993).

Warr, G.G., Evans, D.F. "Spectroscopic Determination of the Effective Dielectric Constant of Micelle-Water Interfaces between 15 and 85°C," *Langmuir* **4**, 217-224 (1988).

Waterman, H.I., Boelhouwer, C., Huibers, D.T.A. Process Characterization. Graphical Statistical Methods of Product Distribution Analysis in Chemical and Physical Operations, Elsevier, Amsterdam, 1960, Chapter 4.

Weiner, H. "Structural Determination of Paraffin Boiling Points," *J. Am. Chem. Soc.* **69**, 17-20 (1947).

Woolfrey, S.G., Banzon, G.M., and Groves, M.J. "The Effect of Sodium Chloride on the Dynamic Surface Tension of Sodium Dodecyl Sulfate Solutions," *J. Colloid Interface Sci.* **112**, 583-587 (1986).

Yalkowsky, S.H., Banerjee, S. Aqueous Solubility. Methods of Estimation for Organic Compounds, Marcel Dekker, New York, 1992.

Yoshida, T., Taga, K., Okabayashi, H., Matsushita, K., Kamaya, H., Ueda, I. "Counterion Binding to Micelles Measured by Sodium-23 NMR Relaxation Times: Enhancement by Anesthetics," *J. Colloid Interface Sci.* **109**, 336-340 (1986).

Zachariasse, K.A., Phuc, N.V., Kozankiewicz, B. "Investigation of Micelles, Microemulsions, and Phospholipid Bilayers with the Pyridinium *N*-Phenolbetaine $E_T(30)$, a Polarity Probe for Aqueous Interfaces," *J. Phys. Chem.* **85**, 2676-2683 (1981).

Zana, R. "Luminescence Probing Methods," in Surfactant Solutions, New Methods of Investigation (R. Zana, Ed.), Marcel Dekker, New York, 1987.

Zecchino, J. R., Krishnaswamy, N., Clement, P. A., Vargas, A. "Oil-in-Water Emulsions Containing Polyethylene," U.S. Patent 5,008,100, Elizabeth Arden Co., April 16, 1991.

Zhao, J., Fung, B.M. "NMR Study of the Transformation of Sodium Dodecyl Sulfate Micelles," *Langmuir* **9**, 1228-1231 (1993).

Zollinger, H. Color Chemistry. Syntheses, Properties and Applications of Organic Dyes and Pigments, VCH, New York, 1987.

Zu, D., Schelly, Z.A. "Investigation of the Microenvironment in Triton X-100 Reverse Micelles in Cyclohexane, Using Methyl Orange as a Probe," *Langmuir* **8**, 48-50 (1992).

BIOGRAPHICAL SKETCH

Paul was born on March 6, 1964, to Elizabeth and Derk Huibers in Summit, New Jersey. He completed high school at Hopewell Valley Central High School in Pennington, New Jersey, and went on to complete his bachelor's degree in chemical engineering from the University of Delaware in June, 1986. Paul started his first career in aerospace research as a scientist at SciTec Inc., later a subsidiary of TRW Inc., in Princeton, New Jersey, engaging in fascinating research in areas related to optical radiation propagation in the atmosphere. Due to unforeseen circumstances, such as the fall of the Berlin Wall and the collapse of the Soviet Union, the prospects for this line of research seemed greatly diminished, and in August of 1992 Paul started his Ph.D. program in the Department of Chemical Engineering at the University of Florida, with Dinesh O. Shah as his research advisor. Completing his degree in the fall of 1996, the future is yet unwritten as to where this newly gained knowledge of surfactants and interfacial phenomena will lead him.

I certify that I have read this study and that in my opinion it conforms to acceptable standards of scholarly presentation and is fully adequate, in scope and quality, as a dissertation for the degree of Doctor of Philosophy.

Dinesh O. Shah, Chairman
Professor of Chemical Engineering

I certify that I have read this study and that in my opinion it conforms to acceptable standards of scholarly presentation and is fully adequate, in scope and quality, as a dissertation for the degree of Doctor of Philosophy.

Chang-Won Park
Associate Professor of Chemical Engineering

I certify that I have read this study and that in my opinion it conforms to acceptable standards of scholarly presentation and is fully adequate, in scope and quality, as a dissertation for the degree of Doctor of Philosophy.

Alan R. Katritzky
Kenan Professor of Chemistry

I certify that I have read this study and that in my opinion it conforms to acceptable standards of scholarly presentation and is fully adequate, in scope and quality, as a dissertation for the degree of Doctor of Philosophy.

Randolph S. Duran
Associate Professor of Chemistry

I certify that I have read this study and that in my opinion it conforms to acceptable standards of scholarly presentation and is fully adequate, in scope and quality, as a dissertation for the degree of Doctor of Philosophy.

Laszlo Prokai
Associate Professor of Pharmaceutics

This dissertation was submitted to the Graduate Faculty of the College of Engineering and to the Graduate School and was accepted as partial fulfillment of the requirements for the degree of Doctor of Philosophy.

December, 1996

Winfred M. Phillips
Dean, College of Engineering

Karen A. Holbrook
Dean, Graduate School